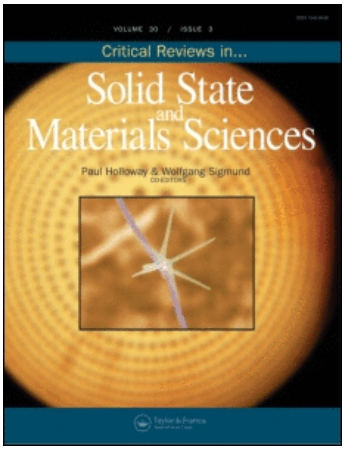

Critical Reviews in Solid State and Materials Sciences
Publication details, including instructions for authors and subscription information:
http://www.informaworld.com/smpp/title~content=t713610945

Nanodiamond Particles: Properties and Perspectives for Bioapplications

Amanda M. Schrand[a]; Suzanne A. Ciftan Hens[b]; Olga A. Shenderova[b]
[a] Nano Etc., LLC, Kettering, Ohio, USA [b] International Technology Center, Raleigh, North Carolina, USA

To cite this Article Schrand, Amanda M. , Hens, Suzanne A. Ciftan and Shenderova, Olga A.(2009) 'Nanodiamond Particles: Properties and Perspectives for Bioapplications', Critical Reviews in Solid State and Materials Sciences, 34: 1, 18 — 74
To link to this Article: DOI: 10.1080/10408430902831987
URL: http://dx.doi.org/10.1080/10408430902831987

Critical Reviews in Solid State and Materials Sciences, 34:18–74, 2009

ISSN: 1040-8436 print / 1547-6561 online
DOI: 10.1080/10408430902831987

Taylor & Francis
Taylor & Francis Group

Nanodiamond Particles: Properties and Perspectives for Bioapplications

Amanda M. Schrand,[1] Suzanne A. Ciftan Hens,[2] and Olga A. Shenderova[2,*]
[1]*Nano Etc., LLC, Kettering, Ohio, USA*
[2]*International Technology Center, Raleigh, North Carolina, USA*

Nanodiamonds (NDs) are members of the diverse structural family of nanocarbons that includes many varieties based on synthesis conditions, post-synthesis processes, and modifications. First studied in detail beginning in the 1960s in Russia, NDs have now gained world-wide attention due to their inexpensive large-scale synthesis based on the detonation of carbon-containing explosives, small primary particle size (∼4 to 5 nm) with narrow size distribution, facile surface functionalization including bio-conjugation, as well as high biocompatibility. It is anticipated that the attractive properties of NDs will be exploited for the development of therapeutic agents for diagnostic probes, delivery vehicles, gene therapy, anti-viral and anti-bacterial treatments, tissue scaffolds, and novel medical devices such as nanorobots. Additionally, biotechnology applications have shown the prospective use of NDs for bioanalytical purposes, such as protein purification or fluorescent biolabeling. This review critically examines the use of NDs for biomedical applications based on type (i.e., high-pressure high-temperature [HPHT], CVD diamond, detonation ND [DND]), post-synthesis processing and modifications, and resultant properties including bio-interfacing. The discussion focuses on nanodiamond material in the form of nanoparticles, while the biomedical uses of nanodiamond coatings and thin films are discussed rather briefly. Specific use of NDs in both non-conjugated and conjugated forms as enterosorbents or solid phase carriers for small molecules including lysozyme, vaccines, and drugs is also considered. The use of NDs as human anti-cancer agents and in health care products is already showing promising results for further development. The review concludes with a look to the future directions and challenges involved in maximizing the potential of these exciting little carbon-based gems in the fields of engineering, medicine, and biotechnology.

Keywords ultradispersed diamond, detonation synthesis, biocompatibility, nanocarbon, cellular imaging, drug delivery

Table of Contents

*E-mail: oshenderova@itc-inc.org

1. INTRODUCTION

Nanodiamonds (NDs) are members of the diverse structural family of nanocarbons, which include nano-sized amorphous carbon, fullerenes, diamondoids, tubes, onions, horns, rods, cones, peapods, bells, whiskers, platelets, and foam.[1] First studied in detail beginning in the 1960s in Russia, NDs have now gained world-wide attention due to their inexpensive large scale synthesis based on the detonation of carbon-containing explosives, small primary particle size (~4 to 5 nm) with narrow size distribution, facile surface functionalization including bioconjugation, as well as high biocompatibility. Although there are only a few carbon nanomaterial-based medicinal products such as adamantane derivatives (i.e., amantadine, memantine, and rimantadine) or derivatized fullerenes,[2,3] preliminary studies with ND suspensions administered to animals and human patients with cancer have shown promising results for further development.

It is anticipated that the attractive properties of NDs will be exploited in a similar manner to other carbon nanoparticles, quantum dots, and metallic nanoparticles, for the development of therapeutic agents for diagnostic probes, delivery vehicles, gene therapy, anti-viral and anti-bacterial treatments, tissue scaffolds, and the development of novel medical devices such as nanorobots.[4–15] More specifically, biotechnology applications have shown the prospective use of NDs for bioanalytical purposes such as protein purification or biolabeling using highly fluorescent synthetic nanodiamond particles. In terms of biodesign, the engineering of a plethora of nanostructured materials (i.e., metallic, ceramic, polymeric, and composite) for interaction at the molecular level with a high degree of specificity demonstrates an almost unlimited potential of bionanotechnology.[16,17] However, the translation of these advances into clinical applications may rely on a diverse set of nanofabrication techniques, further miniaturization of devices (i.e., BioMEMS), as well as the development of new analytical methods.[18–22]

The goal of maximizing therapeutic benefits while limiting adverse-effects has been approached through surface coating of fluorescent semiconductor nanocrystals (quantum dots), magnetic nanoparticles, and metallic nanoparticles (i.e., Au, Ag) before they may be used in molecular imaging, separation, and delivery of substances for demanding biological environments such as living tissues.[23–28] However, there is no escaping the worrisome potential pitfalls of human exposure to nanoparticles, which have been prominently addressed by high-impact scientific journals such as *Science* and *Nature* in an effort to understand their long-term health and environmental implications.[29–37] The journal *Carbon* devoted an entire issue to carbon nanoparticle toxicity, emphasizing that collaboration between toxicologists and materials scientists in the development of "green" nanomaterial formulations is needed to optimize function and minimize negative health impacts.[38] The issue of carbon nanoparticle biocompatibility, or alternatively, cytotoxicity and genotoxicity, as well as the need to advance the experimental methods used in this emergent field of research has also been highlighted in several papers and books.[39–47] Therefore, the development of nanoparticle-based products that either directly or indirectly come into contact with the body is being approached with great caution.

It is the goal of this review to critically examine the use of NDs for biomedical applications based on type (i.e., high-pressure high-temperature [HPHT], CVD diamond, detonation ND [DND], diamondoids), post-synthesis processing and modifications, and resultant properties including biocompatibility. The focus will be on nanodiamond material in the form of nanoparticles, while the biomedical uses of nanodiamond coatings and thin films are discussed rather briefly. Specific uses of NDs as bioanalytical probes, curative agents for cancer, optical labels, and ingredients in health care products will be discussed. Finally, we take a look at the future directions and challenges of ND research in engineering, medicine, and biotechnology.

2. TYPES OF NANODIAMOND

2.1. General Overview

Diamond structures at the nanoscale (length ~1 to 100 nanometers) include pure-phase diamond films, diamond particles, recently fabricated 1-D diamond nanorods and 2-D diamond nanoplatelets. There is a special class of nanodiamond material often called '*ultra-nanocrystalline*' diamond with the characteristic size of the basic diamond constituents

encompassing the range of just a few nanometers that distinguishes it from other diamond-based nanostructures with characteristic sizes above ~10 nm.[1,40,48] Particles with characteristic sizes of 4 to 5 nm, often called in the literature "ultradispersed diamond" (UDD) or "detonation nanodiamond" (DND), were produced by detonation of carbon-containing explosives in the former USSR in the 1960s. Pure-phase UNCD films with characteristic grain sizes of 2 to 5 nm, grown by chemical vapor deposition (CVD), were developed in the United States at Argon National Laboratory at the end of 1990s.[48] DND particles and UNCD films have been the focus of several recent reviews and feature articles,[49–54] books,[1,40,55,56,374] and proceedings of topical nanodiamond conferences.[57–60] UNCD films have been successfully commercialized by *Advanced Diamond Technology, Inc.*[61] The ultra-nanocrystallinity is the result of a new growth and nucleation mechanism, that is due to the use of argon-rich plasmas instead of the hydrogen-rich plasmas normally used to deposit microcrystalline diamond films. UNCD films are superior in many ways to traditional microcrystalline diamond films: they are smooth, dense, pinhole free, phase-pure and can be conformally deposited on a wide variety of materials and high-aspect-ratio structures.[48] While UNCD films are not the focus of the present review, it should be mentioned that UNCD films have emerged as very attractive candidates for coatings on biomedical devices and implants[62] and in biosensors.[63]

A detailed discussion on the known synthesis methods of diamond structures at the nanoscale is provided by Shenderova and Gruen.[40] Below we give a brief outline on the methods of production and related characteristic sizes of diamond particles (Figure 1). The methods for synthesizing diamond powder in the form of single particles with micro- and nanometer sizes were invented in the beginning of the 1960s by DuPont de Nemours, USA and the product has been commercially available since the 1970s under the name *Mypolex*™. DuPont produced polycrystalline diamond particles up to 50 microns in size using shock-wave compression of carbon materials (graphite, carbon black) mixed with catalyst. The size of the *primary* grains in the polycrystalline particles is about 20 to 25 nm (Figure 1). In 1999, the Mypolex polycrystalline diamond business was acquired from DuPont, by *Microdiamant AG*, Switzerland, a company specializing in the micron- and sub-micron diamond market. Since acquiring the Mypolex product, *Microdiamant AG* now manufactures three size classes smaller than any products ever available from DuPont.[64] In addition to *Mypolex* polycrystalline diamond, *Microdiamant AG* also provides the finest fractions of particles down to 0 to 50 nm processed from the starting material high-pressure high-temperature synthetic diamond as well as from natural diamond powders (Figure 1). The commercialization of these nanodiamond materials has become well established in applications requiring high-precision polishing.

An approach for producing even smaller and more uniformly sized ultrananocrystalline diamond powder with a characteristic size of primary particles of ~4 to 5 nm, as mentioned above, is the conversion of carbon-containing explosive compounds into diamond during the firing of explosives in hermetic tanks. The fascinating history of the discovery of the DND particulate was discussed by Danilenko.[65] This method was initiated in Russia in the early 1960s soon after DuPont's work on shock-wave conversion of graphite synthesis. A large scale production foundry, "ALTAI," was founded in Russia in 1983 to commercialize the process of detonation diamond production in bulk quantities, yielding tons of the product per year.[55,66] Currently, there are several commercial centers in the world producing DND particulates by explosives detonation located in Russia, Ukraine, Byelorussia, China, and Japan. Although discovered several decades ago, DND particles became an object of a keen interest outside of Russia only within the last few years[40,59,60,67] as the field of nanotechnology matured.

There are several other approaches for the production of ultrananocrystalline and nanocrystalline diamond particles at the laboratory scale. Diamond with characteristic sizes of several nanometers has been synthesized particularly, by chlorination of carbides,[68] ion irradiation of graphite,[69] electron irradiation of carbon onions[70] and in the vapor phase in a substrate-free tube flow CVD reactor.[71] Moreover, astronomical observations suggest that as much as 10 to 20% of interstellar carbon is in the form of ultrananocrystalline diamonds.[72] The questions of when and how does nanodiamond originate in the Cosmos remain open, although comparative microstructural analysis of nanodiamonds extracted from meteorites, indicates that the majority of cosmic nanodiamonds are formed by low-pressure vapor condensation.[73] Diamond particles attached to quartz substrates with characteristic sizes several tens of nanometers (specifically, 10 to 110 nm) have been synthesized by the CVD method.[74] One benefit of this synthesis technique was the ability to fabricate isolated diamond nanocrystals with single color centers.

For biomedical applications, it is important to have nanodiamond material available in large quantities and with highly reproducible and consistent properties, i.e., commercial nanodiamond is required. Existing commercial diamond nanoparticles can be tentatively categorized into three groups of products according to the primary (smallest monocrystalline) particle sizes: nanocrystalline particles, ultrananocrystalline particles, and diamondoids (Figure 1). Characteristic sizes of nanocrystalline particles encompass the size range of tens of nanometers, while sizes of primary particles of ultrananocrystalline diamond are within several nanometers. Diamondoids are well defined hydrogen-terminated molecular forms consisting of several tens of carbon atoms.

2.2. Commercial Nanocrystalline Diamond Particles

Nanocrystalline diamond particles with characteristic sizes of primary particles in the range of several tens of nanometers can be in the form of isolated *monocrystalline* particles or *polycrystals* (Figure 1). Monocrystalline nanoparticles are obtained by processing micron-sized monocrystalline diamond particles, which are, in turn, a byproduct of natural diamond or HPHT

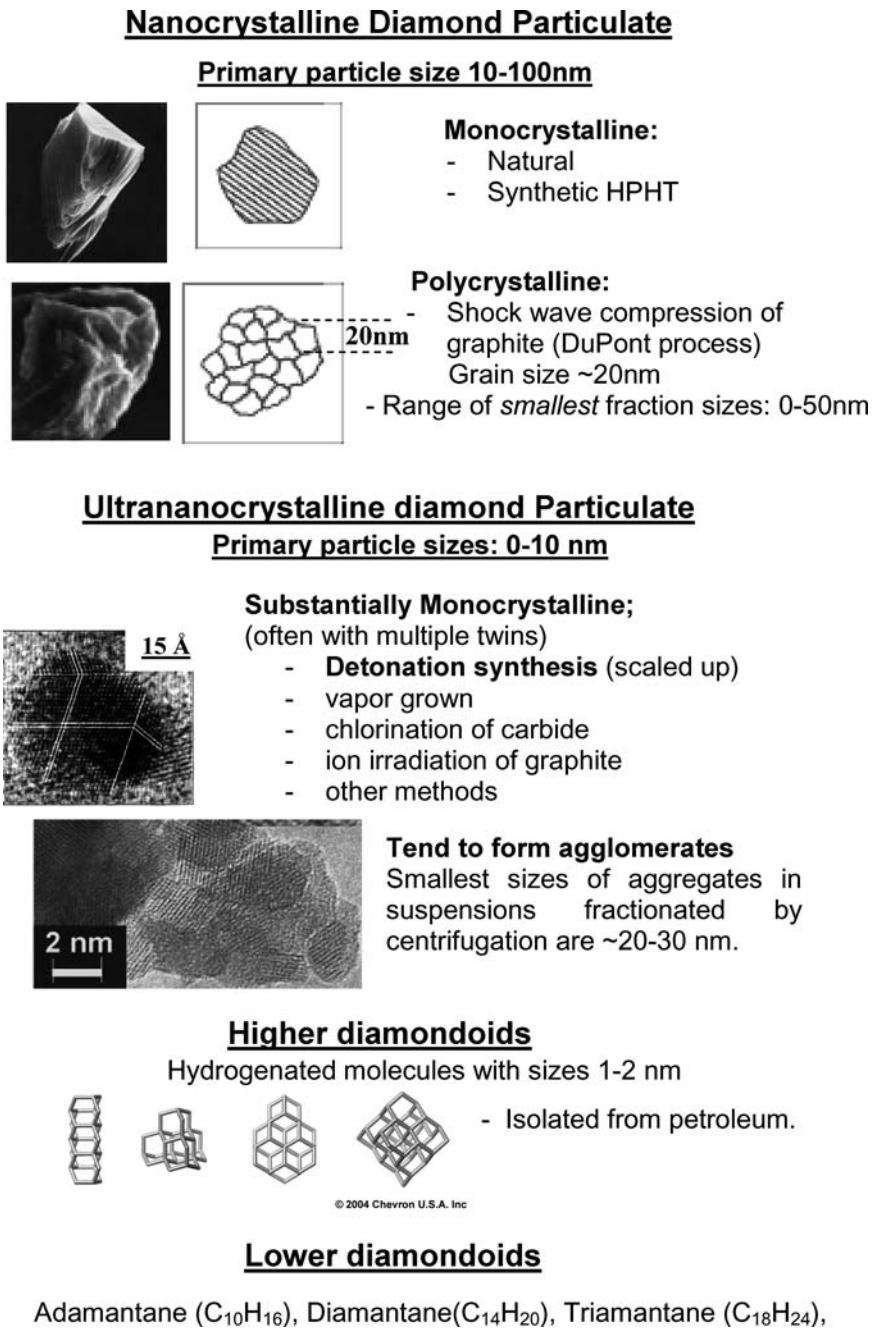

FIG. 1. Summary of the types of nanoscale diamond particles and molecular forms (low diamondoids) according to the *primary* particle size.

diamond synthesis. The processing of micron-sized diamond particles to smaller fractions includes grinding, purification, and grading of the powder. Monocrystalline grinded diamond particles have rather sharp edges compared with other forms of nanodiamond (Figure 1). Monocrystalline natural nanodiamond powder is the purest product within the class of ND (and UNCD) materials. Synthetic HPHT type Ib monocrystalline diamond powders (containing typically 100 ppm nitrogen atoms) with particle sizes of 100 nm, 35 nm, and 25 nm have been used to produce fluorescent ND by irradiation with protons followed by annealing for bio-labeling applications.[75–77]

The polycrystalline nanodiamond powder (Figure 1) is processed from micron-sized polycrystalline diamond particles obtained by shock synthesis[78] (DuPont de Nemours's method mentioned above). Polycrystalline particles consist of nanometer-sized diamond grains (∼20 to 25 nm). The finest

diamond fraction produced by micronizing followed by grading has an average particle size of ∼25 nm. This type of ND has a high content of impurities and thus far has not been used for bioapplications. The shape of primary particles is more platelet-like rather than spherical.[79]

2.3. Commercial *Ultra*nanocrystalline Diamond Particles

Out of several types of ultrananocrystalline diamond particles (Figure 1), only detonation ND has been commercialized. The size of primary detonation ND particles depends on the weight of explosive charge so, in principle, there is no specific maximum size, although most vendors produce particles with an average size of 3.5 to 6 nm. This type of ND is most frequently used for envisioned bioapplications such as broad drug delivery platforms for nanoscale medicine,[80] protein adsorption,[81–83] carriers of genetic material[84] in gene gun ballistic delivery,[85] as enterosorbents,[86,87] as well as other applications (see Section 5). The cost factor is also an important issue for applications of nanodiamond particles. For example, HPHT nanodiamond with an average particle size 25 nm costs $75/gram. However, well purified DND powder costs only about $1 to $2/gram for polydispersed powder (200 nm average aggregate size) and about $10–20/gram for a fraction with 20 nm average aggregate size. Since detonation ND is the most popular starting material within the nanodiamond particle family for biomedical applications, its processing and modification are described in more detail in the Section 3.

2.4. Diamondoids

Recently, a whole family of ∼1 to ∼2 nm sized hydrogen-terminated diamond species was discovered. As highly rigid, well defined, readily derivatizable structures,[2] these so-called "higher diamondoids" are valuable molecular building blocks for nanotechnology. With more than 3 crystal diamond cages, higher diamondoids are intermediate in size to the adamantane molecule, the smallest species of H-terminated cubic diamond containing only 10 carbon atoms, and ultrananocrystalline diamond particles with sizes more than 2 nm as described above. Higher diamondoids are extracted from petroleum as diamond molecules in the form of nanometer-sized rods, helices, discs, pyramids, etc. (Figure 1).[88,89]

However, the formation mechanism of the higher diamondoids in petroleum remains a mystery.[89] So far, it has not been possible to synthesize higher diamondoids except anti-tetramantane, a tetramantane isomer.[2] Certain higher diamondoids are now available in multi-gram quantities through *Molecular Diamond Technologies, Inc.* on a collaborative basis.

By comparison, lower diamondoids (adamantane, diadamantane, and triadamantane), extracted from crude oil much earlier than larger members of the diamondoid series, are currently available in kilograms quantities[2] and can be synthesized. Lower diamondoids such as adamantane derivatives (single-molecule unit of diamond with the formula $C_{10}H_{16}$) have been used in pharmacology, clinical medicine, and biosensing.[90] A review of biomedical applications of diamondoids and their derivatives is provided by Grichko et al.[91]

3. DETONATION NANODIAMOND SYNTHESIS, PROCESSING, AND MODIFICATION

Three major steps in the conversion of carbon-containing explosives to modern DND products include *synthesis*, *post-synthesis processing*, and *modification* (Figure 2), which are discussed in detail in the following sections. The current interest in DND material is so great that even 'traditional' methods of synthesis (composition of explosives and cooling media) and processing (type of oxidizers) are being revisited.[92,93] *Processing* includes purification of detonation soot from metallic impurities and non-diamond carbon and is typically performed in conjunction with detonation soot synthesis by the same vendor. The result of the processing is DND of a certain purity (presently at a level of incombustible impurity content 0.5-5wt.% depending on the vendor) that is available on a large scale (hundreds of kilograms). DND treatments, tentatively called *modification,* can include additional deep purification, surface functionalizations toward specific applications, and de-agglomeration or size fractionation. In the last 3 to 4 years, the development of approaches for DND modifications has been the major focus of

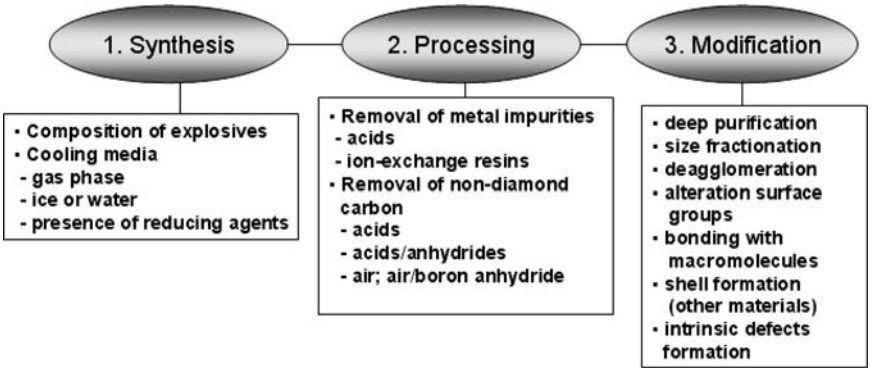

FIG. 2. Three major steps of conversion of carbon-containing explosives to modern DND product.

research activity. Although, initially, DND modifications were performed on a small scale, currently these steps are being implemented on a large scale on site at DND production centers.[94] Of primary importance is the method of disintegration of nanodiamond aggregates by stirred-media milling with micron-sized ceramic beads suggested by Osawa et al.,[115] resulting in diamond slurries containing primary 4 to 5 nm DND particles. The single-digit DND immediately attracted the attention of relatively large number of researchers working in the area of nanoscale materials, which was demonstrated by recent publications in high-profile journals.[80,96,97]

3.1. Synthesis

The explosion method for diamond production results in diamond clusters that are formed from carbon atoms contained within the explosive molecules; thus, only the explosive is used as a precursor material. However, a wide variety of explosive materials can be used.[49,56] For example, a typical explosive is a mixture of TNT and hexogen composed of C, N, O, and H with a negative oxygen balance, so that 'excess' carbon is present in the system. The explosion takes place in a non-oxidizing cooling medium of either gas (N_2, CO_2, Ar, or other medium that can be under pressure) or water (ice), so-called 'dry' or 'wet' synthesis, respectively. To prevent the DND formed in the detonation wave from transforming into graphite at the high temperature generated by the detonation, the cooling rate of the reaction products should be no less than 3000 K/min.[55,66] The initial shock from a detonator compresses the high-explosive material, heating it and causing chemical decomposition, which releases enormous amounts of energy in a fraction of a microsecond. As the detonation wave propagates through the material, it generates high temperatures (3500 to 4000 K) and high pressures (20 to 30 GPa) that correspond to the phase region for thermodynamically stable diamond.[98] During detonation, the free carbon coagulates into small clusters, which might grow larger by diffusion.[99] The product of detonation synthesis, called "detonation soot" or "diamond blend" contains 40 to 80 wt.% of the diamond phase depending on the detonation conditions.[49,56] The carbon yield is 4 to 10% of the explosive weight. Understanding the mechanisms of the DND formation during detonation of high-energy explosives is still unresolved and is an active area of research.[79,100,101]

There are two major technical requirements for DND synthesis using explosives; the composition of the explosives must provide the thermodynamic conditions for diamond formation, and the composition of gas atmosphere must provide the necessary quenching rate (by appropriate thermal capacity) to prevent diamond transformation to graphite.[49] The diamond yield depends to a large extent on the explosive mixture and cooling media.[49,56] The shape of the explosive also influences the yield; the ideal shape is spherical but for convenience a cylindrical charge is regularly used.[49] The relationship between the mass of the explosives and the mass of the surrounding media also influences the yield. Thus, 5 kg of explosive requires $\sim$11 m^3 of detonation chamber with gas media at ambient pressure to provide the necessary quenching rate.[55,66] The mass of the charge influences the average size of the primary particles, although not significantly.[79,95] For example, for charges with a mass of 0.2 to 2 kg, 10 to 20 kg, and 140 kg, the average primary particle size is 4 to 5 nm, 6 to 7 nm, and 8 nm, respectively.[101]

For numerous areas of DND applications, including bioapplications, there are several important questions related to revisiting DND synthesis methods and to the development of a new generation of DND particles. Reducing DND primary particle size to the range of 2 to 3 nm may further increase their capability for penetrating cells and organelle membranes including nuclear pores. ND particles with sizes $\sim$2 nm and smaller show quantum confinement effects.[102] Synthesis of small particles would open perspectives for the development of diamond quantum dots. Another question is related to the possibility of optimizing the detonation process to produce mostly isolated primary particles and only small aggregates in the detonation soot. This would significantly reduce the cost of the final DND product. In fact, it has been recognized that dry and wet synthesis methods influence both of these parameters (the primary size and degree of aggregation) in opposite directions.[79,93] The dry DND synthesis results in smaller primary DND particle sizes and smaller average aggregate sizes as compared with wet synthesis.[79,93,101] This strategy of optimization using dry synthesis for producing small average aggregate sizes has been discussed recently by Gubarevich.[93] Another factor that influences the aggregation of DNDs during synthesis is the mass of the charge and a ratio between masses of the charge and wet cooling media used.[79]

In principle, the XRD data on the size distribution of primary DND particles within detonation soot, which were reported in a limited number of publications,[56,92] include 2 nm peaks. It was reported by Dolmatov[92] that his novel method of using reducing agents agents (for example urea, ammonia) in water cooling media allows the preservation of the DND fraction with a primary particle size less than 3 nm along with a 'typical' fraction of 5 nm primary particles. Estimations of the kinetics of the explosion process by Danilenko[79,101] declares that DND cannot be produced with sizes less than $\sim$2 nm. Also, a method reported by Dolmatov[92] for using reducing agents provides the benefits of increased DND yield from the soot as well as an increased carbon content (up to 96mass%) within DND particle composition, where the total content of C,H,N, and O corresponds to 100mass%.

The new, forseen approaches for DND synthesis are focused on the different combinations of explosive materials with possible solid dopants, as well as on the non-traditional cooling media (both gaseous and liquid) with possible additives to alter the DND composition (both bulk defects/doping content and surface groups), dispersivity, and primary particle sizes.

3.2. DND Post-Synthesis Processing

Biomedical applications set high standards on nanomaterial purity, so the development of DND products of ultra-high purity

remains an important goal. In addition to the diamond phase, the detonation soot contains both graphite-like structures (25 to 45 wt.%) and incombustible impurities (metals and their oxides – 1 to 8wt.%).[49] The metal impurities originate from a detonator and from the walls of the detonation chamber. The impurity content of nanodiamonds produced by detonation synthesis is higher when compared with other artificial diamonds (for instance, HPHT diamonds contain no less than 96% carbon). After typical purification steps, powders of DND can be considered a composite consisting of different forms of carbon (~80% to 89%), nitrogen (~2% to 3%), hydrogen (~0.5% to 1.5%), oxygen (up to ~10%) and an incombustible residue (~0.5% to 8%).[49,65] The carbon phase consists of a mixture of diamond (90% to 99%) and non-diamond carbon (1% to 10%).

Figure 3 illustrates the major structural features of detonation soot and the purified DND product. Non-diamond carbon contains graphite nanocrystals, graphite ribbons, carbon onions, and amorphous carbon, which may be located externally to the tight DND aggregates and be removed during the purification process or can be confined within tight aggregates and remain inaccessible to oxidizing media (Figure 3). Similar features can be attributed to the metallic, incombustible impurities, which can be located externally or internally relatively to the tight DND aggregates. To remove internal metal impurities and internal non-diamond carbon, tight DND agglomerates should be disintegrated. Nevertheless, after deep purification using acid treatment, the incombustible impurity content in *polydispersed* diamond, for example from *New Technologies* (Chelyabinsk, Russia) can be ~0.2wt.% as defined using thermal gravimetric analysis (TGA).[103] It should be noted that metal ions can also form complexes on DND surfaces (Figure 3) after treatment with liquid oxidizers containing metals (for example, using the mixture of H_2SO_4/CrO_3) and contribute to the total content of incombustible impurities. A combination of oxidation of non-diamond carbon and metallic impurities should be performed to effectively remove both non-diamond carbon and metal particles confined within amorphous carbon. The importance of this aspect was demonstrated by Osswald et al.[103] and Pichot et al.[104] by achieving a low metal content only after oxidizing the amorphous carbon during soot treatment.

In general, methods of DND purification as well as DND purity vary from vendor to vendor. For DND purification from detonation soot, mechanical and chemical methods are used. After mechanically removing process admixtures, the diamond-carbon powder is subjected, for example, to thermal oxidation with nitric acid under pressure to separate the diamond phase.[49] In this method, metals are dissolved and non-diamond carbon is oxidized simultaneously. Other 'classical' purification methods, based upon the use of liquid oxidizers for the removal of metallic impurities, include sulfuric acid, mixture of sulfuric and nitric acids, hydrochloric acid, potassium dichromate in sulfuric acid, as well as other schemes.[49,105] A brief review of the numerous methods of detonation soot purification developed in the former USSR is provided by Petrov et al.[105] Pichot et al. reported on soot treatment using hydrofluoric/nitric acids for the efficient removal of metallic particles.[104] For the oxidation of sp^2 carbons, the purification schemes include KOH/KNO_3, Na_2O_2, CrO_3/H_2SO_4, HNO_3/H_2O_2 under pressure, mixtures of concentrated sulfuric and perchloric acids, and other approaches.[49,105,107–109] To remove non-carbon impurities, the chemically purified product is subjected, in some cases, to an additional purification process using ion-exchange and membrane technologies.

Currently, the majority of DND vendors use strong liquid oxidizers at elevated temperatures and pressures.[49] However, liquid-phase purification is both hazardous and costly, contributing up to 40% of the product cost. In addition, the expense of waste pre-treatment and disposal, which is already high, is expected to increase as governmental policy on environmental protection becomes tighter. Alternatively, DND can be very effectively purified from non-diamond carbon in an environmentally friendly manner by a gas phase treatment using ozone at

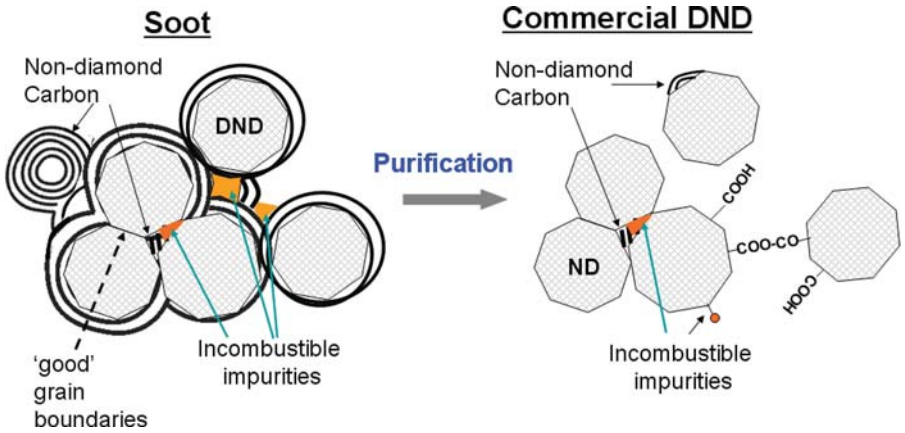

FIG. 3. Tentative scheme of major structural components of detonation soot (left) and commercial DND product (right). Corresponding electronic microscopy images are illustrated in Figure 5.

elevated temperatures[110] to eliminate the need for the use of corrosive liquid oxidizers. Ozone oxidation is also more efficient for sp^2 carbon oxidation than is oxygen. The method was first introduced in 1991,[106,110] and the productivity of the ozone-in-air flow fluidized bed reactor was 6 to 10 kg/month. Now ozone oxidation is the only gas-phase method for soot purification that has been realized at an industrial scale (by *New Technologies*, Chelyabinsk, Russia).

Several efforts have attempted to purify DND by oxidation of detonation soot with air at elevated temperatures. The method allowed for a significant decrease in the non-diamond carbon content. Larionova et al. purified DND using soot treatment with air at 380 to 440°C for several hours.[109] Soot purification through a combination of liquid oxidizers and air treatment at temperatures up to 600 °C was reported by Mitev.[111] Osswald et al.[103] demonstrated that for DND, with a high content of non-diamond carbon (sample UD50[103]), the optimal temperature for the heat treatment in air within several hours is 400 to 430°C. This process allows for the oxidation of sp^2-bonded carbon, but not that of the sp^3 carbon. The purified DND contained 95% sp^3 carbon, as was measured with XANES, and was substantially lighter in color than the original material.[103] Chiganov purified DNDs from soot through thermal oxidation in air, using boric anhydride in order to selectively oxidize the non-diamond carbon.[107]

3.3. Detonation Nanodiamond Modification

DND obtained from commercial vendors often requires additional processing and modification, since the content of incombustible impurities (ash) and non-diamond carbon can be too high, average aggregate size too large, and surface chemistry not suitable for an envisioned application. The low stability to sedimentation of commercial DND powders after liquid dispersion is a common problem (Figure 4). Besides, there is no universal material called 'detonation nanodiamond.' Materials from every vendor are specific to the synthesis and post-synthesis purification methods adapted by the vendor. Accordingly, the modification strategy would be different for DND from different vendors. For example, DND of wet synthesis purified from soot at the vendor site (VNIITF, Snezinsk) using a mixture of CrO_3/H_2SO_4 was additionally purified with heat treatment in air.[112] This treatment followed by dispersion in water using a high-powered sonicator and multi-step ultracentrifugation resulted in stable hydrosols of DND fractions.[112] DND from 'dry' synthesis purified from soot at the vendor site (FSPC "Altay") using a mixture of H_2SO_4/HNO_3 was also subjected to heat treatment in air, resulting in a high-purity product.[103] However, the water dispersion of the treated DND[103] was unstable and sedimented easily, thereby requiring an additional treatment in HCl to improve its colloidal property.[113] While both samples contained abundant carboxylic groups after heat treatment in air,[103,112] dissimilarities in other types of surface groups might explain the differences in colloidal stability of these two DND samples. As a means to improve quality of the DND product, deep purification, fractionation, deaggregation, and surface functionalization are discussed below.

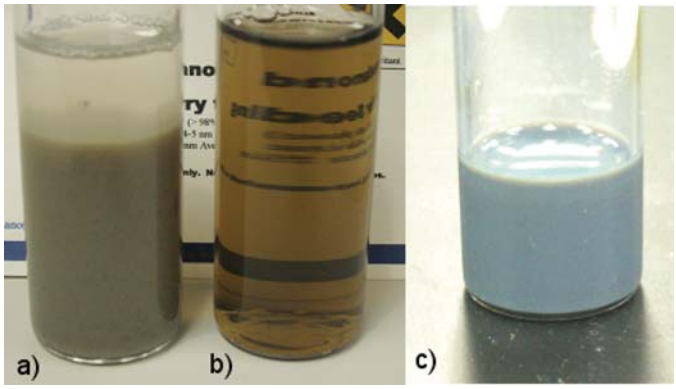

FIG. 4. Photos of commercial DND (Ch-St) in DI water 10 hours after sonication (a) and same after purification and fractionation, forming a stable colloidal suspension of DND with 20 nm average aggregate size (b). Note the high transparency of the suspended sample (b) and amber-like color originating from Raleigh scattering, which is stronger for shorter wavelengths of visible light. Narrow-size distribution fraction of ND in DMSO with average aggregate size 50 nm depleted of primary ND particles (c) exhibits bright blue color due to uniformity of the particles size distribution.

3.3.1. Deep Purification

Back in the 1990s tons of DND were produced at the Federal Science-Production Centre "Altay," Biisk, Siberia, Russia;[55,66] hundreds of kilograms of DND were produced at VNIITF center, Snezinsk, Ural region, Russia,[114] and at other centers in Russia, Belorussia, and the Ukraine; these products are still available in the DND market. At that time, achievement of low ash content in DND was not a high priority. The incombustible impurities content in DND produced at Altay and VNIITF was 2.39wt.%[115] and 1.4wt.%,[112] correspondingly. The purity of commercial DND from a large manufacturer in Lanzhou, China, Gansu Lingyun Nano-Material Co., Ltd., was reported as 1.19wt%.[115] Additional purification of these DNDs is required for modern applications, especially for biomedical use. Table 1 illustrates that additional treatment with liquid oxidizers reduced the ash content in the sample (Ch-St DND) that was produced at VNIITF.[113] The sample was purified with HCl, HCl/HNO_3, HF/HCl, and H_2O_2-NaOH.[116] The most efficient purification in this series was achieved using treatment with HF followed by HCl acids. While the initial Ch-St sample had a very low colloidal stability (Figure 4, left), the colloidal stability of the samples after deep purification was significantly improved, and the average aggregate size decreased by more than twofold (Table 1). Table 1 also contains data on the average aggregate size of the DND purified from soot with ozone.

TABLE 1
Comparison of incombustible impurities content and average aggregate size for the same initial soot purified with either a wet oxidizer or ozone (rows 1 and 2, correspondingly) as well as for different additional purification treatments of the Ch-St DND

ND treatment	Incombustible Impurities, wt.%	Size in H2O, nm
Soot purified with CrO_3/H_2SO_4 (Ch-St ND)	1.5	300
Soot purified with O_3	0.9	190
Ch-St purified with air		210
Ch-St purified with HCl	1.2	177
Ch-St purified with HCl/HNO_3	0.9	175
Ch-St purified with HF/HCl	0.2	171
Ch-St purified with H_2O_2-NaOH	0.8	202

The average aggregate size is much less than for DND purified with CrO_3/H_2SO_4 (Ch-St) from the same batch of the soot. The colloidal stability of the ozone-purified DND in water is very high. For example, a suspension of 10% ozonated DND in water was stable for 5 years. This illustrates the importance of using ozone treatment of DND for both soot purification, and, possibly, for additional deep purification of DND. Examples of the lowest reported incombustible impurities content obtained on a small scale using hot nitric acid for DND purification include samples containing only 0.08wt.%[115] and 0.07%[92] of ash.

Heat treatment in air can be considered as an efficient means for deep purification of DND from non-diamond carbon, as demonstrated in a thorough study by Osswald et al.[103] using the XANES technique for identifying sp^2 and sp^3 carbon content. Gordeev et al.[117] heated DND in air at 440 to 600°C and obtained DND with a significantly improved stability for their dispersions in water. The effects on stability for DND with an average primary particle size of 8 to 10 nm, heated in air at a temperature exceeding 557°C, were studied by Xu et al.[118] Shenderova et al.[112] carried out oxidation of commercial DND products (Ch-St DND) with air at 400 to 450°C and achieved high colloidal stability for DND hydrosols. In an alternative approach of DND purification with gases, a significant decrease in sp^2 carbon content and a significant reduction in Al, Cr, Si, and Fe content was achieved by applying Cl_2 treatment at 850 degrees C.[119]

3.3.2. Fractionation

While the primary detonation ND particle size is 4 to 5 nm, the primary particles form tightly and loosely bound aggregates. The typical commercial polydispersed ND powder solutions that are subjected to powerful ultrasound treatments routinely exhibit 200 to 400 nm average aggregate sizes, which are unbreakable by the ultrasonic treatment (Figure 5 e–g). An alternative approach to effectively separate the particles and narrow the size distribution is centrifugal fractionation.[94,112,120,121] Importantly, DND solutions must possess high colloidal stability for centrifugal fractionation. It is difficult, if not impossible, to fractionate an unstable suspension.

DND fractionation has several attractive aspects. First, it is a contamination-free approach as compared, for example, with bead milling, which introduces impurities from ceramic beads. It is also convenient to be able to fractionate DND into different, narrow distribution of sizes for different niche applications (Figure 6). For example, only DND with aggregate sizes of more than 100 nm can form photonic structures that diffract light in the visible region.[122] Finally, after deep purification or treatment with ozone/air, the content of DND with small-sized aggregates can be significantly increased and the production of suspensions with small fractions of pure DND without added contaminents becomes economically feasible. In fact, suspensions of 5wt% of 25 nm size DND fraction in water have been produced using this method.[94] Suspensions of DND with an average 15 nm aggregate size in water can be obtained by centrifugation (Figure 4, right). The purity of small aggregates can be very high. First, as it was discussed in the previous subsection, the content of incombustible impurities even in the polycrystalline sample after deep purification is very low. Second, the small aggregates consisting of several primary DND often have both elongated shapes (Figure 7) and atomically sharp grain boundaries (Figure 5 c,d),[123] preventing confinement of amorphous carbon in the intergrain regions. It might be expected that content of non-diamond carbon would be relatively low. Future characterization of small fractions of DND is required to test these parameters.

The content of individual primary DND particles within the fractions with small average aggregate size is quite substantial (Figure 7). It is expected that the content of surface groups on these individual primary DND particles is more uniform than for those obtained by bead milling when 'fresh' diamond surfaces are being formed during disintegration of the agglomerates, which can interact with surfactant and other molecules from the liquid media.[124,125] The development of methods of extraction of the primary DND particles from DND suspension would definitely advance DND applications.

The centrifugal fractionation approach has drawbacks that mostly originate from the highly irregular shapes (spherical vs. elongated chains) of the DND aggregates (Figures 5 and 7). While the centrifugal force depends upon the particle shape, the resulting separation is done based upon the combined size/shape factor rather than solely on the size. Importantly, it was recently shown that it is possible to extract 4nm primary DND particles by ultracentrifugation.[126]

3.3.3. Deagglomeration

Deagglomeation if nanodiamond into their primary particle size is an important goal for biomedical applications. Osawa

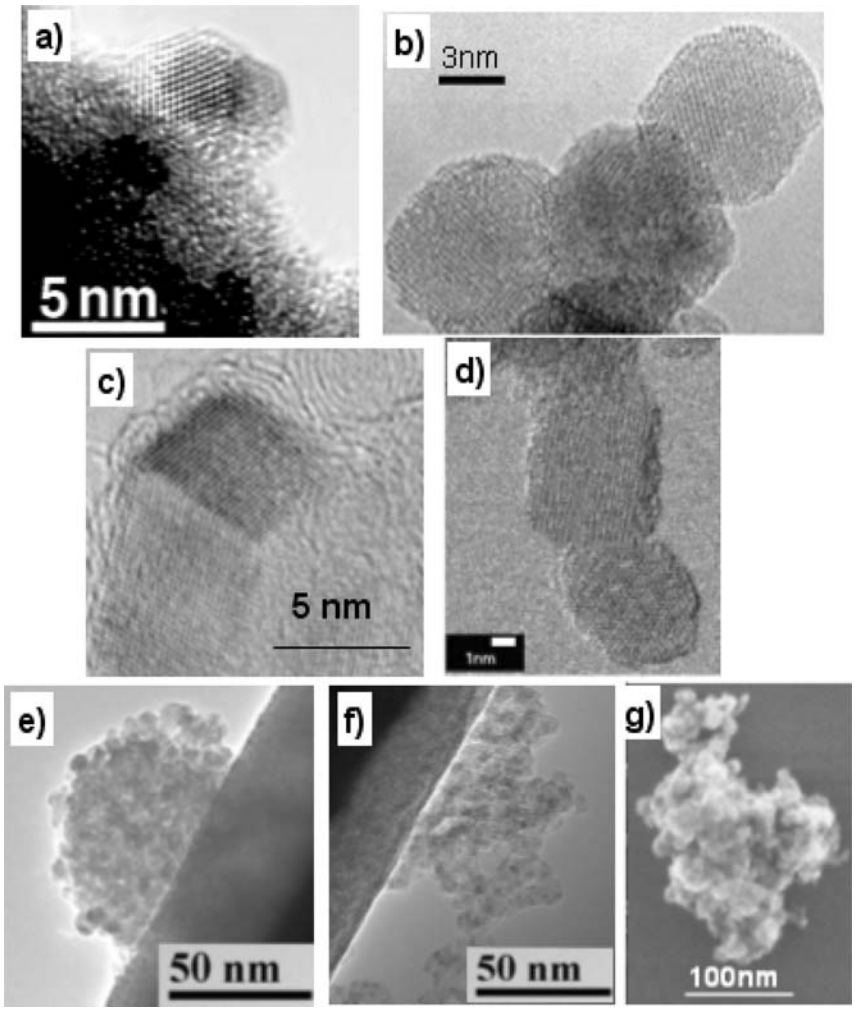

FIG. 5. HRTEM images of primary DND particles (a,b), primary DND particles forming small agglomerates with atomically sharp grain boundaries (c,d); medium-size agglomerates with high (e) and low (f) DND packing density and a large aggregate with highly irregular shape (g). Images (a) and (e-g) are courtesy of Talmage Tyler, NCSU, ITC. Image (b) is courtesy of Bogdan Palosz, IHPP, Warsaw, Poland. Image (c) is courtesy of Vladimir Kuznetsov, BIC, Novosibirsk. Image (d) has been adapted from Iakoubovskii, et al.[123] with permission.

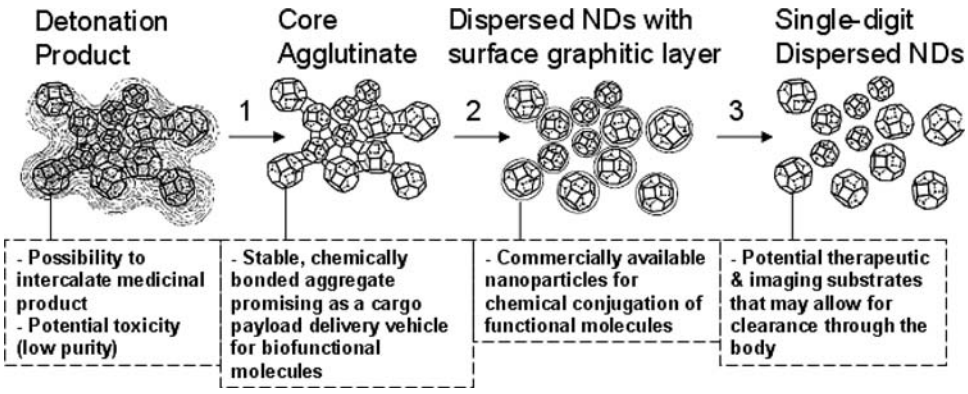

FIG. 6. Detonation nanodiamond structural changes and proposed uses for controlled and sustained release of small molecules or medicinal products during different stages of purification: (1) Nitric acid oxidation, (2) Bead milling, and (3) Removal of graphitic surface layer. (Adapted with permission from Ōsawa.[392] Also see Huang et al.[80])

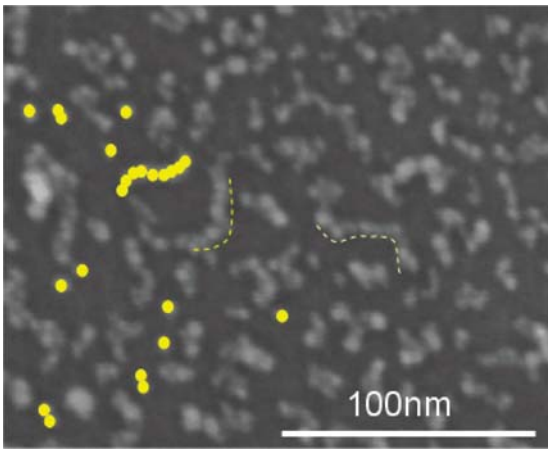

FIG. 7. SEM image of the fraction of DND particles with average aggregate size 20 nm dispersed over a Si substrate. Highlighted in yellow are selected primary particles, aggregates consisting of one or two particles as well as elongated worm-like DND aggregates.

and coworkers developed proprietary methods of mechanical deagglomeration of DND dispersion in suspensions by stirred media milling[115] or bead-assisted sonic disintegration.[127] Suspensions of individual 4 to 5 nm DND particles containing a very small fraction of ∼30 nm particles (less than 1vol.%) have been produced.[127] Since the small fraction of particles with coherent scattering region of more than 5 nm in size was observed in the X-ray diffraction studies,[128] the fraction of 'un-milled' particles can originate from these large monocrystalline particles. Besides, the high cohesive energy between primary DND particles at atomically sharp grain boundaries (Figure 5 c,d) produces unbreakable bonds, that upon bead milling, lead to undesirable side effects such as contamination with zirconia and generation of graphitic layers on the particle surface.[129] Attempts to purify bead-milled DND with liquid oxidizers lead to aggregation of the primary particles.[129] While using NaOH solution in water can be a way to purify the bead-milled material,[130] purification of the single-digit DND to a chemically acceptable level has not been yet reported.[129,130] Despite this, several kilograms of this so called single-digit, bead-milled "Nanoamando" nanodiamond has become the most popular nanodiamond material for biomedical research and has permitted the successful development of applications thereof.[129] Figure 6 illustrates DND structural changes during Osawa's approach and proposed uses for controlled and sustained release of small molecules or medicinal products during different stages of purification.

Several other methods have been proposed for DND deagglomeration. Xu et al. developed a two-step deagglomeration procedure that included graphitization of by-products of detonation in N_2 atmosphere at 1000°C for 1 h followed by their oxidation with air at 450°C for several hours.[131] The final powdered product contained at least 50% DND with the particle size of less than 50 nm. Krueger reported using DND reduced in borane (accompanied by ultrasonic treatment) resulting in significantly smaller sized aggregates.[97] Treatment of DND powder in atmospheric pressure plasma also reduced the average DND aggregate size by ∼20%.[132]

A concern that requires thorough study is the possible reagglomeration of single-digit DND or small-sized fractions subjected to further surface functionalization after purification or drying for storage. Kruger et al. observed an increase in size of DND agglomerates after silanization due to the condensation reaction between silanized particles.[124] At the same time, reduction reactions did not lead to further agglomeration.[124] Typically, during drying of ND from water and other solvents, ND aggregation is further increased, making ND functionalization, which often involves drying of the ND from a solvent, more difficult. Recently, a technique of ND fractionation has been developed that allows for drying of the ND to a powder form without concomitant agglomeration.[133] In this case, the size of the ND powder aggregate (20 to 30 nm) is preserved after dissolving the fractionated powder in a variety of solvents, facilitating ND functionalization and further processing. Puzyr et al. developed a modification based upon sonication-assisted treatment of NDs in a NaCl solution,[134,135] which results in the purification of the NDs and possibly the incorporation of Na^+ ions into the ND surface. The attractive feature of the NaCl-treatment method of ND modification[134,135] is the possibility of drying NDs from a hydrosol to a powder form with subsequent re-suspension without agglomeration. DND powder with average aggregate size ∼40 nm after dispersion in water was obtained through this method.

3.3.4. DND Surface Functionalization

Nanodiamonds are unique among the class of carbon nanoparticles because of their intrinsic hydrophilic surface, which is one of the many reasons that these nanocarbon particles are envisioned for biomolecular applications. The surface of nanodiamond particles contains a complex array of surface groups, including carboxylic acids, esters, ethers, lactones, amines, etc. Alterations in detonation nanodiamond surface groups can produce a high density of chemical functionalities, as compared with nanoscale diamond powders, since almost 15% of all atoms in the DND primary particle are located on the surface and therefore are solvent-accessible.

Nanodiamond surface groups have been altered using various reaction chemistries. Radical based reactions were one of the first chemistries to be investigated on diamond powder samples. In these reactions, the surface terminated hydrogen was abstracted creating reactive radical species that bond to groups such as carboxylic acids,[136] NO_2,[137] benzoyl peroxide, and dicarboxylic acids.[138] Furthermore, modifications to DND surfaces have been made without wet chemical methods. Liu and coworkers showed that fluorinated nanodiamond improves the solubility of these particles for efficient chemical modification into alkyl, amino, and amino acid groups.[139] Earlier work on a gas-phase treatment of DND particles with fluorine, chlorine,

and hydrogen was done by Loktev et al.[140] Spitsyn et al. performed annealing of DND in a CCl_4/Ar mixture and demonstrated a decrease in the hydrophilicity by a factor of 20.[119] The authors also performed high temperature treatment of DND in H_2 and NH_3. RF plasma was used for biofunctionalization with amino silanes[141] and an atmospheric, cold plasma source to fluorinate ND within minutes.[142]

Kulakova et al.[143,144] analyzed the modification of the nanodiamond surfaces in gaseous and liquid media and the influence of modification on the sorption and catalytic properties of nanodiamonds, their compactibility, and sintering. A procedure for the photochemical chlorination of DND by molecular chlorine in the liquid phase was described by Lisichkin et al.[143] The possibility of disintegrating the initial aggregates (<60 um) to finer aggregates (<200 nm) was shown. The reactions of a series of C-nucleophiles (organolithium reagents, CN^- ion) with the chlorinated surface were also carried out.

Because of the myriad chemical surface groups found on DNDs, prior to chemical surface modifications, it is necessary to reduce these groups in order to decrease the number of chemical products formed and to increase the yield of product. To achieve this goal, Krueger et al. have reduced DNDs with borane to eliminate surface oxygen groups, such as carboxylic acids, producing a product with increased OH surface groups.[97,145] Using this product, it was then possible to attach alkyl silanes to the DND surface. Starting with this alkyl silane, a small peptide, as well as biotin were then synthesized onto the DND surface.[97,145] Lithium aluminum hydride has also been used to reduce DND surface groups prior to the formation of aminated DND. This aminated DND was attached to both a dye and a biotin linker using their succinimydl ester derivatives.[146] In addition to these biofunctional groups, nanodiamond hydrophilic and hydrophobic polymer brushes have been synthesized.[147] Krueger et al. modified the surface of hydroxylated DND with alkyl chains of different length by an esterification reaction of carboxylic acid chlorides with the surface hydroxyl groups.[148] The resulting materials had a surface loading of 0.3 to 0.4 mmol/g and showed a much better dispersibility in several organic solvents along with a smaller particle size of the remaining agglomerates.

A recent review[149] summarized the state of the art of chemical, photochemical, and electrochemical strategies for the grafting of different organic functionalities on diamond surfaces. Depending on the envisioned application, halogenated, aminated, carboxylated and oxidized diamond surfaces have been proposed. Chemical functionalization strategies have been used on oxygen-terminated diamond, while other methods have been developed for the formation of C–C, C–X, and C–N bonds on hydrogen-terminated diamond.

Characterization of surface groups on nanodiamonds is usually achieved by FTIR and XPS. FTIR analysis is complicated by the fact that ND surfaces strongly adsorb water causing Lewis Acid/Lewis Base interactions[149] and water's stretching and bending frequencies overlap other regions of interest, including amine and amide groups. Therefore, it is necessary to use temperature-programmed vacuum FTIR for DND surface group characterization.[146,150,151] X-ray photoelectron spectroscopy (XPS) can be used for the quantification of binding energies of nitrogen,[146] fluorine,[152] oxygen,[153] and carbon atoms on DND surfaces. Other methods for characterizing ND surface groups are emerging, such as solution phase C13 NMR.[154]

3.3.5. *DND Zeta Potential*

The type of charge DND acquires in colloids becomes important in its sorption and electrophoretic applications. Remarkably, there are classes of commercial and modified DNDs with highly positive and highly negative zeta potential values (Figure 8). Different groups, both acidic and basic, found on the ND surface form during the chemical treatment of the nanomaterial. DNDs processed with soot oxidation using either singlet oxygen (RUDDM) in NaOH, air treated in a presence of catalyst (Kr series), ozone purified, or oxidized with a mixture of

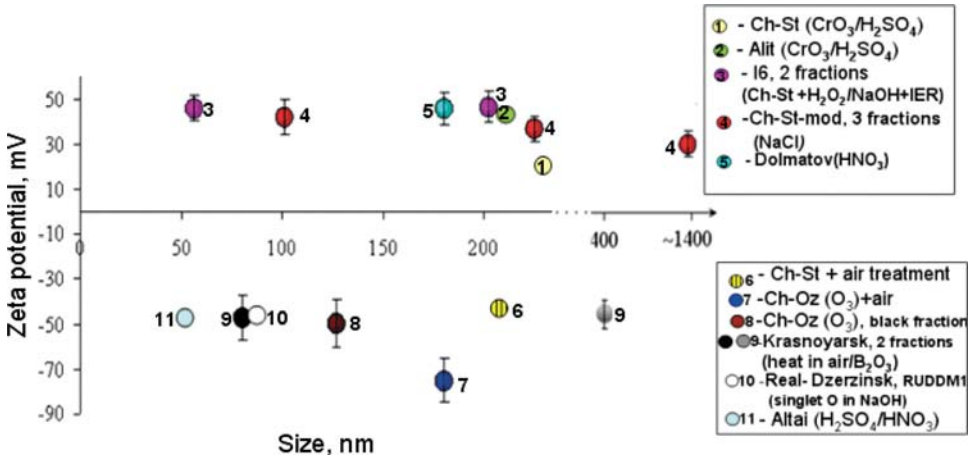

FIG. 8. Zeta potential and average aggregate size for different types of commercial DND.

H_2SO_4/HNO_3 have negative zeta potentials (Figure 8). Additional oxidation of Ch-st sample (with zeta potential +17mV) in air resulted in a material with high negative zeta potential, -45mV.[112] DND oxidized from soot with HNO_3, CrO_3/H_2SO_4, $NaOH/H_2O_2$ have positive zeta potentials (Figure 8). DND samples after deep purification with HCl, HCl/HNO_3, HF/HCl (Table 1) exhibit high positive zeta potentials ($\sim$ +40mV) (not shown in Figure 8).

Thus, presently it might be suggested that some processes of oxidation of soot or further oxidation of ND containing non-diamond carbon such as the use of singlet oxygen in liquid media, oxygen, or ozone[106] in a gas phase result in rather deep oxidation with predominant carboxylic acids groups on the ND surface. When ND is dispersed in DI water, dissociated acidic groups cause a negative charge on the ND surface.[155] The amount of carboxylic acid species on the surface of dehydrated ND with negative and positive zeta potential is the major difference observed in FTIR spectra for these groups of nanodiamond.[132]

Revealing the origin of positive zeta potential of ND is more complicated. Previously a positive charge on the ND surface was attributed to protonation of amino groups in acidic media. The spectra were taken in air, so the presence of adsorbed water might obscure signatures from amines.[156] However, FTIR spectra taken in a vacuum cuvette revealed a negligible amount of amino groups on the surface of Ch-series ND with a positive zeta potential. For comparison, the FTIR spectra of aminated DND taken in vacuum demonstrated a very pronounced peak at 3420 cm^{-1} related to amines.[146] At the same time, the amount of alcoholic groups that might also be responsible for a positive zeta potential is also small. From numerous studies of the nature of oxygen-containing groups on the surface of carbons,[157,158] two families of surface groups have been identified relative to their acidic or basic character in aqueous solutions. Carboxyl groups, lactones, phenol, and lactol groups contribute to the acidic character of carbon materials. Several models of basic oxygen-containing functionalities still being debated include chromene structures, diketone or quinone groups, pyrone-like groups and electrostatic interactions of protons with the π-electron system of the graphene structures.[157–159] Quantum chemical calculations on a large series of polycyclic pyrone-like model compounds demonstrated high relevance of the model to carbon basicity.[158,160] Pyrone-like structures, are combinations of non-neighboring carbonyl and ether oxygen atoms at the edges of a graphene layer (Figure 9). Signatures for both ketone and ether groups are present at FTIR spectra of ND. The underlying reason for the basicity of pyrone-like structures is the stabilization of the protonated form via the electronic π-conjugation throughout the sp^2 skeleton.[160] In principle, this model, which attributes the basicity of the carbon surface to pyrone-like structures, can be adapted to nanodiamonds with positive zeta potential. It is known, that the sp^2-like carbon shell might be present at the surface of ND, as well as buckyfication of (111) surfaces that can take place on the surface of nanodiamond,[102] providing a π-conjugated system. HRTEM images (Figure 5) reveal the presence of sp^2 carbon on the surface of some DND samples. The presence of sp^2- and sp^3-type oxygen has also been observed in FTIR spectra, making the presence of pyrone-like structures plausible at the nanodiamond surface. Never the less, studies on the surface modification of NDs, by chemical and mechanical processing, in combination with FTIR measurements, may help reveal the origin of positive or negative zeta potentials. Zhu et al. found that the addition of DN-10 oligomer converted the zeta potential from positive to negative.[125] Additional studies using titration[157] are required to reveal the nature of the positive zeta potential for DND.

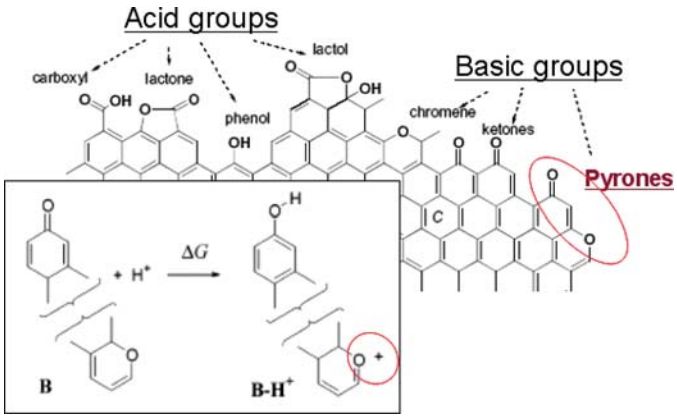

FIG. 9. Illustration of acid and basic groups on the edge surface of graphene. Pyrones surface groups can be responsible for the positive zeta-potential of the DND possessing residual aromatic rings at the surface. The inset illustrates a model of the basicity of carbon surface attributed to pyrone-like structures. Both figures were adapted with permission from Montes-Moran et al.[160]

3.4. "Modern" Detonation Nanodiamond

DND specification has been significantly tightened lately due to growth of interest in their use for new applications, specifically in the biomedical field. Figure 10 schematically illustrates the most important structural aspects of modern DND and key questions and goals that must be addressed before the 'ideal' DND will appear on the market. Major structural characteristics that need to be carefully controlled are the size of DND particles (both primary particles and their aggregates), their 'external' composition (surface groups), and 'internal' lattice defects responsible for important physical properties such as photoluminescence (Figure 10).

To date, suspensions of DND primary particles 4 to 5 nm in size obtained by bead milling, as well as fractions of DND agglomerates obtained by centrifugal fractionation, have been developed (Figure 11). Both approaches have positive and negative facets in terms of purity of bead-milled DND and consistency of DND aggregate shapes within fractions as was discussed in Section 3.3.3. It was also demonstrated that full deagglomeration

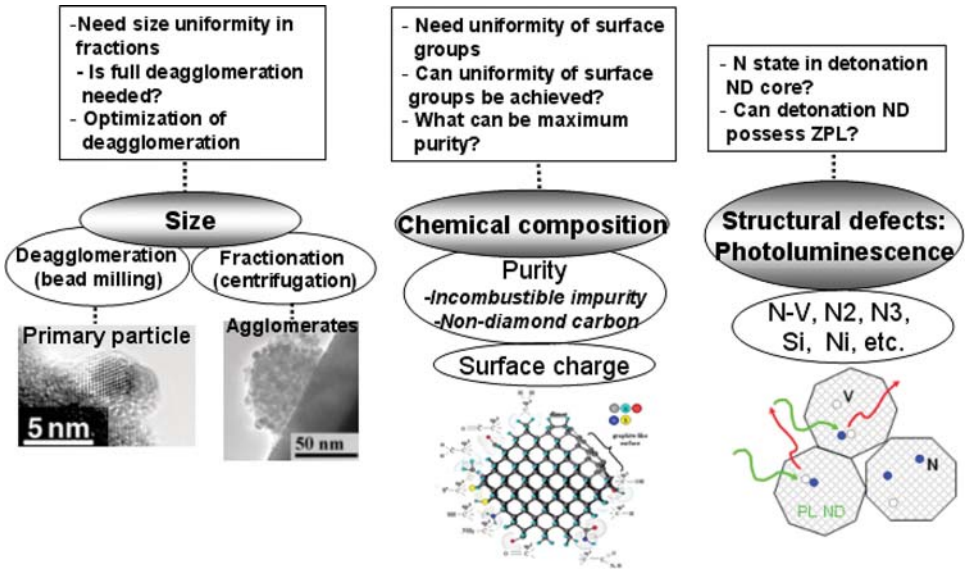

FIG. 10. Schematics of the most important structural aspects of modern DND and key questions and goals that need to be addressed before 'ideal' DND will appear on the market.

of DND should not be an ultimate goal, since a wide variety of applications require particle sizes much larger than the size of the primary particles (Figure 11), such as use of DND for efficient UV protection[161] or formation of photonic structures.[122] Logically, two methodologies should be advanced in parallel: development of slurries of DND primary particles free from contamination and attempts to obtain DND fractions with a narrower size distribution. Importantly, the strategy of optimization of DND deagglomeration shifted from the stage of modification to DND synthesis and purification from the soot.

The key requirements for the chemical composition of the modern DND are purity (absence of incombustible impurities and non-diamond carbon) and uniformity of surface groups (Figure 10). It was demonstrated at the laboratory scale that incombustible impurity content in DND can be extremely low, less than 0.1wt% (Section 3.3.1). Previously, using X-ray diffraction and small angle X-ray scattering, it was postulated that a DND cluster in detonation soot has a complex structure consisting of a diamond core and a shell made up of sp^2-coordinated carbon atoms, implying that the content of non-diamond carbon in DND is relatively high.[162] At the same time, HRTEM images demonstrate that DND particles can be purified to a level where sp^2 carbon on DND surface is visually absent (Figure 5 a,b); this was also demonstrated by Iakubovslii et al.[123] Very low sp^2

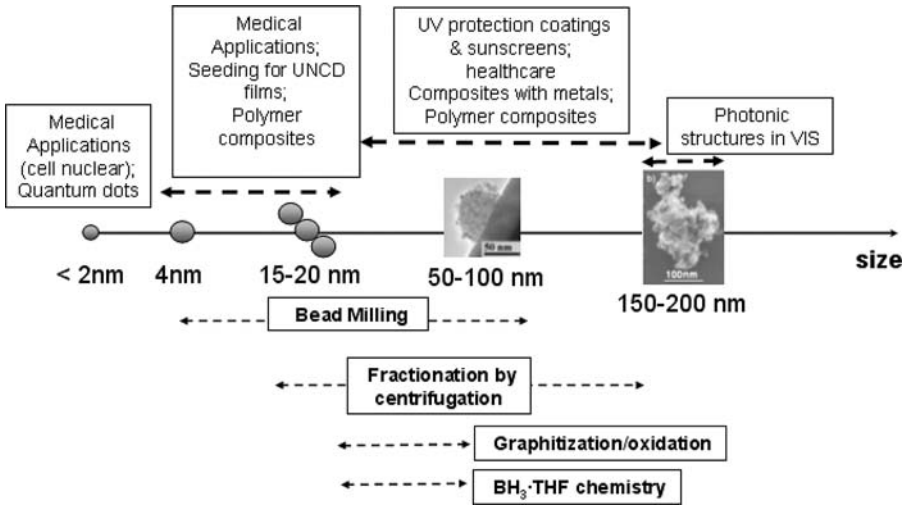

FIG. 11. Schematics of the size ranges of DND primary particles and aggregates in relation to different possible areas of biomedical and healthcare applications as well as current approaches for obtaining DND product within these size ranges.

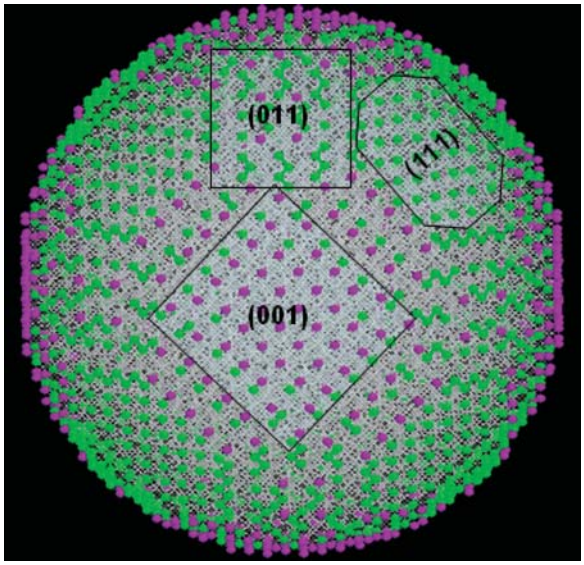

FIG. 12. Illustration of the 4.2 nm diamond particle with a shape, close to spherical. Purple and green colored atoms correspond to 2- and 3-coordinated carbon surface atoms, correspondingly. 1-coordinated atoms had been removed from the surface. Facets with low Miller indexes are denoted.

carbon content in DND heat treated in air was also demonstrated by Osswald et al.[103] These data imply that the high purity DND can be available in the nanodiamond market.

Inhomogeneity of pristine DND surface groups hampers control of the surface functionalization including modification with biologically active moieties.[145] However, the question of whether homogeneity of DND surface functional groups can be achieved might have a negative answer. A nanodiamond particle of 4 to 5 nm in size with a shape, approximating that of sphere has multiple low-index facets, such as (001), (011), and (111) types, exposed at its surface (Figure 12). Surface energies of these facets are very different, involving possible surface reconstructions for (111) and (001) surfaces. Binding energies with different surface groups can be rather different as well.[163] For example, as reported by Kern et al.,[164] the hydrogen adsorption energy (difference between the hydrogenated surface and the stable clean surface) differs by 0.4 eV for C(111) and C(100) diamond surfaces. It might be possible that binding of different surface groups will be energetically preferable for different DND facets. This question requires further atomistic simulation work. Moreover, as pointed out by Chiganova,[155] the hydrophilic-hydrophobic mosaic structure of the surface of DND particles has a strong influence on the aggregation behavior of the low-concentration DND aqueous dispersions. Zeta potential of DND suspensions is another characteristic defined by DND surface composition. Modern commercial DND may have positive or negative charge in solvents (Section 3.3.5), which facilitates applications where the type of the charge is important.

Finally, the internal structure of the DND core and the development of methods for its control also must be addressed (Figure 10). An important aspect of DND bio-related applications is a question of DNDs strong internal photoluminescence, originating particularly from lattice structural defects. It is important to have a well pronounced unambiguous zero phonon line (ZPL) signal in the spectra rather then than just a broad PL emission peak. While a well pronounced ZPL has been observed from N-V centers created by proton irradiation and annealing of HPHT diamond nanoparticles 25 nm in size,[75–77] after similar treatment of DND powder only a broad structureless emission peak was observed.[165] Although it was demonstrated that the content of nitrogen in a DND core is high,[166] nitrogen states in the DND core are far from understood. So far, the ZPL in the photoluminescent spectra of 4 to 5 nm DND has not been observed, to the best of our knowledge, and the development of bright, intrinsically photoluminescent DND remains an important target.

4. BIOMEDICAL PROPERTIES OF ND

The benefits of using nanodiamonds in biomedical applications, including purification, sensing, imaging, and drug delivery, are based upon their desirable chemical, biological, and physical (optical, mechanical, electrical, thermal) properties (Table 2). As discussed in Sections 2.3 and 3.1, NDs can be synthesized at low cost (i.e., detonation synthesis) and in large quantities, while their[55,167] particle and film forms have exhibited high biocompatibility and low toxicity. Although nanodiamonds have recently become commercially available (*Alit*, *Diamond Center*, *Sinta*, *Real Dzerzinsk*, *ITC*, *Nanoblox*, *Aldrich*, and others), there remains a large variety of size distributions and purities with variable uniformity. For example, the small size of primary monocrystalline ND particles (∼4 to 5 nm) can be useful for interactions at the same size-scale as biomolecules. Because the primary core of detonation NDs is sp^3 hybridized carbon, sharing the carbon-based composition with many biocomponents, they are stable and present a biocompatible interface with no generation of reactive oxygen species (ROS).[168] Indeed, ND particles are efficiently internalized at a variety of concentrations by individual cells and through animal systems.

The hope for NDs as biomedical probes is that they can provide maximum therapeutic benefits while avoiding damage to healthy cells or tissues. In medicinal preparations used for oncology, gastroenterology, or dermatology (burns, skin diseases), NDs can be used as additives to intensify the action of other components. Purified NDs have already been shown to normalize blood pressure, detoxify the gastrointestinal system, and remedy cancerous conditions.[169] The significant amount of unpaired electrons on the surface of NDs makes each particle a powerful multi-charged radical donor, able to scavenge free radicals, which accompany many serious illnesses.[169] Another property of NDs that promotes beneficial effects is its large specific surface area (300 to 400 m^2/g) and high affinity for adsorbing proteins, enzymes, and other biological molecules.

TABLE 2
Physicochemical properties of NDs for biomedical applications

Property	Characteristics	Application
Structural	Small size of primary monocrystalline particles (∼4–5 nm)	Unique interactions with bio-compounds on same size-scale
	Availability of variable sizes and narrow size fractions	Diverse applications based on size (UV protection, photonic structures)
	Different forms (i.e., particulate, coating/film, substrate)	Tailorability for different bio environments
	Large specific surface area (300–400 m^2/g)	High affinity/adsorption capacity for binding proteins, enzymes; enterosorbents, purification
	Low porosity/permeability of films	Component of small pore membranes for ultrafiltration or non-porous membrane for extended time storage
	High specific gravity (3.5 g/cm^2)	Dense structure for solid phase support
Chemical	Chemically resistant to degradation/corrosion, pH stability	Implants, coatings, films, substrates for cell growth
	High chemical purity	Biocompatible interface
	Possible sp^2 carbon shells	Adsorption of hydrophobic biomolecules; EM radiation absorption for thermal therapy
	Numerous oxygen containing groups on surface	Hydrophilic, water-dispersible suspensions for further coupling to bio entities/into other matrices
	Ease of surface functionalization (chemical, photochemical, mechanochemical, enzymatic, plasma- and laser assisted methods)	Attachment of drugs and biomolecules; polymer, metal composite materials
	Radiation/Ozone resistance	X-ray, protective coatings and surfaces, detection devices
	Large number of unpaired electrons on the surface	Free radical scavenger/multiple radical donor; electrochemistry
Biological	High biocompatibility, low toxicity	Cell, tissue, organ, and organism studies
	Readily bind bio-active substances (i.e., proteins, DNA, etc.) with retained functionality	Targeted therapeutics/ molecules, labels, hormones, inhibitors, antigens, drugs
	Solid phase carrier	Multiple cell delivery methods including ballistic, transfection
Optical	Photoluminescence: non-photobleaching, nonblinking, originates from N-vacancy defects	Fluorescent probe and imaging tool for biolabeling
	High refractive index, optical transparency	Scattering optical label for live cells, possible UV sunscreen
	Unique Raman spectral signal	Non-destructive detection with living cells
Mechanical	High strength and hardness	Composite additive; possible cell lysis; ballistic delivery to tissues and cells; autoclaving
	Fine abrasive	Homogenization of composites/cosmetics, skin polishing
Electro-chemical	Electrochemical plating with metals	Improves durability, life of medical instruments/implants
	Redox behavior of DND	Chem/biosensors; potential production of ROS
Thermal	Can withstand very high/low temperatures	Sterilization (i.e., autoclave), composite manufacturing, liquid nitrogen storage
Technical	Inexpensive, mass production (i.e., detonation synthesis)	Commercial availability
	Exist naturally in meteorites and laboratory synthesized by diverse techniques	Availability of various quality/purity samples

For example, the extremely large surface area of NDs has a high propensity for binding pathogenic viruses and bacteria, absorbing, removing, or destroying them.[86,169] As super-active sorbents, NDs can also be used to purify solutions of proteins or act as an enterosorbent in the body.

Although the surface of bulk diamond has been considered to be chemically inert, NDs contain numerous oxygen-containing surface functional groups (i.e., -COOH, -OH) that are introduced during purification and modification stages. For example, acid treatment yields high purity samples through the removal of sp^2 carbon atoms and metallic residues while introducing hydrophilicity for aqueous dispersibility. Facile surface functionalization has been accomplished by chemical, photochemical, mechanochemical, enzymatic, plasma and laser assisted methods. The use of strong chemical treatments or extreme temperatures (i.e., autoclaving for sterilization or liquid nitrogen for storage) render the NDs suitable for medical use without degrading the crystalline structure (sp^3 bonding) of the all carbon, chemically inert core.

Due to multiple methods of surface functionalization, NDs can be readily incorporated into other matrices useful for binding biological entities such as proteins, enzymes, hormones, antigens, DNA, or drugs via both electrostatic and covalent interactions, see recent reviews.[51,53,170] The complexity of the ND aggregates as delivery systems is continuing to evolve with the goal of controllable release of immobilized substances, which may occur by specialized enzymes such as lipases, esterases, and proteases. Of critical importance to this mechanism of action, is the retained conformation and functionality of the bound biomolecule and tailorability of the delivery method for targeted therapeutics. As solid phase carriers, NDs can be distributed by multiple methods, including ballistic delivery.[85]

The optical properties of NDs are exceptional due to their transparency in the visible wavelength range, which is greater than glass, and high index of refraction. These characteristics allow both *in vitro* and *in vivo* imaging and detection with or without surface functionalization by multiple methods. As shown in Figure 13, the labeling of cells in culture with NDs can produce intense scattering after illumination with ultrahigh resolution light microscopy.[171] As fluorescent labels, NDs display stable, non-photobleaching, bright internal fluorescence from nitrogen vacancy defects within the crystal lattice.[74,75,172,173] The unique Raman spectral signal for NDs allows non-destructive detection with living cells.[174,175] All of these labeling schemes have shown good biocompatibility with live cells, which is in contrast to other nanoparticle-based imaging labels such as quantum dots that can release toxic substances over time.[172] Of particular interest is the emission in the red region (700 to 900 nm), which may prove useful for *in vivo* imaging, while green emission is also possible with type 1a diamonds containing H3 defects.[176,177] Furthermore, the non-blinking and

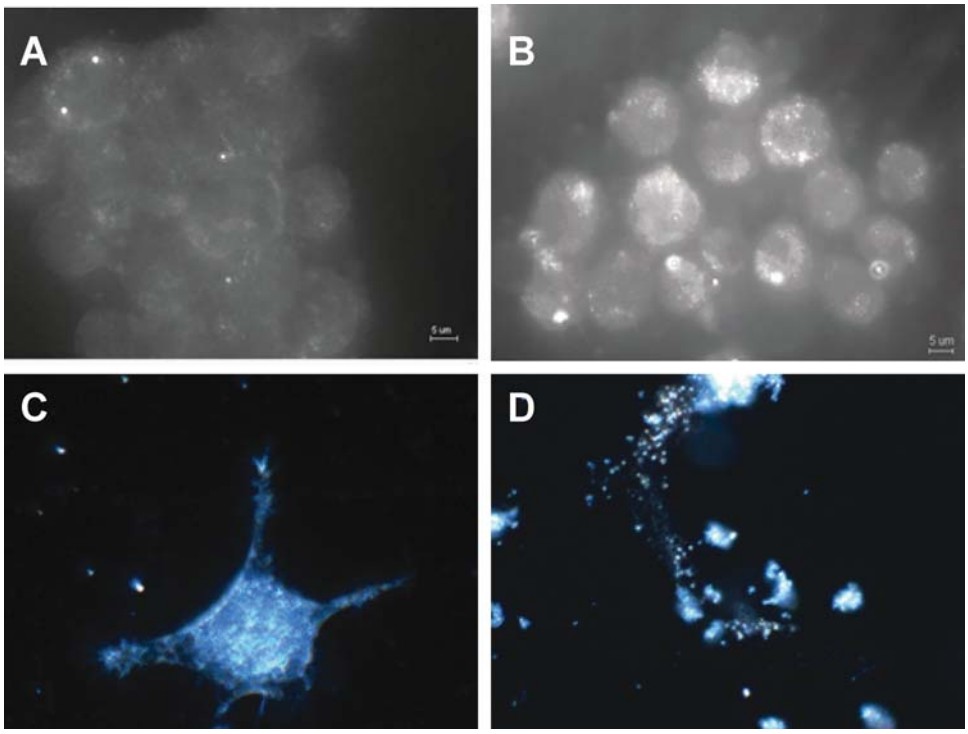

FIG. 13. Ultrahigh resolution light microscopy of neuroblastoma (N2A) cells. (A,C) Control cells and (B,D) Cell incubated with NDs demonstrating the intense light scattering capability. Images were taken with a 60x lens on a phase contrast microscope equipped with the Cytoviva system. Figures used from Schrand.[193]

non-photobleaching characteristics of photoluminescent nanodiamonds are unique among nanoparticles and dyes.

In more traditional materials-related biomedical applications, NDs can be incorporated either into or onto other materials to enhance their properties. For example, ND films improve the wear resistance of metallic implant coatings or medical instruments due to their controllable roughness, high micro-hardness (3000 to 3500 kg/mm^2), low coefficient of friction, lubricating quality, and fatigue durability.[40] ND particles can also be used in the electrochemical plating of metals, enhancing mechanical properties of the metal coatings on medical instruments. The compatibility of ND coatings with bio-fluids while resisting bacterial colonization has possible benefits in circulatory usage in small devices such as MEMS.[19] In polymer matrix composites, NDs can increase the dispersion of other additives while improving polymer strength, hardness, and radiation/ozone resistance. As a fine abrasive, NDs can be used on both hard and soft surfaces for polishing purposes (i.e., ceramics or skin). The low porosity and low permeability of compacted NDs could be used in developing biofiltration and separation devices composed of small pore membranes for ultrafiltration or non-porous membranes for extended time storage under very high or low temperatures. As experiments with NDs continue, it is anticipated that more uses based on their attractive biomedical properties will be discovered.

5. ND OPTICAL LABELS AND THEIR APPLICATIONS

The photoluminescent (PL) properties of nanodiamonds are outstanding; they have high quantum yields, little photobleaching, no blinking characteristics, and long luminescence lifetimes as compared with small-molecule dyes. When these PL properties are coupled with ND's noncytoxic effects and stability (in terms of biological, physical, and chemical), it is certain that NDs will be exploited for applications in biotechnology and medicine.

5.1. Innate PL of NDs

Diamonds possess over 500 different color centers originating from impurity atoms,[178,179] including nitrogen vacancy centers in the crystal lattice.[180] Diamond particles of different origins have been compared based upon their luminescence spectra and it was concluded that natural diamond shows the most pronounced luminescence characteristic peaks (from 400 nm to 500 nm using a 337 nm laser source) as compared with the broad bands seen for synthetic and ultradispersed diamond materials.[181] DND particles have an optical absorption value of 236.4 nm, close to that for natural diamond, which occurs by radiative recombination at the nucleus of the DND diamond cluster. Their characteristic broad-band luminescence (350 to 380 nm) may be due to nitrogen defects from the nitrogen containing explosives.[182] Furthermore, the luminescence bands become somewhat sharper when the DND powder is cooled from 300 K to 100 K. Additionally, surface modification does not affect the photoluminescence spectrum. Natural diamond has distinct peaks at 365 nm and 370 nm; however, related broad bands may be present in the luminescence spectra of DND.[181] It was suggested that the intrinsic structural defects of single crystal diamond are responsible for the broad band PL;[181] however, other interpretations of the featureless PL spectra have been made, including the effect of structural disorder in carbon surface groups that cause radiative recombination resulting from a range of band gap energy levels.[153]

The photoluminescence spectra measured using a pulsed UV laser showed that the relaxation times are different for natural diamond, as well as for DND films and powders in the near-UV to blue spectral region.[183] Ultrafast optical emission measurements of nanodiamond showed processes with decay times of 60 and 350 ps, which were attributed to the large number of defect states found in the large surface-to-volume ratio of diamond crystallite aggregates.[184] The irreversible conversion of nitrogen vacancy color centers (NV^-) to the neutral state (NV^0) has been observed using femtosecond pulsed illumination, in addition to two unstable color centers.[185]

Both HPHT and detonation nanodiamonds exhibit innate PL. Excitation of nanodiamonds by photons may be caused from a single photon-excited PL, multiphoton PL, or PL from emission of carbon plasma induced by laser vaporization of the sp^3 carbons to graphitic sp^2 carbon forms.[186] Synthetic HPHT nanodiamonds exhibit PL intensities that can be detected using confocal microscopy or flow cytometry without requiring high-energy-treatment.[187,188] There also appears to be a size-dependence of the PL spectra of nanodiamond particles, suggesting different kinds of defects/impurities predominantly sustain the luminescence from nanodiamonds of different sizes.[189]

5.2. Enhanced PL of NDs

The nanodiamond PL contrast enhancement has been extensively studied using high-energy irradiation by electron, proton, and helium ions and can be detected with standard microcopy methods. In 1997, Wrachtrup and coworkers irradiated synthetic type Ib nanodiamond powder with a high energy ($\sim$2 MeV) electron beam and then annealed the powder to form NV^- centers.[180] None of the vacancy centers showed either photobleaching or fluorescence spectral changes, as observed by scanning confocal microscopy,[180] thus long-term imaging was possible. More recently, studies with continuous-wave laser excitation at 514.4 nm also showed photostable emission from a zero-phonon line at 575 nm, after electron beam irradiation, and it was inferred that the PL originates from a neutral NV^0 defect center.[172] Electron beam irradiation for this type of nanodiamond appears to be noncytoxic to human HeLa cells,[96] thus promoting their *in vivo* applications, such as imaging.

When synthetic type Ia ND powder is irradiated with protons and annealed, similarly red fluorescent particles are observed. A 3 MeV proton beam source with a flux of $\sim 10^{14}$ ions/cm^2 produces a zero phonon line at 638 nm with an intensity that increases by two orders of magnitude, as compared with the untreated, annealed nanodiamond (Figure 14). Similar to

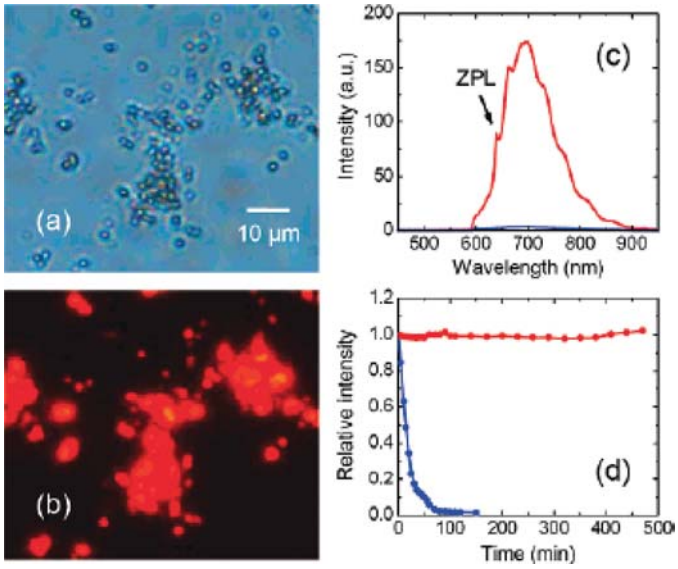

FIG. 14. Synthetic type Ib nanodiamond can be made highly fluorescent by irradiating the particles with high energy proton beams. Bright field (a) and epifluorescence (b) images of cells after uptake of fluorescent NDs. PL spectra taken under illumination with 510 to 560 nm and captured using a long-pass filter (580 nm) (c). Irradiated nanodiamonds (*red*) show greater photostability compared to fluorescent polystyrene nanospheres (*blue*) under the same conditions (d). (Reprinted from Yu et al.[75] with permission.)

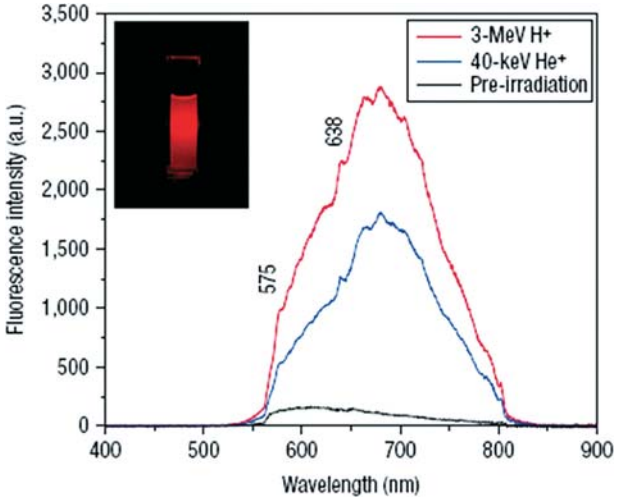

FIG. 15. Fluorescence spectra of the synthetic type Ib nanodiamonds irradiated with helium ions at a dose $\sim 1 \times 10^{13}$ ions cm^{-2} (*blue*) and protons at a dose $\sim 1 \times 10^{16}$ H^+ cm^{-2} (*red*). Spectral features of PL ND obtained under these two drastically different bombardment conditions are essentially the same, except relatively small ($\sim$30%) difference in intensity. (Reprinted from Chang et al.[167] with permission.)

electron-beam irradiation, no photobleaching is observed after 8 hours of continuous excitation with a mercury lamp. These fluorescent nanodiamonds appear to be noncytotoxic to human kidney cells[75] as well. Further investigation of the particles showed two ZPLs (576 nm for the NV^0 defect and 638 nm to the triplet transition of the NV^- center) and no fluorescence blinking within 1 ms (Figure 14). It was also found that the photostability of the particles is size-dependent for 35 nm and 100 nm particles. The fluorescence lifetime of 17 ns is significantly longer than for dye molecules.[76]

It is possible to evaluate the photophysical characteristics of irradiated nanodiamonds and to compare the effects of electron and proton irradiation on nitrogen vacancy centers using an optical set-up that allows for the collection of two-photon absorption and emission spectra. Because the number of defect centers is expected to be 10 for a 10 nm particle, nanodiamonds should exhibit similar brightness as compared to quantum dots. In fact, it was measured that proton irradiation and annealing has an enhancement factor of over four orders of magnitude compared with untreated nanodiamonds, producing up to 100 photostable N-V^- centers for a particle size of 35 nm. The authors suggest that specialized van der Graaff accelerators having a 3 MeV electron source are not required, and therefore the mass production of PL nanodiamonds is feasible. The number of vacancy centers produced by proton irradiation is 100 times greater than that for electron irradiation, however the penetration depth is significantly diminished with heavier protons. In contrast to the one photon emission spectra, two photon emission spectrums show larger ZPL peak intensities attributed to NV^0 defects.[190]

Two photon fluorescence imaging was shown to be practical for imaging PL NDs in live cells due to an increased emission signal by eliminating autofluorescence and background-light-scattering effects of the particle. Furthermore, it was also shown that irradiation of nanodiamonds using He^+ ions can effectively increase nitrogen vacancy centers to enhance photoluminescence of the particles (Figure 15). The photoemission spectra and non-photobleaching characteristics for particles treated with He^+ and H^+ ions were similar (Figure 15). Particles as small as 35 nm were imaged inside mammalian cells using photoluminescent NDs, which were separated by centrifugal fractionation after irradiation. Importantly, employing helium irradiation of synthetic diamond nanocrystallites, bright fluorescent nanodiamonds can be produced in large quantities.[167]

Besides nitrogen vacancy centers, the development of other defect centers would broaden the utility of diamond particles with varied PL colors and lifetimes. It has been shown that different color centers can be created by irradiating diamond with different types of ion beams. With the control of dose and location of ions, nitrogen vacancy centers were "written" on type Ib diamonds with a spatial resolution below 180 nm using a focused gallium ion beam.[191] In a similar manner, Si ions were implanted in type IIa diamond, which produced a sharp ZPL at 738 nm with a short lifetime of < 4 ns.[192] In a different

study, applying proton irradiation to a PDMS polymer (with -Si-O- backbone) containing embedded DNDs, a strong dose-dependent photoluminescence was observed. It was suggested that this photoluminescence may be attributed to the defects formed at the interface of DND/siloxane matrix.[165]

5.3. Fluorescently Labeled NDs

The development of nanodiamond optical labels has tremendous potential in many areas of biomedicine and biotechnology, and it is for this reason that additional fluorescent labeling methods are being explored. One of these methods is labeling nanodiamonds directly with fluorophore tags. In this way, it is possible to fabricate the desired spectral property by choosing an appropriate dye molecule. It was demonstrated by Huang and coworkers that Alexa Fluor dye could be conjugated directly to poly-L-lysine, which was physisorbed onto nanodiamonds.[82] In this way, chemical functionalization of nanodiamonds allows for high loading efficiency of dyes to the surface of the particle. This experimental method was used for the localization of nanodiamond using biolistic delivery methods.[85] In another study, it was shown that dyes can be directly conjugated with an amide bond using aminated nanodiamond and the NHS ester of TAMRA.[146] The TAMRA-ND conjugate was useful for fluorescent cellular tracing of nanodiamonds in cytotoxicity studies; the conjugate was chemically stable, being viewed over a 24-hour period, and was noncytotoxic while the particle localized in the cytoplasm after being transiently located in the lysosome region—it did not penetrate the cell nucleus.[193,194] For a larger scale reaction, FITC may be conjugated to ND using the acid chloride derivative of ND, see Figure 16.[195] Interestingly, it was recently reported that the chemical modification of DND surfaces with octadecylamine resulted in a highly fluorescent material.[113]

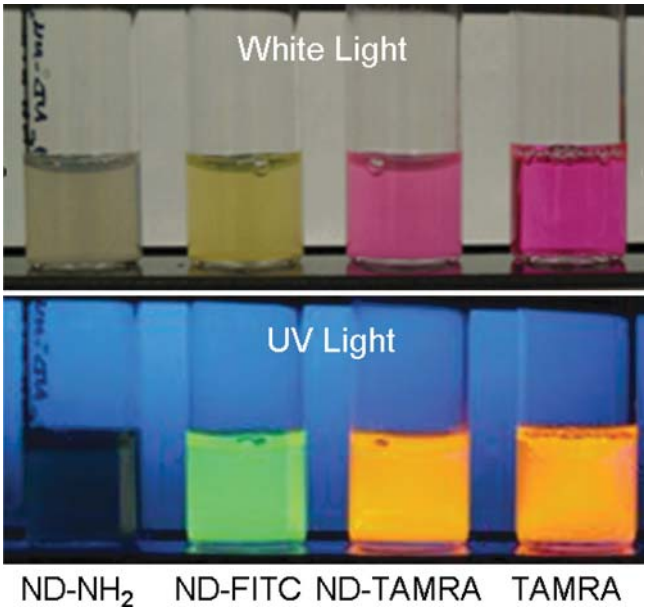

FIG. 16. Photograph of vials containing colloidal suspensions of ND and ND-dye conjugates, whereby the FITC and TAMRA are chemically attached to the surface of the nanoparticle. The advantage of ND-dye conjugates is their intense, tunable photoluminescence properties. Notice that the photoluminescence color of TAMRA bound and unbound is unchanged.

5.4. Nonfluorescent Optical Labels

Unlike other labels, such as gold or silver plasmon resonant scattering particles or luminescent optical labels (such as quantum dots), nanodiamonds are noncytotoxic, immune to their environment, have a large separation between the excitation and emission bands, and are photostable.[46,171,196] In addition to PL detection, NDs are good scattering optical labels. Because of their high index of refraction, a 55 nm diamond particle will appear 300 times brighter than a cellular organelle of the same size.[196] Using up to 1,000 nanodiamond particles loaded per cell, it was possible to exploit the Raleigh scattering property of NDs to visualize the particles by contrast enhancement microscopy, which is useful for larger (∼40 nm) particles,[197] see (Figure 17). The optical detection by scattering and photoluminescence of NDs, for which these images showed almost complete overlay, were both exploited to visualize the uptake of NDs into human cells.[96]

Raman spectroscopy in the 1332 cm^{-1} absorption region has also been used to trace these nanoparticles within cells. The Raman signal was mapped and showed that lysozyme-attached nanodiamond penetrated *E. coli* cells, unlike uncoated nanodiamonds.[175] In addition, the conjugation of small molecules to the ND surface does not disturb the Raman mapping of the particles inside cells, see Figure 18. Raman measurement is advantageous because it does not require physical or chemical treatment of nanodiamonds. Thus, the *in vivo* effects of the nanodiamond particle itself, as compared with ND treated with high energy irradiation, may be determined.[174,175,198]

6. BIOANALYTICAL APPLICATIONS

Recent advances in the chemical manipulation of nanodiamonds have shown the practicality and uniqueness of NDs as compared with other well studied nanoparticles. For example, NDs are chemically and physically stable, but their surface can be chemically modified. ND optical properties include transparency in the visible wavelength range and have photoluminescence with nonblinking and no photobleaching properties. NDs can now be fractionated into stable colloidal solutions of narrow sizes, while the smallest primary DND particle of 5 nm has recently been made available.[129] Although the use of NDs in biotechnology is in its infancy, recent ND studies highlight the utility of these particles for bioanalytical applications.

6.1. ND Binding Capability

6.1.1. Nonspecific

There are many reported biotechnical uses of nanodiamonds. Early research shows that DND nanoparticles are capable of

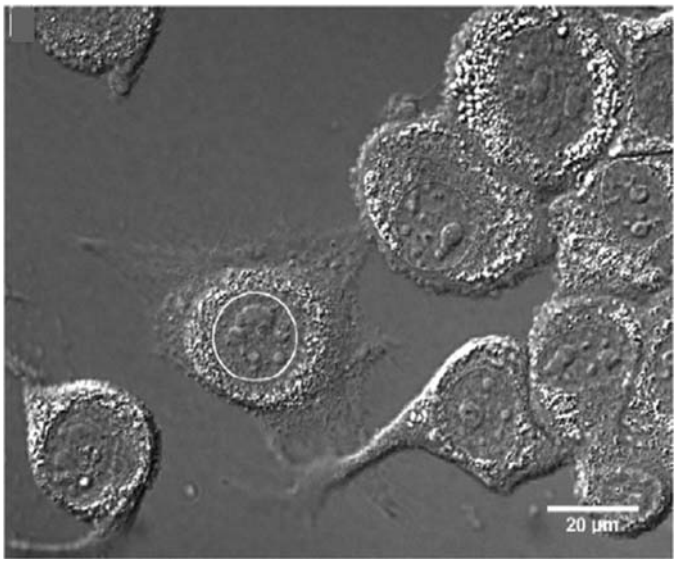

FIG. 17. Nanodiamonds may be visualized by differential interference contrast microscopy due to their high refractive index that causes strong elastic scattering, as seen using live 293T cells that were transfected with nanodiamonds using liposomes. (Reprinted from Smith et al.[197] with permission.)

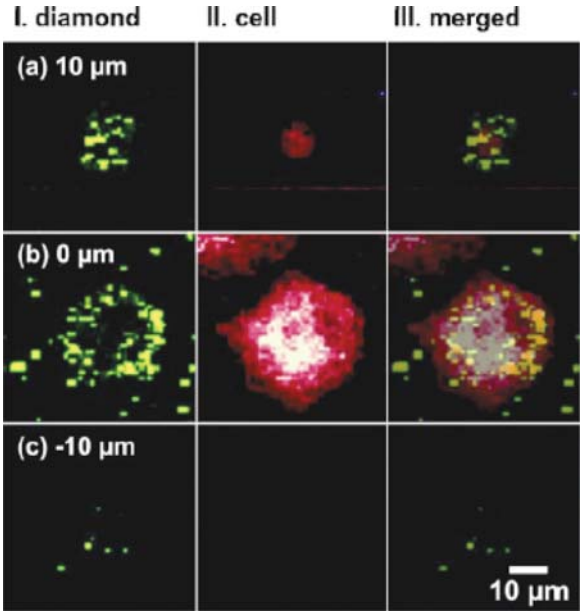

FIG. 18. Confocal Raman mapping in the z-direction for a A549 cell using 1320 to 1340 cm^{-1} and 1432 to 1472 cm^{-1} signal collected for the nanodiamond and cell, correspondingly. (Reprinted from Cheng et al.[174] with permission.)

adsorbing recombinant apoobelin and luciferase proteins.[81] It was suggested that the use of chromatographic methods for isolating proteins could be side-stepped in favor of the more rapid physisorption-based collection of proteins. For this application, the thermodynamics of lysozyme binding was compared for DND and nanosilica using Langmuir isotherms. DNDs have a binding capacity that is ten times greater as compared to nanosilica, which may be due to the five times greater surface area of porous nanodiamond aggregates.[199] In addition to the physisorption of proteins, DNDs can be used to adsorb small molecules and may replace traditional alumina silicate enterosorbants for the removal of aflotoxin during the feeding of corn to livestock.[86,87]

6.1.2. Specific

A more complex preparation of the ND surface has been accomplished through a combination of physisorption and chemical conjugation. For example, positively charged poly-L-lysine was physisorbed onto the negatively charged nanodiamond surface.[82] Then the amines from poly-L-lysine were used for subsequent reactions with succinimidyl conjugate dyes and proteins, resulting in novel probes for cellular targeting see (Figure 19). Free sulfhydryl groups on cytochrome c were also chemically linked to the sulfhydryl group of one end of a heterobifunctional linker, while the opposite end containing a free succinimidyl group was bound to the amine of poly-L-lysine.[82] In this study, UV-VIS, FTIR, and IR spectroscopy were used to characterize protein binding. It was estimated that a spherical 5 nm DND may carry up to two molecules of cytochrome c.[82]

Methods for directly attaching small molecules and biomolecules onto diamond films are now being translated for the functionalization of DND nanoparticle surfaces. One of the first reports of direct ND surface conjugation was the synthesis of a peptide-ND conjugate.[145] Chemical attachment to ND surfaces affords greater robustness of the biomolecular tag, since it does not rely on electrostatic binding[145] (see Figure 20). It is also possible to attach streptavidin protein onto the DND surface using chemically modified, biotinylated DNDs.[96,97,146] Thus, by chemically attaching a protein-specific probe on the DND surface, protein-specific selection can be made. In this way, it is possible to select a protein or other biomolecular target of interest from a biological matrix. Furthermore, the collection of the biomolecule can be completed using electrophoresis. In this way, it is possible to analytically quantitate the amount of protein in a biological sample. This method of collection and capture was demonstrated using the biotinylated nanodiamond conjugate probe (ND-biotin) that was used to bind streptavidin from solution and was subsequently collected by electrophoresis,[146] see Figure 21. For this method of collection (see Figure 22), it is important to use ND probes that form stable colloidal solutions.[146] NDs can also be linked to form ND-DNA probes for the collection of the complementary DNA target[195] (see Figure 23), which may be used in the future to construct ND-based DNA microarrays (see Section 9).

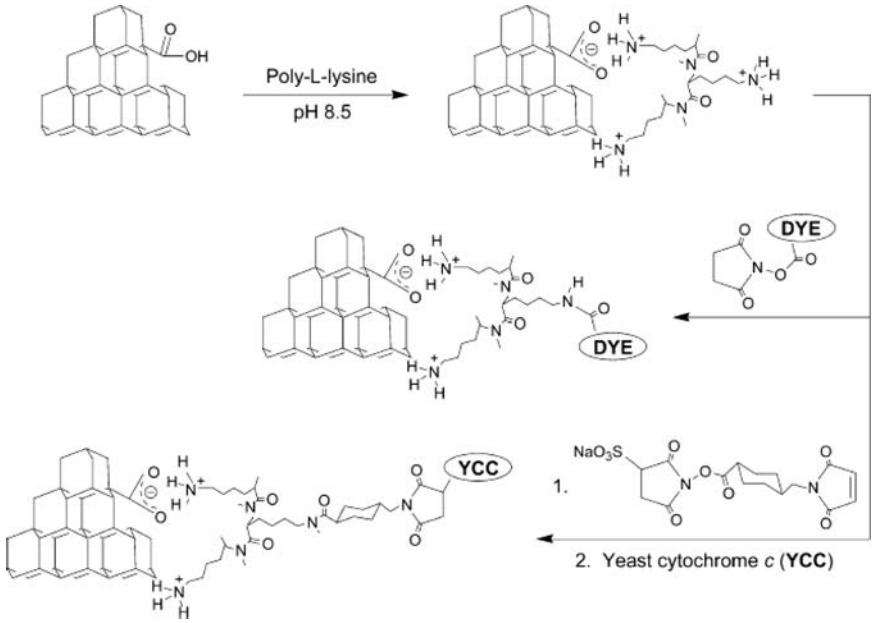

FIG. 19. A schematic representation for the combination of indirect-direct conjugation of a dye and protein to ND surface. Poly-L-lysine is physisorbed onto the ND surface by charge-charge interactions, thus providing amine surface groups on the ND for conjugation to either a NHS-dye or -protein conjugate. (Reprinted from Huang et al.[82] with permission.)

6.1.3. Analytical Methods

Advances in biotechnology research are being made using the unique properties of DNDs as analytical substrates. One well studied area is protein identification by matrix assisted time of flight mass spectrometry (MALDI-TOF-MS), whereby NDs are used as substrates for simply concentrating biomolecules by physisorption. The detection limit of proteins was improved by two orders of magnitude.[83] For poly-L-lysine coated DNDs, it is also possible to collect and separate DNA oligonucleotides from proteins.[84] In addition, enzymatic digestion has been used for the DNA attached to the ND surface. In 2008, Yeap et al. chemically functionalized ND with a small molecule through a silane linker to specifically bind glycoproteins for separation in a protein matrix and identified the attachment of glycoproteins to the ND by the same MALDI-TOF-MS method.[200] NDs are well suited for biological samples due to their high collection affinity of biomolecules, hydrophilicity, and high surface area to volume ratio. Also NDs are compatible with the MALDI matrix, allowing facile blending, and are optically transparent to the ionizing laser source because of their UV transparency and nanometer size, which results in less interference compared with microbeads.[83,84,200] These MALDI-TOF-MS studies pave the way for future proteomic and genetic assay development using DNDs. Using a different analytical method, but exploiting

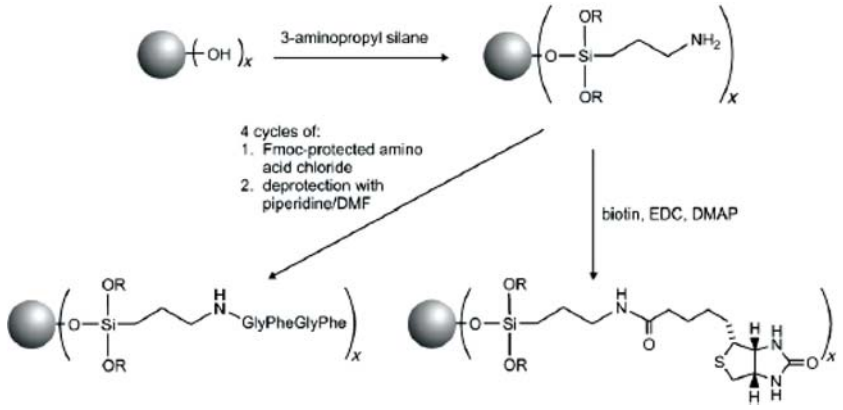

FIG. 20. Schematics for the direct reaction of reduced nanodiamond particles that are functionalized with silanes for modification of a ND-polypeptide and ND-biotin conjugate. (Reprinted from Krueger[53] with permission.)

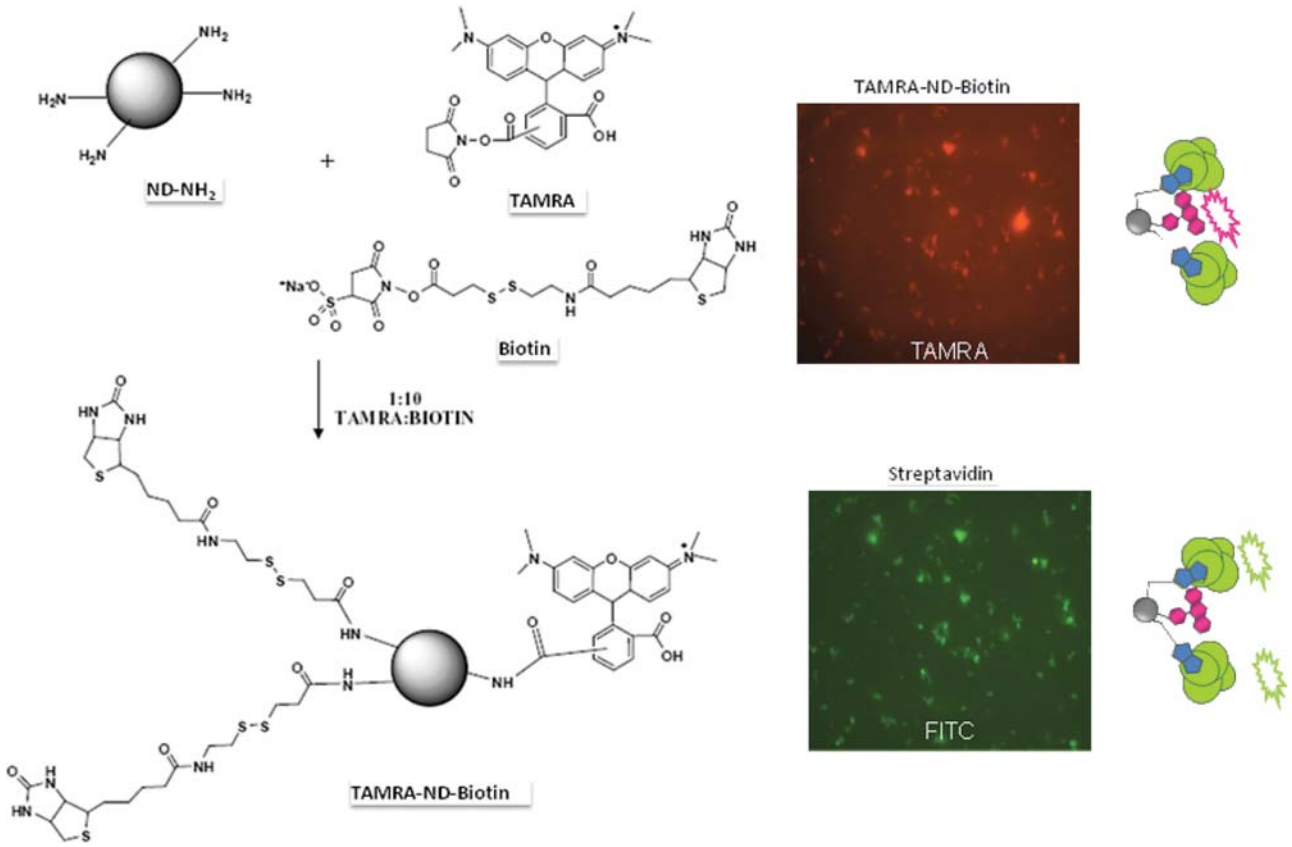

FIG. 21. A schematic representation of aminated ND surface coupled with the conjugates of TAMRA-NHS dye and biotin-NHS, making a visible nanodiamond protein-probe complex. By fluorescence microscopy (1,000x magnification), the red fluorescence emission of TAMRA localizes ND particles (*top*), while the green fluorescence emission of FITC identifies ND-bound streptavidin (*bottom*). (Adapted from Hens et al.[146])

the high binding capacity of DNDs for proteins, high pressure liquid chromatography (HPLC) was capable of separating luciferase protein from other contaminants based upon the specific adsorption affinity of this protein to the DND matrix.[201] This biotechnological advance was based upon early studies of the binding of this protein to DNDs.[81] HPLC using sintered nanodiamonds was also recently shown to be capable of separating small molecules.[202]

6.1.4. Biochips

ND particles seem an obvious choice as a materials platform due to their high biocompatibility and affinity for both small and large molecules. This is no surprise, considering the success of diamond films[203] as biocompatible materials[63] in electrochemical sensors[204] and biochips.[62] Further, a recent study shows that diamond powders, grown by two different CVD methods and detonation nanodiamond, deposited on substrates affect cells on the molecular level in terms of gene expression through stress (oxidative, cellular, genotoxic) inhibition leading to anticarcinogenic and antioxidant activities.[205] Along these lines, ND-based biochips may be fabricated in a number of ways, for example, by using electrophoresis, by seeding NDs, or through direct covalent attachment. In 2004, Puzyr et al. demonstrated that luminescent ND biochips could be fabricated using bacterial luciferase protein.[206] More recently, UNCD films were found to be more biocompatible than platinum or silicon films, allowing for greater adhesion, proliferation, and growth, using different cell lines, including human cells.[62] Additionally, surface properties such as hydrophobicity or hydrophilicity, crystal structural peculiarities, roughness, and the ability of proteins to tightly bind NCD substrates by mere physisorption appear to influence cell growth as well.[207,208] For example, human osteoblast cells (SAOS-2) cultured on O-terminated NCD films displayed increased metabolic activity as a function of surface roughness.[208] Therefore, tailoring the surface properties of NCD films is expected to provide a greater level of sophistication for devices, 3-D tissue scaffolds, diagnostic tools, and therapeutics.

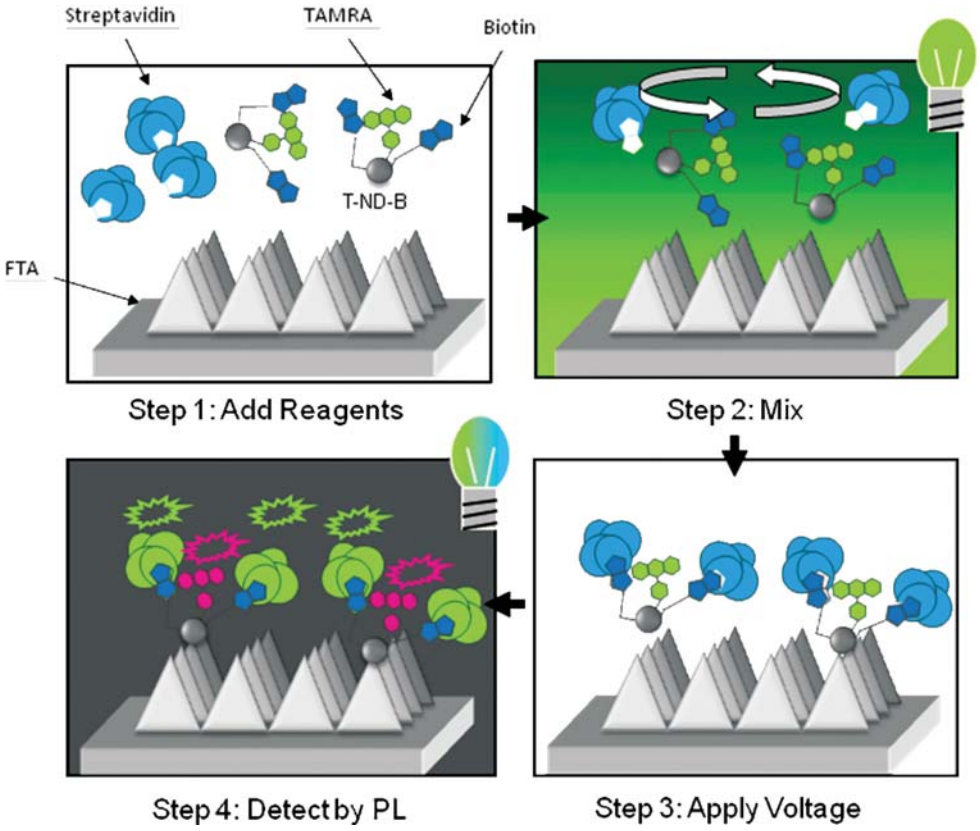

FIG. 22. A schematic representation for the ND capture-probe process. After the addition of reagents (Step 1) the solution is mixed (Step 2) to capture targets onto the nanodiamond-probe complex. The solution may be mixed in a remote fashion by using a visible light source for a closed system such as a microfluidic platform. Next, the targets are collected by electrophoresis (Step 3) on a conductive surface from which the capture efficiency of targets can be identified by fluorescence emission (Step 4). (Adapted from Hens et al.[146])

6.2. Cellular Applications

The uptake and effects of NDs on cells has been investigated for biotechnological applications, such as the delivery of physisorbed DNA vectors for transformation experiments. It has shown that DNDs can be traced within cells for bare DNDs,[197] TAMRA fluorophore conjugated DNDs,[193,194] as well as with enhanced photoluminescent DNDs[76] (see Section 5). The biolistic delivery method was successful for forcibly delivering physisorbed DNA plasmid vectors and small molecules attached to DND particles into cells. In this study, it was possible to transfect *E. coli* and yeast cells for cellular expression analysis with DNA-coated Poly-L-lysine DNDs. In addition, small molecules coated onto DNDs were capable of controlling fruit ripening, while the particles were traced using Alexa Fluor 488 dye coated DNDs.[85]

6.3. Manipulation of ND

6.3.1. Electrodeposition of ND

Two electrically induced phenomena can be used to manipulate dielectric and/or charged nanoparticles in suspension: dielectrophoresis and electrophoresis.[209,210] In dielectrophoresis, a dielectric particle is suspended in a spatially *nonuniform* electric field; the applied field induces a dipole in the particle. Due to the presence of a field gradient, electric forces acting on the charges induced on each side of the dipole are not equal, resulting in a net force and particle movement. The dielectrophoretic particle movement depends on a particle volume, relative complex permittivities of the media and a particle, electric field gradient and angular frequency of the applied electric field. Overall particle charge does not affect its dielectrophoretic mobility.

On the other hand, in electrophoresis, electrically charged particles in suspension move in an applied electric field. The electrophoretic mobility is directly proportional to the magnitude of the charge on the particle, and is inversely proportional to the size of the particle. In practice, quite often both phenomena, electrophoresis and dielectrophoresis, take place simultaneously. Electromanipulation of nanoparticles plays an important role in the concentration of colloids from solution, nanoparticle separation, transport, and formation of coatings

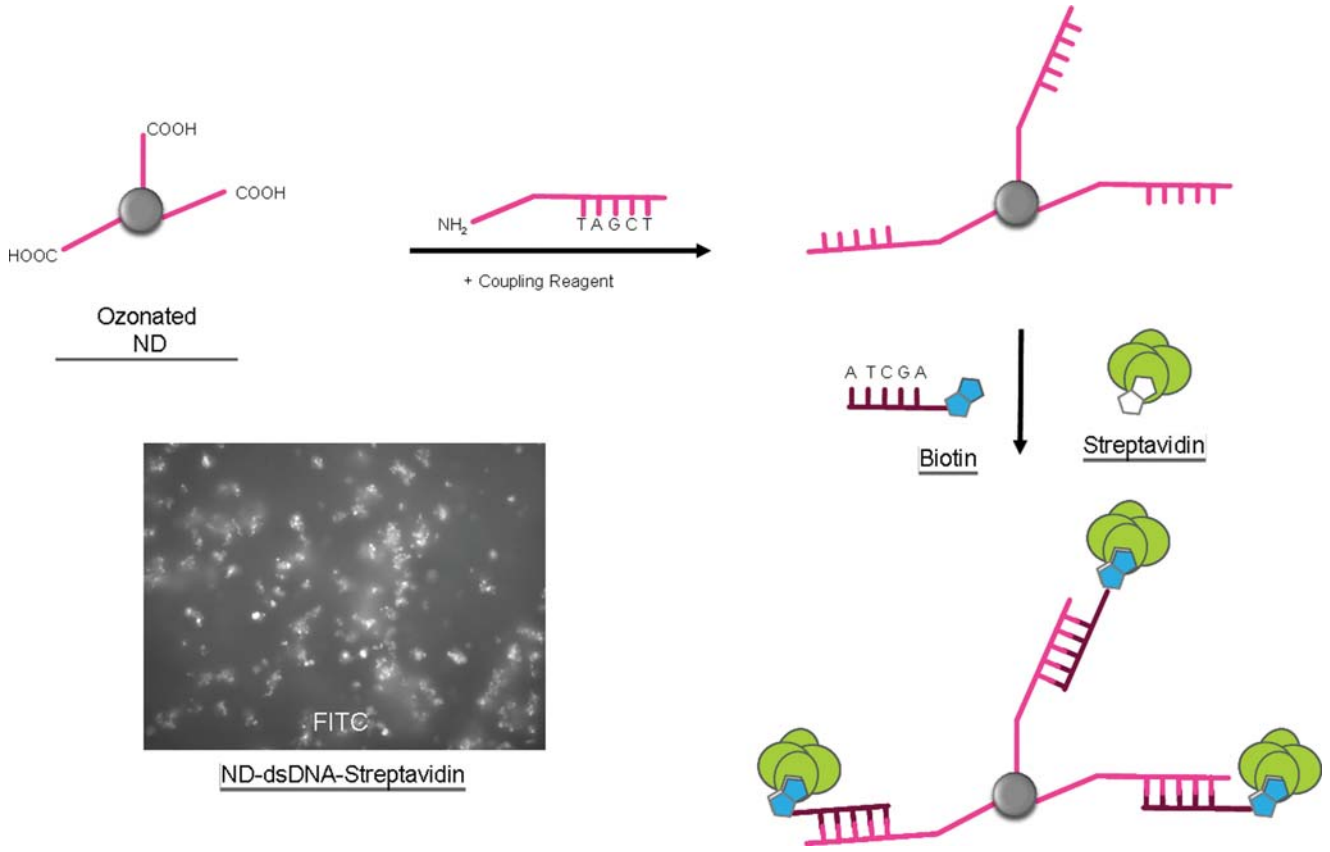

FIG. 23. Schematic for the reactivity of carboxylated nanodiamond with an aminated DNA oligomer strand using the coupling reagent EDC. Once the conjugate ND-ssDNA probe is constructed, hybridization to its complementary DNA strand may be detected through the binding of streptavidin to the biotinylated DNA target moiety (photo taken with fluorescence microscope at 1000× magnification).

on a substrate, including the formation of micropatterns in biosensors.[209,210]

Electromanipulation of DND has been demonstrated to be useful in a variety of applications. Combined dielectrophoretic/electrophoretic deposition of DND has been used by Alimova et al. to coat microscopic silicon tips with nanodiamond for cold cathode applications.[211] Electrophoretic seeding of substrates with submicrometer diamond particles for the growth of diamond films was also explored.[212] Currently, however, ultrasonic seeding of substrates using DND particles is the most popular approach.[213,214] Affoune and coworkers[215] performed electrophoretic deposition of nanodiamond particles in order to convert them to nanographite by heat treatment for the studies of nanographite properties. They also investigated the potentials, solution conditions, and the structure of electrodeposited nanodiamonds and were able to deposit ND seeds without agglomeration. The commercial DND particles used by this group were negatively charged. To collect particles at the cathode, H^+ ions were generated in situ by a reaction between iodine and acetone, resulting in a positive surface charge of the solvation shell formed by H^+ ions on DND.[211,215] As was shown in Section 3.3.5, modern commercial DND are available with both positive and negative zeta potential, facilitating both cathodic and anodic electrodeposition of DND. The DND coatings on electrodes for the detection of small molecules has been formed by electrophoretic deposition of DND particles by Riveros et al.[216]

Application of detonation nanodiamonds (NDs) as probes for protein capture and electrophoretic collection was explored by Hens et al.[146] The field strength and time dependence for the electrophoretic collection of nanodiamonds on a silicon substrate were studied. It was found that the substrate becomes saturated quickly (see Figure 24) showing a concomitant drop in current from the electrode (Figure 24e). This method was used for the collection of target-bound NDs, whereby the target streptavidin was collected using a ND-biotin probe, by applying a potential across an electrically conductive field tip array (FTA) substrate (Figure 25). Because the ND was labeled with both a fluorophore and biotin, it was possible to see that the protein was located on the nanodiamond probe.[146]

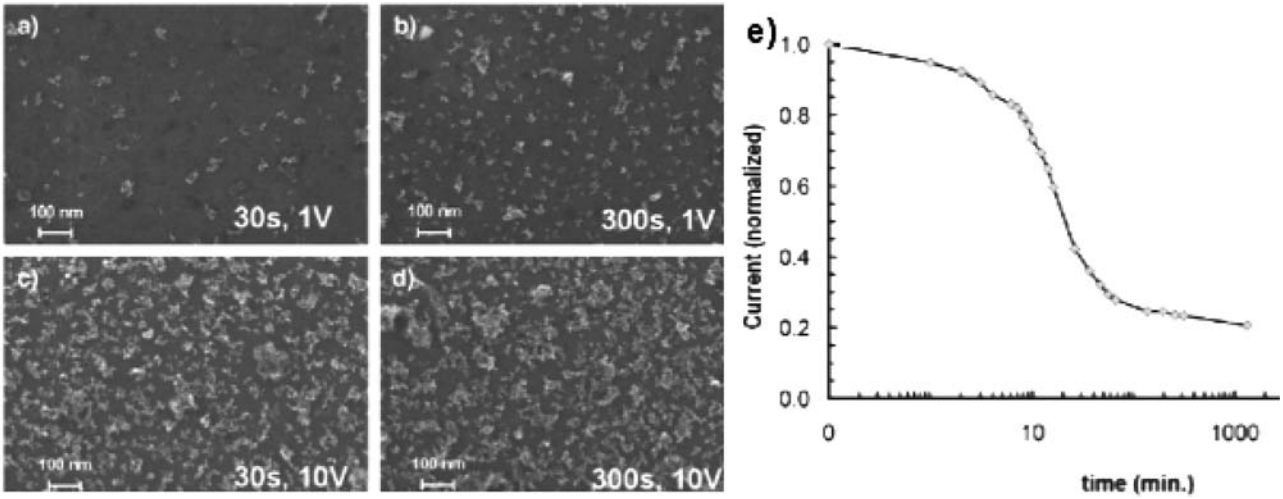

FIG. 24. Photographs are shown for the time and potential dependence of ND collection on the surface of a conductive Si substrate (a-d). After a certain threshold of ND adsoprtion is reached, the electrode becomes more insulating as can be seen from the dependence of electrode current with time (e). (Adapted from Hens et al.[146])

Electrophoretic and dielectrophoretic manipulation of nanodiamond particles opens up a wide range of potential applications for trapping, manipulation, and separation of biomolecules. Due to the possible high surface charge of DND and relatively high dielectric constant, DND movement in the electric field can be controlled with high precision by properly designing the electrode configurations.[209]

6.3.2. ND Electrode Properties

Microcrystalline and nanocrystalline doped diamond films are important electrode materials (see two most recent reviews).[217,218] Boron is by far the most widely used dopant to produce conducting diamond electrodes. Microcrystalline boron-doped HPHT diamond particles immobilized into a substrate are also being used in electrode applications.[217] The most striking feature of diamond electrodes is their very high overpotential for both oxygen and hydrogen evolution, which leads to the widest potential window (~3.5 V) currently known for aqueous electrolytes. Diamond electrodes are also distinguished from conventional electrode materials by their very low capacitance (high signal-to-noise ratio) and by the absence of surface oxide formation and reduction reactions which are present in conventional metal or metal oxide electrode materials between oxygen and hydrogen evolution.[217,218] Because of their unique electrochemical properties, doped diamond electrodes can be used for numerous applications, including the destruction of organic and inorganic pollutants in water, water disinfection, inorganic and organic electrosynthesis, electroanalytical applications, electrochemical energy technology, and

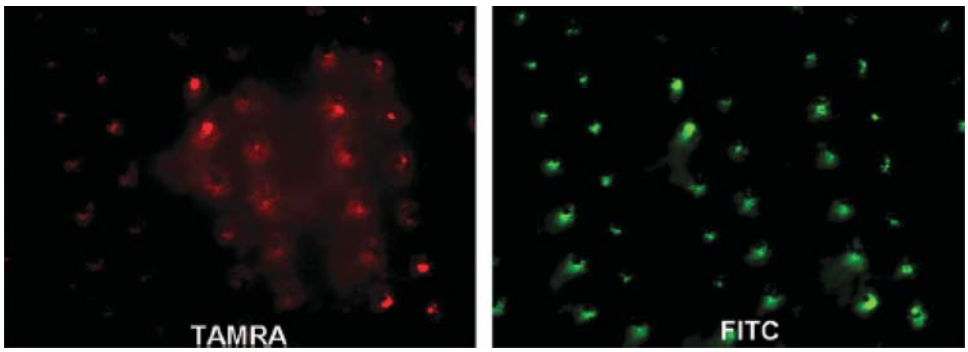

FIG. 25. Photographs of TAMRA-ND-biotin with TAMRA illumination and with FITC-streptavidin conjugate bound. The ND probe was collected on the tips of a conductive field tip array (FTA) by applying a low potential. Notice the similar intensity of TAMRA and FITC emission intensity across the tips of the FTA. Images were taken with a fluorescence microscope at 1000x magnification. (Reprinted from Hens et al.[146])

bioelectrochemical applications.[217,218] Examples of bioelectrochemical applications of diamond electrodes are neurodynamic studies in an animal model[219] and biosensors.[217,220,221]

As a seed material for doped CVD diamond growth, DND particles play an important role for the construction of electrochemical sensors.[213,214] However, in addition to this 'passive' role of DND in development of electrochemical and bio-sensors, DND are considered as an 'active' component for coating electrodes for the detection of small molecules.[216,222,223] While DND possesses an electrically insulating core, surface atoms constituting 15at.% can play important role in charge transfer in electrode-immobilized DND. Novoselova et al.[224] fabricated electrodes from DND by sintering the powder into the compacts at high temperature and pressure. Using different redox probes, the authors observed reduction and oxidation peaks for the redox couple, as well as other peaks (for the $Ce^{3+/4+}$ couple) that could only be attributed to the ND itself.[224] Zhao et al. incorporated DND powder into an electrochemical glucose biosensor based on the covalent immobilization of glucose oxidase on DND.[222] Zang et al. also fabricated an electrode using DND powder and reported electroactivity of DND in ferricyanide solution. The authors attributed DND conductivity to sp^2 groups on the surface of the particles.[225] Holt et al. confirmed that 5 nm undoped DND is indeed electroactive, but argued that it can not be considered conducting. Holt formed a thin layer of ND by drop-coating onto a gold electrode. A significant enhancement in the redox response of ferricyanide and oxygen reduction was observed as compared with the unmodified gold electrode. The oxidation of the powder by heating in air resulted in an increase in its redox activity, while hydrogenation of DND inhibited the electrochemical behavior. Differential pulse voltammetry of electrode-immobilized DND layers in the absence of solution redox species revealed oxidation and reduction peaks that could be attributed to direct electron transfer (ET) reactions of the DND particles themselves. A mechanism was suggested explaining DND inner electroactivity. While DND consists of an insulating sp^3 diamond core, DND surface contains unsaturated carbon bonds as well as double bonds with other elements (for example, in carbonyl groups). Due to presence of unsaturated active bonds at the DND surface, ET is taking place between these essentially insulating particles and a redox species in solution or an underlying electrode. Holt et al. hypothesized that a reversible reduction of the DND may occur via electron injection into the surface states at well defined reduction potentials so that the DND particles act as a source and sink of electrons for the promotion of solution redox reactions.[223] The observed redox behavior of DND raises important questions that needs further investigation on types of reactions that can take place over potential ranges applicable to the cellular environment.

Nanodiamonds have been shown to be biocompatible substrates,[63] as compared with silica and glass, thus it is highly feasible that these nanoparticles will be used in electrochemical detection methods in the near future. The incorporation of DND to electrodes may also enhance signals for detection of bound substrates. There are numerous reasons suggesting that DNDs may one day advance current redox reactions, such as those used for the detection of cancerous genes through the identification of genetic mismatches.[226]

6.3.3. Interaction of NDs with Electromagnetic Radiation

The illumination of ND suspensions with a light beam leads to active directional movement of the NDs. When realized in a microliter volumes, rigorous turbulent flows are formed resulting in efficient mixing of NDs with other components dispersed in the suspension. A possible explanation for this phenomena could be a process called thermophoresis, or thermodiffusion, the effect of a temperature gradient on mixtures of particles. During the illumination of nanoparticles, which can interact with EM radiation and acquire local heating, thermal gradients can arise at the boundary of the illuminated and non-illuminated nanoparticles causing particle movement. This phenomenon may be applied for efficient mixing of ND conjugates for target capture in solution, which is especially critical in microfluidic platforms since laminar flow prevents mixing. Presently, mixing in microfluidics is achieved by texturizing the fluid channels; however, using light exposure of NDs in solution platforms may provide a simplified means of remotely controlling the mixing location and duration without modifying channel architectures. Researchers from ITC have been able to mix NDs with other particles (carbon nanotubes and carbon onions) using light from colored filters with a Xenon lamp on a fluorescence microscope.

The utility of NDs used purely as mixing reagents would require that these particles be coated in an inert film to prevent adsorption of solution organics or biomolecules. For example, silanation of NDs with alkane chains may be a means of preventing adsorption. Also, removal of NDs may be necessary downstream of the mixing chamber, so electrophoretic mobility of coated NDs and accompanying analytes must be tested. However, when using NDs as a target probe, these considerations are unnecessary and allow for direct attachment and collection of biomolecular targets.

7. BIOCOMPATIBILITY OF ND

7.1. Overview

Before nanoparticles are fully integrated into biomedical applications, their unique interactions with biological systems demands special consideration. Of particular concern is the greater toxicity found for nano-sized particles compared with larger or soluble materials of identical composition.[227–230] To fully assess the life cycle impact of nanoparticles, from synthesis to disposal, the new sub-field of 'nanotoxicology' was coined in 2004.[231] Prior to and during this time, studies began to uncover the new and unpredictable ways that nanoparticles were internalized by cells, localized to critical organelles such as mitochondria,[232] see Figure 26, translocated from regions of the respiratory tract to various nerves[233] and penetrated through the

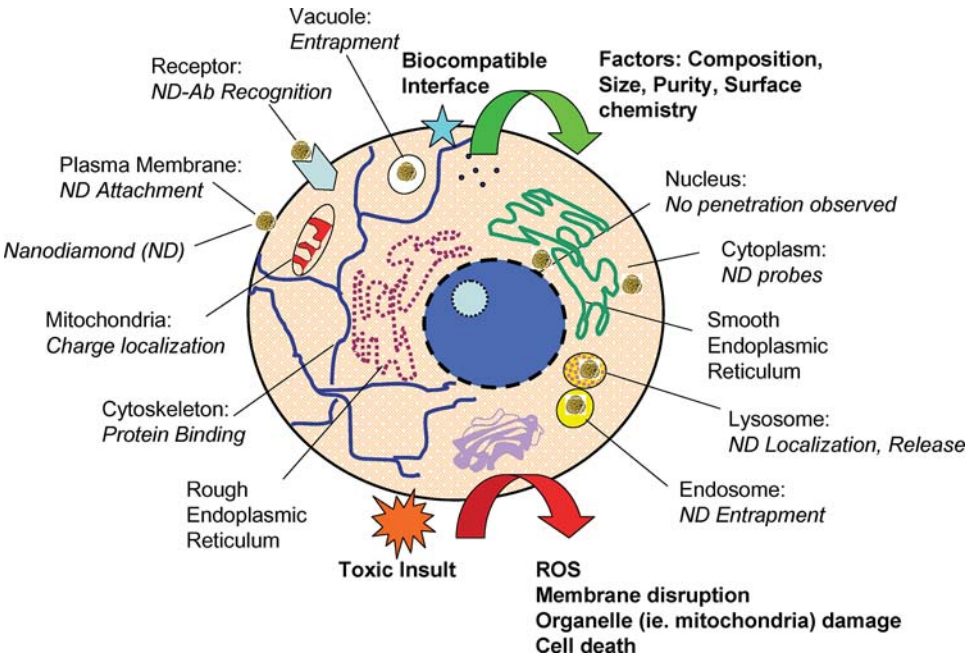

FIG. 26. Schematic representation of a mammalian cell showing some possible interactions nanodiamond (ND) particles including biomolecular binding interactions, entrapment within organelles, and localization to areas within the cell resulting in biocompatibility or unforeseen toxic insults. (Reprinted from Schrand.[193])

blood brain barrier.[234–240] In addition to their small size, a multitude of other physicochemical properties have been implicated in their distinct effects. Therefore, during the pursuit for novel uses of nanoparticles, it is imperative to independently assess the biocompatibility of nano-sized particles even if materials of similar composition are currently being used in biomedical applications.

7.2. Cell Lines, Animal Models, and Assays

The evaluation of possible therapeutic applications or the potential health threat of nanomaterials is routinely performed with both *in vitro* cell cultures and *in vivo* animal studies.[241,242] *In vitro* studies rapidly and inexpensively provide an initial risk assessment in cell models that representative likely routes of nanomaterial exposure such as alveolar macrophages (respiratory inhalation), keratinocytes and fibroblasts (integument breech), neuroblastoma or PC-12 cells (nervous system translocation), or blood and epithelial cells (circulatory injection). However, differences based on the model biological system chosen (i.e., cell line, animal) can introduce experimental variability considering the physical arrangement of organ systems (i.e., respiratory, digestive) and the unique role that each cell type has in the body.[233,243–246] White blood cells (i.e., neutrophils, lymphocytes, and monocytes) are primarily responsible for mounting an immune response after exposure to foreign materials. The general mechanistic paradigm to explain the toxic effects of nanoparticles is the generation of reactive oxygen species (ROS) and subsequent oxidative stress[37] (see Figure 26). The cascade of events that amplifies the inflammatory response can include lysosomal membrane damage causing leakage of lytic enzymes and increased expression of proinflammatory mediators and cytokines, which signal a variety of immune and other cells to migrate to the vicinity working to remove and repair the tissue through inflammatory, proliferative, and remodeling processes.

Polymorphonuclear neutrophils (PMNs) quickly arrive within an hour from the bloodstream to the site of exposure and release a variety of proteolytic and hydrolytic enzymes in a process known as degranulation.[247] Shortly thereafter, PMNs die and are replaced within 2 days by monocytes, which mature into macrophages. Macrophages continue to phagocytose bacteria and damaged tissue and may contribute to the formation of inflammatory lesions called granulomas. The release of other growth factors and cytokines by these blood cells signal to recruit additional cells involved in angiogenesis (endothelial cells), fibroplasia and granulation tissue formation (fibroblasts), and epithelialization (epithelial cells, keratinocytes). Therefore, the choice of cell type in biocompatibility studies may be based upon the ability of nanomaterials to interfere with or contribute to an immune response at the site of exposure (i.e., keratinocytes in the epidermis) or for targeting of the nanomaterials to certain locations to aid in recovering normal function (i.e., destruction of cancer cells).

The primary assay that has been used to evaluate cell health after exposure to nanomaterials is the MTT assay. The ability of mitochondria in living cells to chemically reduce a tetrazolium salt, thereby changing its color from yellow to purple,

TABLE 3
Biocompatibility studies of nano-sized diamond particles

ND Type	Processing	Dose/Time	Cell Line/ Animal	Locale Imaging	Cellular Assay/ Bio-marker	Outcome	Ref.
5-300 nm NDs, GE	A, cellobiose and MAP antigen coated	500 μg/mL, 1mL injection	White rabbits	N/A	ELISA Ab	Antigen carrier	[367]
DND	S, #5 & 6 BioNDs	1.25 mg/ml, 1.5 h	White Blood Cells	N/A	TB, CLR	85 to 93% hemolysis	[314,315]
DND	S, #5 & 6 BioNDs	310 μg/mL, 1.5 h	Red Blood Cells	N/A	TB, CLR	3 to 50% hemolysis	[314,315]
Synthetic type Ib powder, 100 nm	PBI, F, A	20–400 μg/mL, 3 h	293 T	Cyto, LM, EP, CF	MTT	Non-toxic	[75]
2-10 nm DNDs	Raw, A, B, S>3h, 5–10 s before dosing	5–100 μg/mL, 24 h	N2A	Cyto, FM, LM, TEM	MTT, ROS	Non-toxic	[168,193,246]
2–8 nm DNDs	S 30 min	20–100 μg/mL, to 24 h	RAW macrophage, HT-29	Cyto, CF, LM, TEM	MTT, gene	Non-toxic	[80,372]
Synthetic type Ib powder, 35 & 100 nm	PBI, F, S 30 min	0.8 μg/mL, 5 h	HeLa	Cyto, FM, BF, 3-D	See [75]	See [75]	[76,167]
Commercial type 1b powder 50 nm and DND 4 nm	EBI, SDS, S 10s PBS	NC, 3h	HeLa	Cyto, CF, RL	N/A	N/A	[96]
5 nm DND & 100 nm NDs, carboxylated	A, B, C, S 20 min	0.1–1000 μg/mL, 4h (RC 24–48 h)	A549 HFL-1	Cyto, Bio-AFM, CF, PC, RM, FC	MTT, protein	Non-toxic	[187,188]

Acid purification treatment (A), active oxygen generation (AOG), antibody (Ab), base purification treatment (B), brightfield microscopy (BF), centrifuged to sediment (C), chemiluminescent luminole reaction (CLR), confocal microscope (CF), cytoplasm (Cyto), electron beam irradiated (EBI), enzyme-linked immunoassay (ELISA), epifluorescent microscope (EP), flow cytometer (FC), fluorescent (F), fluorescent microscope (FM), light microscope (LM), mitochondrial viability assay (MTT), nanodiamond (ND), no concentration listed (NC), phase contrast microscope (PC), phosphate buffered saline (PBS), proton beam irradiated (PBI), Raman Mapping (RM), reactive oxygen species generation (ROS), recultured (RC), reflected light (RL), sodium dodecyl sulfate (SDS), sonicated (S), transmission electron microscope (TEM), trypan blue supravital stain (TB).

provides a method to spectroscopically monitor reductions in cell viability after nanomaterial exposure compared with untreated cells. Similar tetrazolium dye assays include XTT and WST-1. Other complementary methods of evaluating the cellular effects of nanomaterials include, but are not limited to, morphological examination, trypan blue dye exclusion, neutral red uptake by lysosomes (NR assay), thymidine uptake, propidium iodide staining, cell counts, reactive oxygen species (ROS) production, cellular permeability barrier breakdown (i.e., lactase dehydrogenase (LDH) assay), mitochondrial membrane permeability (MMP), chemiluminescent luminole reaction (CLR) measurement, glutathione alterations (i.e., GSH), genetic analyses, protein expression, and activation of pro-inflammatory cytokines (i.e., IL-6, IL-8, TNF-α)[46,47] (see Table 3).

The choice of animal for studies of nanomaterial biocompatibility may be influenced by several factors, including genetic similarity to humans, size, cost, ease of handling, and reproduction rate. However, neither *in vitro* nor *in vivo* studies can ultimately predict the consequences of some drugs and chemicals in humans, which can produce unique effects even amongst different rodent species.[233,248–250] For example, rat studies have shown that nanoparticles can translocate from the lungs to the blood circulation and other organs, while most of the human studies of short-term exposure to carbon nanoparticles have not.[251] Additional differences in the breathing patterns and the structure of the respiratory tract between rodents and humans result in differences in delivered dose to the upper and lower airways.[252]

7.3. Factors Influencing Carbon Nanomaterial Biocompatibility

Historically, carbon-based materials have been considered chemically inert with minimal reactivity toward cells of the body.[4] However, nano-sized forms of carbon (i.e., nanotubes, fullerenes, nanodiamonds), with very small sizes, high surface-to-volume ratios, and reactive surface chemistries, have greatly impacted cellular permeability and dynamics.[38,253] Regarding biocompatibility, the predominant factors responsible for the cellular response to carbon nanomaterials are the elemental impurities and structure (i.e., ropes, aggregates) of the final product. Some examples of impurities include metallic species remaining from the synthesis of carbon nanotubes (i.e., Fe, Ni, Co),[254–258] other materials containing Fe and transition metals,[259–261] or metal residues from the containers used in the detonation of ND.[129] Other contaminants to the underlying elemental composition of some nanoparticles include ceramic or other abraded materials from mechanical or ultrasonic processing for aggregate disruption (i.e., ZrO_2 in ND from stir-media milling for dispersion), graphitic or amorphous material formed on surface during heat treatment, nitrogen from deliberate doping,[262] or residual solvents such as tetrahydrofurane or dimethyl sulfoxide to aid dispersion.[263,264] These results are in agreement with the greater toxicity found for Ni, Co, and Ag compared with TiO_2[230,265] and for 20 nm Ni or TiO_2 compared with 500 nm counterparts.[266,267] However, the structure-property relationship is not as straightforward because the as-produced nanomaterials typically undergo standard purification and processing treatment with strong acids (i.e., hydrochloric, nitric, sulfuric) and at high temperatures.[268–271]

Although there has been no direct link between the primary dimension of carbon nanomaterials and their resultant biocompatibility, Jia et al.[272] found that the toxicity of carbon nanomaterials followed a mass sequence of biocompatibility with C60>quartz>MWNT>SWNT in alveolar macrophages after exposure for 6 hours. In agreement with these studies, Schrand et al.,[246] found similar results with ND>CB>MWNT>SWNT in a variety of cell types including neuroblastoma cells, keratinocytes, and macrophages after 24 hours while Grabinski et al. 2007 found that larger carbon fibers or carbon nanofibers were more biocompatible than MWNTs or SWNTs in mouse keratinocytes (HEL-30).[273] Smaller sized carbon black (14 nm) compared with larger-sized carbon black (260 nm) increased the production of ROS and MIP2 mRNA expression.[274,275] In contrast, other studies have shown that smaller or shorter carbon nanotubes were more biocompatible than larger-sized carbon nanotubes or carbon fibers.[268,271,276,277] Other physicochemical properties such as shape (i.e., carbon nanotubes vs. nano-onions or nano-horns; TiO_2 rods vs. dots, Au spheres vs. rods), crystal structure (i.e., TiO_2 anatase vs. rutile or amorphous vs. crystalline SiO_2), porosity, surface chemistry (i.e., hydrophilic vs. hydrophobic), charge, and release of soluble impurities are suggested to play a role in the biocompatibility of nanomaterials.[227,233,278–293]

To date, research shows that NDs are consistently better tolerated by cells than many other carbon-based nanomaterials, such as carbon nanotubes or fullerenes, which continue to undergo scrutiny for determining their *in vitro* toxicity or biocompatibility.[256,257,269,271,273,294–301] Therefore, it is the aim of this section to summarize the suitability of ND to interface in a biocompatible manner with cells in culture or after various routes of administration to animals. Factors such as particle size, concentration, exposure time, and cell-type-specific responses will be examined with an appropriate comparison between micron-sized diamond particles to nano-sized diamond particles.

7.4. *In Vitro* Studies of Micron-sized Diamond Particles

As previously mentioned, the body responds to injury and foreign materials by initiating an inflammatory response by blood cells called platelets that signal immune cells such as neutrophils and monocytes and connective tissue cells called fibroblasts. Any disruption in this chain of highly orchestrated events can lead to negative consequences such as infection, excessive scar formation, implant rejection, or other disease conditions. Subsequently, many early scientific studies of particulate wear debris from implantable materials or coatings and respirable dusts (i.e., asbestos, quartz) were examined in these cell types for possible links to disease conditions (i.e., inflammation, arthritis, fibrosis).

Due to its low reactivity, diamond was frequently chosen as an inert, negative control particle. Results showed that diamond particles internalized by PMNs resulted in no chemotactic activity,[302] did not produce reactive oxygen species,[303,304] and had no effect on degranulation or secretion of cell motility factors.[247] *In vitro* studies of macrophages exposed to micron-sized diamond dust demonstrate that it is non-fibrogenic,[305] does not affect cell viability for at least 30 hours,[306] and does not activate or change the cell morphology or production of interleukin 1-β.[307] In fibroblasts, micron-sized diamond particles did not induce fibrogenic activity[306,308] did not induce the release of proliferation factors,[305] and had no mitogenic effect.[309] In mouse embryo 3T3 Balb/c cells or differentiated human

umbilical venous endothelial cell (HUVEC), a variety of ceramics (Al_2O_3, ZrO_2/Y_2O_3, AlN, B_4C, BN, SiC, Si_3N_4, TiB_4, TiC, TiN), including diamond and graphite powder, were not found to induce any cytotoxic effect.[310] Additionally, rabbit blood exposed to diamond powder did not produce any detectable hemolysis after 60 minutes compared with 100% lysis of blood cells in water or 0% lysis in saline solution.[311] Therefore, these studies collectively indicate that diamond particles do not provoke an inflammatory response in cell types relevant to foreign particle response.

7.5. *In Vitro* Studies of Nano-sized Diamond Particles

Smaller, nano-sized diamonds are being examined much differently than their larger-sized counterparts due to their superior physicochemical properties for incorporation into cutting edge biomedical innovations (i.e., nano-sized carriers, probes, labels) as introduced in Sections 5 and 6.2, and to be further discussed in Section 8. Nanodiamonds (NDs) not only have a large surface area and high adsorption capacity, but are able to penetrate a wide variety of cell lines while remaining biocompatible.[75,80,188,193,246] Similar to micron-sized diamonds, NDs do not induce inflammatory or cytotoxic responses such as ROS production, morphological alterations, viability changes, or cytokine production in a wide variety of cell lines including, but not limited to, macrophages, fibroblasts, and epithelial cells (Table 3).

7.6. Differential Biocompatibility of ND

Compared with other nano-sized forms of carbon, NDs show greater biocompatibility irregardless of their purification method, concentration, or size. For example, Schrand et al., demonstrated differential biocompatibility between neuronal and lung cell lines after exposure to aqueous suspensions of carbon nanomaterials (ND, CB, MWNT, SWNT) at concentrations from 25 to 100 μg/mL for 24 hours with the MTT assay.[246] The trend for biocompatibility was ND>CB>MWNT>SWNT. The lung cells (macrophages) were more greatly affected by the presence of carbon nanomaterials generating up to five times the amount of ROS compared with the neuroblastoma cells after exposure to either MWNTs or SWNTs. However, there was a lack of ROS generation from either cell line after incubation with the NDs as well as intact mitochondrial membranes further supporting the low toxicity of NDs.

Similar studies by Liu et al. examined the biocompatibility of carboxylated and uncarboxylated NDs and CNTs in human lung A549 epithelial cells and HFL-1 normal fibroblasts.[188] Treatment with ND or carboxylated ND (cND, 5 nm and 100 nm) at concentrations ranging from 0.1 to 100 μg/mL for 4 hours followed by recovery for 24 to 48 hours did not affect the overall cell morphology including the cytoskeleton or nuclei, did not reduce cell viability per the MTT assay, and did not alter the expression of protein extracts via sodium dodecyl sulfate-polyacrylamide gel electrophoresis (SDS-PAGE) analysis. The smaller 5 nm cNDs slightly reduced viability compared to the larger 100 nm cNDs, but with no significance. In contrast, uncarboxylated CNTs (10 to 50 nm and 100 to 200 nm) significantly decreased cell viability at concentrations as low as 0.1 μg/mL in A549 cells, or 1 μg/mL in HFL-1 cells, compared to concentrations greater than 10 μg/mL for carboxylated CNTs (cCNTs). There was also a more pronounced cytotoxic effect for the longer 100 to 200 nm cCNTs compared with the shorter 10 to 50 nm cCNTs.[188]

7.7. Effect of ND Surface Chemistry and Impurities

Unfortunately, the detailed purity and surface chemistry of the NDs used in many experiments has not been mentioned alongside the biocompatibility results, making it difficult to ascertain the significance, if any, of the impurities and surface functional groups. In a study of blood hemocompatibility with diamond powders by Dion et al.,, the elemental impurities in the diamond powder were 0.05 wt.% Al, 0.05 wt.% Fe, 0.15 wt.% Si, and 1.00 wt.% Zr.[311] However, these low concentrations of impurities were not cytotoxic to other cell lines in culture.[310] Regarding the purity of newly developed DNDs, there may be some residual zirconia from the process of bead milling used to destroy the agglutinate structure, fragments of graphitic structure at grain boundaries, and approximately 2 wt.% fullerene-like conjugated sp^2 carbon,[115,129,130] see Section 3.2 for further discussion on DND impurities. Other remnants from interactions during detonation with the container may contribute metallic residues, but the majority of these impurities are removed during subsequent purification steps, which alter the ND surface chemistry. For example, some initial ND powders contained $\sim$5.7% Fe, which was reduced to $\sim$1.2% Fe.[134]

The impact of surface chemistry on 2 to 10 nm detonation-produced NDs, purified with strong acids or bases, on cell viability was examined by Schrand et al.[246] At concentrations up to 100 μg/mL, all of the NDs were non-toxic to a variety of cell types including neuroblastomas, macrophages, PC-12 cells, and keratinocytes after 24 hours with the MTT assay. The most noticeable difference between two cell types (neuroblastoma and macrophage) was in the amount of carbon nanomaterials internalized by the cells, which was likely related to the greater decreased viability and increased ROS for the macrophages. The inherent function of the macrophages to initiate an inflammatory response or programmed cell death may also occur to a greater extent in this immune cell. However, despite these proposed cell-specific differences, there was a lack of ROS generation and a retention of mitochondrial membrane integrity in cell lines incubated with NDs. This suggests that the presence of impurities (i.e., Fe) has a greater influence on the oxidative stress response of the cells.

Follow-up studies on the biocompatibility of acid purified NDs in RAW 264.7 murine macrophages by Huang et al. monitored the response of genes involved in inflammation including the production of three different cytokines: interleukin-6 (IL-6), tumor necrosis factor α (TNFα), nitric oxide synthase (iNOS), and the Bcl-x gene involved in apoptotic behavior/toxicity.[80]

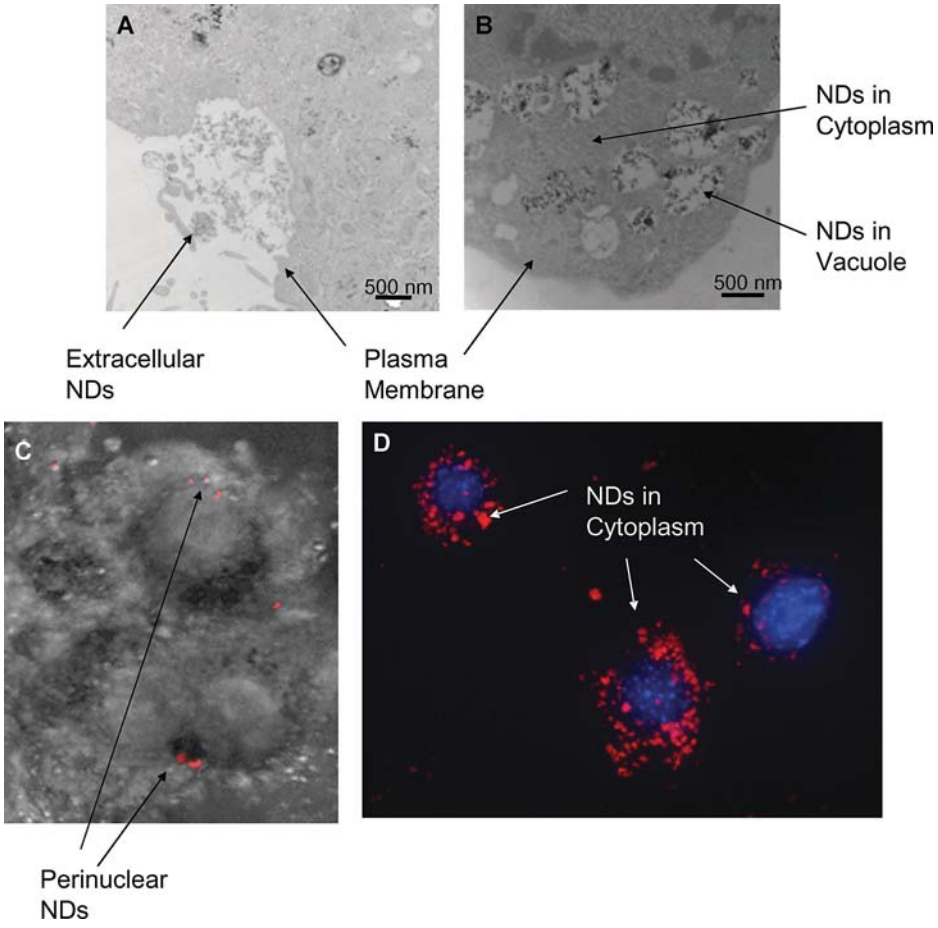

FIG. 27. Internalization and localization of NDs in neuroblastoma (N2A) cells. (A, B) TEM images of thin sections of N2A showing NDs interfacing with the plasma membrane as well as internalized into the cytoplasm and vacuoles. (C, D) Confocal images of N2A cells incubated with T-ND taken with a 60x lens. (C) Overlay of transmitted light and rhodamine signal after incubated with 50 μg/mL of T-ND (*red*) for 1 hour showing perinuclear localization. (D) Demonstration of T-ND (*red*) accumulation over 24 hours into the cytoplasm after incubation with 25 μg/mL of T-ND and counterstaining of nuclei with Hoechst dye (*blue*). T-ND is a TAMRA-ND conjugate supplied by ITC, Inc. (Raleigh, NC). (Reprinted from Schrand[193] and Schrand et al.[194])

After 24 to 72 hours of incubation with 100 μg/mL NDs, no significant change in the expression of the cytokines was detected with the real time polymerase chain reaction (RT-PCR) compared with controls. Additional experiments examining morphological changes and DNA fragmentation in macrophages as well as viability with the MTT assay in HT-29 human colorectal adenocarcinoma cells revealed the high innate biocompatibility of the NDs.

Subsequent studies with stable and fluorescent rhodamine-labeled NDs (T-ND) incubated with both animal and human cell lines did not induce morphological changes, but maintained high viabilities at concentrations up to 100 μg/mL,[193,194] (see Figure 27). The internalization of T-ND increases over time with localization to endosomes at 1 to 6 hours, to lysosomes at 3 to 6 hours, and aggregation in the cytoplasm after 24 hours suggesting an endocytotic uptake mechanism, see Figure 27. In addition, nerve growth factor, which has been shown to be important in inducing neuronal proliferation,[312] was disrupted by SWNTs and MWNTs, but not T-ND, which provides further impetus for considering NDs as biological platforms.[194]

7.8. ND Studies with Blood Cells

In contrast to the previous studies of ND biocompatibility in various cell types, studies with blood cells have yielded some disconcerting results. One study of red blood cells incubated with ND in the presence of $NaNO_2$, a potent peroxidation initiator, showed positive effects by protecting the cells' main antioxidant enzymes (superoxide dismutase and catalase). In this case, ND may have been directly acting as an antioxidant or stimulator for these antioxidant enzymes by promoting enzyme levels similar to control cells after co-incubation with ND.[313]

However, several other studies found damage to both white and red blood cells after incubation with NDs.[314–316] Careful diagnosis of hemolysis, defined as the destruction of red blood cells and the release of hemoglobin, is required for evaluating blood-contacting materials and artifical organs.[317] In general, the factors found to influence hemolysis include material chemical composition, reactivity, solubility, and surface state with a correlation between toxicity results and hemolysis.[311] Previously, it was shown that a variety of powders (Al_2O_3, ZrO_2, Y_2O_3, B_4C, BN, SiC, Si_3N_4, TiC, TiN), in addition to graphite and diamond powders, did not produce hemolysis of fresh rabbit blood after a standard test (ISO/TR 7405-1984F) to measure the release of hemoglobin.[311] In contrast, Puzyr et al. found that the addition of 0.125wt.% (1.25 mg/mL) NDs for 90 minutes to activated whole blood samples from healthy human donors changed the reaction kinetics for active oxygen generation (AOG).[315] The change in AOG was measured by the chemiluminescent luminole reaction (CLR), which is directly related to cell death. Specifically, the maximum intensity for AOG was reached more quickly after exposure to latex particles opsonized with human blood serum proteins or the addition of NDs; indicating blood cell activation. While suspensions of greater stability (BioNDs) more efficiently increased AOG compared with the initial ND suspensions, the damaging effects of BioNDs could be remediated after coating the surface of the BioNDs with donor blood plasma proteins. The authors hypothesized that the surface properties and dynamic aggregation behavior of the NDs were responsible for the passive or reactive nature of the different types of NDs used in the study.

In another study by Puzyr et al., the ND sample that most greatly influenced CLR kinetics contained the highest mass fraction of non-diamond carbon (3.4 wt.%) in the solid phase and volatile compounds (12.1 wt.%).[314] However, there was no general trend for changes in reaction kinetics based on these parameters or the pH of the suspension after assessing seven different ND samples. Therefore, the impact of different synthesis methods or varied surface modifications, as in the case of the BioNDs, have not been sufficiently understood. It does, however, seem reasonable to presume that the source of cellular damage was related to the surface properties, aggregation behavior, purity, or sterility of the NDs used in the previous studies.[314–316] because many recent studies of NDs have shown good biocompatibility and earlier studies with micron-sized diamonds in blood cells, in particular, showed no hemolysis.[318]

7.9. Effect of ND Concentration

In comparison with other studies with NDs, the concentrations used in Puzyr's studies were slightly higher (1.25 mg/mL compared with up to 1 mg/mL,[187] see Table 3. However, the influence of concentration was not directly studied and is not likely to have contributed to the negative impact on the cells because earlier studies with micron-sized diamonds were performed at much higher concentrations ranging from 4 to 10 mg/mL for 12 min to 4 hours.[302,303,319] Most recent studies have limited the dosage to 100 μg/mL to avoid excessive aggregation and also to avoid biological overloading, which would be unrealistic from the standpoint of either accidental or therapeutic exposure. However, Chao et al. found that A549 human lung epithelial cells incubated with 5 nm and 100 nm carboxylated NDs at concentrations up to 1000 μg/mL did not result in altered morphology or cell viability (MTT assay), but could be easily detected on or in living cells with Raman mapping and fluorescent confocal microscopy.[187]

7.10. Effect of ND Size

Liu et al. found that there were slight, but not significant, reductions in cell viability after incubation with smaller 5 nm carboxylated NDs compared with larger 100 nm carboxylated NDs.[188] However, several other studies have confirmed the high biocompatibility of NDs produced by a variety of methods with sizes ranging from 2 nm to 100 nm. Yu et al. investigated the biocompatibility of relatively large synthetic abrasive diamond powders (type 1b, 100 nm, Micron+ MDA, synthesized by Element Six, acid purified) that were proton beam irradiated to introduce very stable, bright, and internal fluorescent nitrogen vacancy defects.[75] They found very high viability, indicative of *in vitro* biocompatibility, with human kidney cells (293T) after 3 hours of incubation at concentrations up to 400 μg/mL assessed with the MTT assay. Smaller, non-fluorescent, detonation NDs (2 to 10 nm, supplied from the NanoCarbon Research Institute, Inc.) at lower maximum concentrations ($\leq$100 μg/mL) over longer periods of time (typically 24 hours) were studied by Schrand et al.[193,246] and Huang et al. in other cell lines.[80]

Although the effect of ND size has not been shown to play a role in biocompatibility, smaller 5 nm NDs have >15% of the carbon atoms on their surface and have shown different properties than larger sized 100 nm NDs.[320] Examination of the ND aggregate behavior and size in solution as well as interaction and uptake amount may help clarify any size-dependent effects on biocompatibility. However, in order to properly pursue the use of NDs in blood contacting devices and other biomedical applications, the mechanism and extent of direct ND interaction with cellular membranes, proteins, and fluid electrolyte/osmotic balance should be elucidated in more complex systems.

7.11. *In Vivo* Studies of Nanodiamonds

The use of animals including mice, rats, and rabbits for *in vivo* nanotoxicity studies allows a more in-depth understanding of nanomaterial kinetics. However, even within the same animal model, there has been a great divergence in toxicity results for pulmonary studies of carbon nanotubes in animals [243–245,262,321–323] or C60 in aquatic species and animals.[264,324–329] It is suspected that differences in the starting materials, such as metal impurities or residual solvent, may be responsible for the varied biocompatibility results. In contrast, micro- or nano-sized diamonds show consistently positive

TABLE 4
In vivo studies with detonation nanodiamonds

Type	Route	Animal/Patient	Dose	Time	Outcome	Ref.
DND-1	OS, IV, IM	White Mouse	0.002–0.05 wt%	3–6 mo.	No change in weight or reproductive ability, ↓ cholesterol and bilirubin levels, ↑ leukocyte level, NDA	332,334,335,336
DND-1	IM	White Rat			Localized, gelatinous clot at site of injection, abundant proteins on DND surface, no inflammation[1]	332,334
DND-1	IV	Dog	0.3–20 mL 0.001–5wt%		NDA	336
DND-2	SC	White Mouse	0.2-0.5 mL, 0.1 wt%	3 mo.	Aggregates adjacent to cells, seen through skin as dark areas	170
DND-2	IV	Rabbit	20 mL, 50–125 mg	0.25-96 h	No change in rbc or hemoglobin levels, general ↑ liver function parameters, ↓ cholesterol content and ↑ triglycerides, NDA	170
DND-3	OS	Af Mouse*	Up to 2.5–3%		Lifespan ↑38% compared to untreated mice, No change in sex cells	169
DND-3	OS	Dog			↓cancer pain, ↑ intestinal function, ↑ immune system	169
DND-3	OS	Human Cancer Patients	1 tbsp of o.015 mass %	3x/day	↓pain, ↑ function of stomach and intestines, ↑ appetite, ↑ immune system, excretion of toxins in urine, ↑ lifespan	338,374

DND-1: produced at Krasnoyarsk Research Center, Russia, sterilized, modified by sonication-assisted treatment in NaCl solution and washed.
DND-2 (RUDDM): produced by Real-Dzerzhinsk, Russia, modified by the same method as DND-1. DND-3: produced at Diamond Center, Russia, purified with nitric acid. Oral suspension (OS), Subcutaneous injection (SC), Intravenous injection (IV), Intramuscular injection (IM), No Death of the Animal (NDA), Red blood cell (rbc). Arrows denote overall increase (↑) or decrease (↓) in parameters.
*Mouse line with acute Erlich carcinoma.

results for *in vivo* applications, see Table 4. For example, micron-sized diamond particles did not contribute to inflammation when introduced to implant traversing canals in rabbits,[330] canine knee joints,[302] or the complement system [331] and NDs do not affect the weight or reproductive ability of mice or induce inflammation in rats.[169,332–337]

However, the early *in vivo* studies with detonation NDs were complicated by the low colloidal stability and high polydispersity, which made it difficult to establish dose-response relationships. In one study, ND suspensions in starch gel were orally introduced to animals with a catheter in order to increase the sedimentation stability.[338] Other treatments to remove contaminants and further functionalize the surface of NDs with hydrophilic surface moieties (i.e., oxy, carboxy, carbonyl groups) were used to produce medical-quality ND hydrosols. The ability to prepare stable and sterile ND hydrosols, that could be cryogenically stored and administered by various methods, led to a series of long-term experiments in animals including mice, rats, and dogs. The species-specific responses to 0.002 to 1.0 wt.% ND administered by different means (i.e., oral, intravenous, intramuscular) were studied and summarized below.[168,332,333,335–338]

In mice, completely replacing water in the animals' diet with 0.002 to 0.05 wt.% ND hydrosols from three to six months neither caused death nor affected the growth or internal organ (liver, lungs, heart, kidneys, and pancreas) weight dynamics compared with control animals.[332,335,336] Further, the substitution of water with ND hydrosols did not influence mouse reproductive ability, for at least the first three generations as animals consuming ND hydrosols from birth produced healthy offspring.[332–334] Within the duration of the experiments, the total amount of ND delivered to the animals was between 16 mg to 450 mg per mouse depending on the concentration of ND in hydrosols.[336]

The effects of NDs on blood cells and blood plasma chemistry were examined after prolonged substitution of water with ND hydrosols,[333–335] see Figure 28. There appeared to be a slight decrease in cholesterol content and a more pronounced decrease in bilirubin content with negligible change as the time period increased from 1 to 6 months, see Figure 28A,B. In contrast, there were slight increases in iron content after 1 month and elevated protein concentrations after 3 to 6 months (see Figure 28C,D). Although there were increases in the level of leukocytes after 1 month of treatment with ND concentrations ranging from 0.002

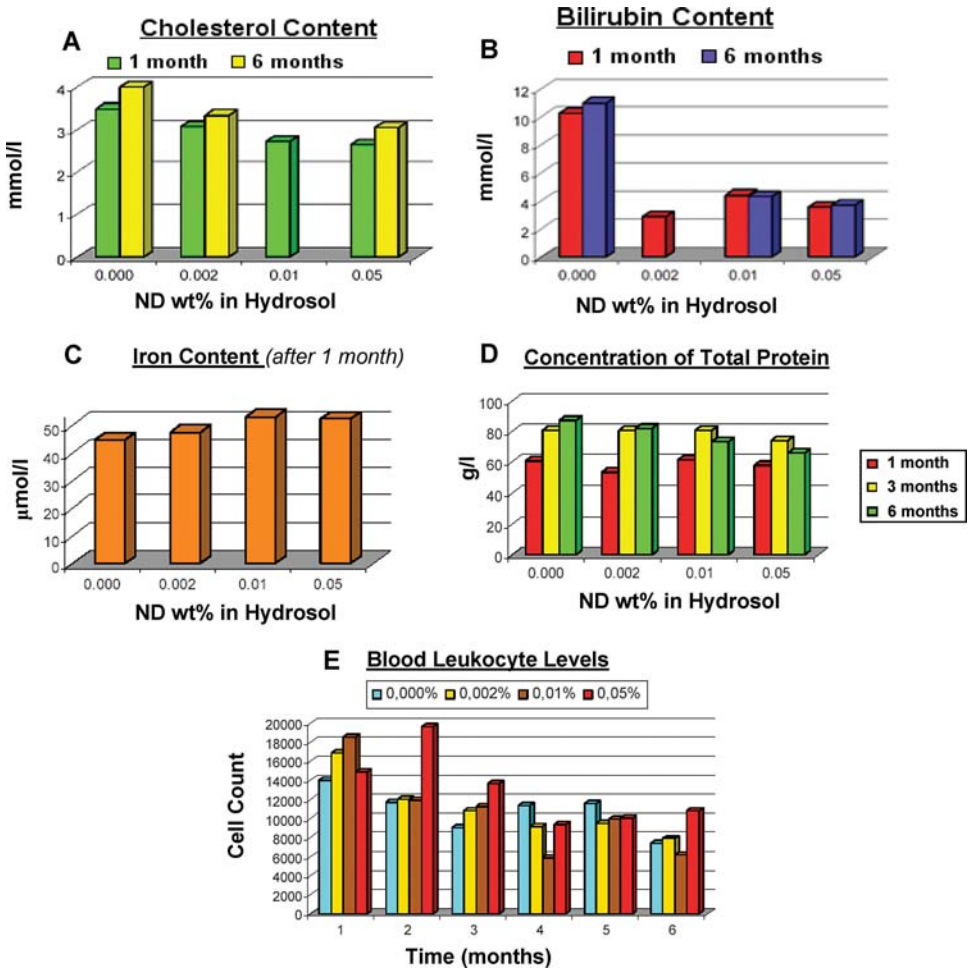

FIG. 28. Dynamics of blood chemistry (A-D) and blood leukocyte levels (E) in experimental mice as a function of ND hydrosol concentration and time. (Figures courtesy of A. Puzyr and V. Bondar.)

to 0.01 wt.%, these levels declined over the following 2 to 6 months, with no obvious difference from the untreated animals, except at 2 months where there was an increase compared to the other doses at the highest concentration of 0.05 wt.% NDs, see Figure 28E. However, the significance of this change is not understood as most leukocyte levels appear to decline in the subsequent months to similar levels as in the control animals. The authors hypothesized that the increased level of leukocytes may be a result of interactions between orally administered ND with macrophages of the gastrointestinal tract leading to a non-specific immune reaction in the animals.[333,335] Therefore, the obtained results demonstrated that ND possesses biological effects *in vivo* and, more importantly, that NDs showed properties characteristic of an enterosorbent (detoxifying agent).

Similar studies in rats showed that intramuscularly injected NDs localized at the injection sites as gelatinous clots that contained considerable amounts of protein components on their surface.[333,335] However, no pronounced visual or histological manifestations of inflammation were detected. The low toxicity was confirmed with an estimated median lethal dose (LD_{50}) of >7000 mg/kg compared with an LD_{50} of 3000 mg/kg for sodium chloride orally administered to rats,[169] In another series of experiments, dogs intravenously injected with 0.3 to 20 mL of sterile ND hydrosols in glucose (0.001 wt.% to 5 wt.%) did not die after the dosage.[337]

7.12. Word of Caution

Although the preliminary biocompatibility studies of NDs with cells in culture and animals are encouraging, extensive fundamental studies will be required before clearly understanding their long-term bio-effects. Questions remain regarding the effects of their hardness, very small primary particle size, adsorption of proteins, and resistance to degradation, which could result in mechanical damage similar to micron-sized diamond particles,[339,340] contribute to respiratory ailments, alter fluid composition,[81,82,341] influence transport properties,[75,188,246] or lead to accumulation and resistance to elimination by cells or tissues. Along these lines, most nanoparticle studies purport

that negative consequences are to be expected with decreasing particle size. However, at this point, it is not known if the synthesis method and resulting properties of NDs leads to greater compatibility with the body compared to micron-sized fragments of diamond. In support of this notion, nano-sized silica, prepared through hydrothermal synthesis, possesses a smooth and fully hydrated surface, which was less toxic than highly inflammatory, larger sized crystalline silica (quartz) particles that were prepared by grinding.[342]

8. MEDICAL APPLICATIONS OF ND

8.1. Overview

The use of NDs, alone or attached to small molecules, has led to their proposed use as remedies in diverse fields such as oncology, cardiology, gastroenterology, and dermatology,[4] see Table 2. The open carbon atoms at the surface of both polydispersed diamond (PDD) and ultra-dispersed diamond (UDD) products allow the linkage of amino acids, peptides, proteins, carbohydrates, nucleic acids, and drugs. Conjugated NDs have demonstrated preserved efficacy, efficient elution, and stable interfaces for use in cancer therapy, and other targeted cell delivery, while retaining the critically important conformation and activity of the attached molecules.[85,80174] However, the attached surface moieties must be considered in the context of their unique interactions with cells, even if the core nanomaterial appears biocompatible or toxic. For example, quantum dots can be made biocompatible with coatings, but retain the toxic In, Ga, Zn, Cd, or Pb core.[343–356] Alternatively, the effective coupling of biocompatible NDs to enzymes or drugs has been shown to effectively kill bacteria[175] or cancer cells.[80] Therefore, the attachment of bio-active molecules to any of the variety of ND forms (i.e., substrate, film, or particulate) can lead to a profound effect on ND distribution, targeting, and medicinal effectiveness throughout the body.

8.2. NDs as a New Class of Carbon-based Enterosorbents

Carbon and clay-containing adsorbents are commonly used in medical and pharmacological industries to bind ingested toxins, which can be potentially fatal to both animals and humans.[357–360] As a remedy after the accidental ingestion of mycotoxins, which are low-molecular-weight by-products of mold growth, enterosorbents are designed specifically to bind the toxins while remaining biocompatible, well dispersed in aqueous solution, and stable for transportation and administration. However, safe, practical, and effective strategies for the use of enterosorbents in the gastrointestinal tract to decrease the bioavailability of specific mycotoxins such as aflatoxin are not readily available.[360]

Due to the high biocompatibility, small size, large surface area, rich surface chemistry, inexpensive production, and variety of available samples, NDs were considered as potential enterosorbents for binding a group of mycotoxins called aflotoxins.[86] After examining the role of particle size, surface chemistry, sonication time, concentration, and zeta potential across different pH levels, the main property found to contribute to the greatest aflotoxin adsorption onto the NDs, measured with fluorescent spectroscopy and high-performance liquid chromatography (HPLC), was a positive zeta potential. Although decreasing the ND concentration from ~0.1 wt.% to 0.01 wt.% increased the zeta potential from +46 mV to +51 mV in one sample, these suspensions would already be considered stable because values above +30 mV (or below -30 mV) lead to electrostatic repulsion between particles and little agglomeration. Alternatively, in a different sample, both the direction of the titration (from pH 1 to 12 or pH 12 to 1) and the concentration of the sample had an effect on the zeta potential. Therefore, at 0.1 wt% concentrations, the two samples with adsorptive capacities of over 100 mg of aflotoxin per kg of ND were purified detonation NDs 185 nm and 300 nm in size with surface charges of +47 and +18, respectively. Further controlling the ND surface chemistry, determining optimal concentrations and reducing the size of the ND aggregates for applications in low pH environments such as the stomach would be desirable.

8.3. Conjugated NDs in Ballistic Delivery

The usefulness of ND as a general solid phase support was demonstrated in experiments using the Bio-Rad PDS-1000/He instrument for the delivery of bio-active molecules to yeast, fall armyworms, cacti, and bananas.[361] In comparison with other delivery methods, the combination of ND bioconjugates and ballistic bombardment instrumentation, which uses He pressure and vacuum circuits to generate a shock wave, can precisely target small areas with bio-active molecules over a wide range of velocities and distances. One example included the use of ND-assisted ballistic delivery of diphenylcyclopropenone, an ethylene antagonist, which was used to prevent the ripening of bananas. Compared with the most potent ethylene antagonists that are currently used to control fruit ripening, flower senescence and biotic/abiotic stress, the ND bioconjugates are less toxic, non-explosive, non-volatile, water soluble, cost efficient, and potent.

The immobilization of DNA onto 1 to 2 μm diamond particles via covalent attachment[362] and more recently onto NDs led to its use in plasmid delivery via ballistic bombardment.[361] After ~50% of plasmid DNA containing ampicillin-resistant genes was adsorbed onto the surface of 5 nm NDs or their 100 to 200 nm aggregates, *E. coli* were bombarded, transformed, and bioluminescent or blue colonies were selected due to their conferred resistance to the antibiotic. The particular advantages of using ND as a carrier for DNA include its ability to stabilize DNA without nicking under longer storage times compared with traditionally used heavy metal nanoparticles. Further optimization of the ND surface could not only increase the efficiency of DNA binding, but introduce multifunctionality for extending its

applications. This work on biolistic delivery of nanodiamonds has been published by a single team of scientists; however, there is great potential for extending these applications to vaccine delivery and gene therapeutics.

8.4. Lysozyme Conjugated NDs for Anti-bacterial Use

NDs may be useful as antibacterial surfaces on implants by attachment of enzymes, such as lysozyme, or possibly using silver-ND hybrids, to reduce infections. Lysozyme is a globular antimicrobial protein widely used in food and pharmaceutical industries. The enzyme lyses the bacterial cell wall by catalyzing the hydrolysis of the sulfur backbone of the peptidoglycan component thereby distorting the normal packing between the phosphate groups of the phospholipids and lipopolysaccharides.[363–365] The retention of ~60% hydrolytic activity of lysozyme after adsorption onto carboxylated/oxidized 100 nm NDs compared to free lysozyme in solution was earlier demonstrated by Nguyen et al.[365] In studies with *E. coli*, Perevedentseva et al. found that lysozyme electrostatically conjugated to carboxylated 100 nm NDs, producing ~131 nm ND-lysozyme complexes, could readily be detected on the bacteria with Raman mapping and scanning electron microscopy.[175] There appeared to be no specific binding or interaction between the non-conjugated NDs and *E. coli*, but ND-lysozyme was visually shown to attach and perturb the outer cell membrane resulting in significant decreases in bacterial colonies compared with controls and similar activity to lysozyme in solution. Other experiments with NDs loaded into sol-gel synthesized epoxy-silicate coatings were found to have mild antimicrobial effects against seven different mold fungi.[366] The investigation of antimicrobial formulations using ND-Ag hybrid materials has not been reported but appears promising to the authors of this review.

8.5. Conjugated NDs for Immunogenic Effects

The recognition of antigens by immunocompetent cells involves interactions that are specific to the chemical sequence and conformation of the epitope.[367] Any alteration to the conformation of the antigen after surface adsorption or shielding of critical functional groups can decrease the availability, stability, and activity of the antigen. Additionally, antigen carriers and adjuvants are selected to enhance the immunogenicity of the attached protein antigens, and as such they must maintain a stable, functional, and intimate contact. Many studies by Bianco and colleagues with carbon nanotubes have shown antigen binding and immune recognition capabilities.[7,368–371]

As antigen carriers, NDs have been shown to maintain the conformational stability of mussel adhesive protein (MAP) after injection into mice leading to antibody production.[367] The weak immune response to the MAP antigen hindered the development of a simple antibody-based purification method for its use as a corrosion inhibitor and surgical adhesive. Solid-phase, high surface area, high surface energy of nanocrystalline diamonds ranging in size from 5 to 10 nm, with some 100 to 300 nm polygonal particles, were coated with cellobiose, a disaccharide that was capable of hydrogen-bonding to MAP to minimize surface denaturation of the adsorbed antigen, which produced 4 to 20 nm ND-cellobiose complexes, which were then coupled to MAP resulting in ~300 nm aggregates. The ND-MAP conjugates were intramuscularly injected into white rabbits and after 1 month the production of anti-MAP antibodies was quantified by enzyme-linked immuno sorbent assay (ELISA) demonstrating a strong and specific antibody. The success of the ND-MAP conjugate was attributed to the nature of the cellobiose matrix and protein-cellobiose interactions at the surface of the NDs. In particular, hydrogen bonding within the glassy sugar matrix conferred 3-D stability and retarded dissolution while the protein was adsorbed rather than embedded in the matrix, which allowed its surface to retain high mobility, hydration, and low packing density for accessibility to antibodies.

8.6. Anti-cancer Properties of NDs in Cell Culture

The anti-cancer properties of diamond in both natural and functionalized forms have been explored with exciting results. In human promyeloblastic leukemia (HL60) cells exposed to dual radio-frequency/microwave plasma activated chemical vapor deposition (RF/MW PCVD) diamond powders showed a decreased stress response demonstrated by human gene expression.[205] By comparison, drugs attached to NDs or ND composite films have been used to effectively deliver anti-cancer medications such as doxyrubin hydrochloride (DOX) and dexamethasone (Dex) see Figure 6. After electrostatic loading of the apoptosis-inducing drug DOX onto the surface of 2 to 8 nm NDs or into ~50 nm ND aggregates, the cellular response of RAW 264.7 murine macrophages and HT-29 human colorectal carcinoma cells was monitored.[80] Cell viability was examined with the MTT assay and fragmentation of DNA was studied with electrophoresis after the cells were incubated with 25 μg/mL unconjugated ND, 2.5 μg/mL DOX, or the composite ND-DOX of equal concentration.[80] The results showed the inherent biocompatibility of ND, the toxicity of DOX, and an intermediate, attenuated response for the ND-DOX composites, respectively. The authors hypothesized that the shielding effect of the ND aggregates could be utilized for delaying DOX desorption in sustained drug release applications while protecting surrounding healthy tissues and cells from harmful drug side effects (see Figure 6). The mechanisms involved in the induction of apoptosis by ND-DOX composites was examined with longer cellular incubation leading to progressive apoptotic cell death suggesting the slow elution of DOX from the ND surface and interior of aggregates. Further evidence for DOX-mediated apoptosis upon addition of ND-DOX composites was shown after pre-treatment with lipopolysaccahride (LPS), a known inhibitor of DOX-mediated apoptosis, which significantly decreased cell death.

Follow-up studies were performed on stable composite ND and poly-l-lysine (PLL) thin films that were synthesized through layer-by-layer assembly onto glass substrates.[372] The biocompatibility of the single or multi-layered ND-PLL

films was examined after seeding with RAW 264.7 murine macrophages. Similar to free-floating NDs, the ND-PLL films did not induce any changes in pro-inflammatory cytokine (TNF-α, IL-6, and iNOS) secretion by the macrophages, which is relevant to multitude of cancer signaling pathways. Additionally, the incorporation of dexamethasone (Dex), a potent synthetic glucocorticoid steroid hormone that acts as an anti-inflammatory and immunosuppressant, into the ND-PLL thin films was shown to attenuate LPS-induced cytokine production.[130] To confirm the desorption and elution of Dex from the PLL-ND composite substrates, the levels of fluorescently labeled Dex into water were measured with UV-Vis spectroscopy. The mechanism of Dex release was hypothesized to be driven by a diffusion process due to sustained release over 24 hours corresponding to a similar time frame as the cell experiments.

8.7. Conjugated NDs for Specific Cell Receptor Targeting

Other studies of NDs for the detection and monitoring of cancer cells have been shown by targeting conjugated bio-active molecules to specific cancer cell membrane receptors.[174,373] (see Figure 26). Covalent attachment of recombinant fish growth hormone (GH) onto carboxylated 100 nm NDs enabled confocal Raman mapping of A549 cells after incubation with 10 μg/mL of ND-GH for 4 hours.[174] Although ND-GH specifically localized to the outer membrane of the cells, where the extracellular domain of the GH receptor resides, unconjugated NDs were found inside the cell cytoplasm near the nucleus of the cell.[174] The adaptation of this labeling technique could be used in the detection of early phase carcinoma or to monitor the status of cancer development at the cellular level where GH receptors have been found in a variety of cancer cells. Alternatively, alpha-bungarotoxin (α BTX), a neurotoxin that specifically binds to the alpha7-nicotinic acetylcholine (α 7-nACh) receptor, was electrostatically conjugation to carboxylated NDs. The nACh receptor is involved in regulating a wide range of physiological functions, such as cell proliferation and neuroprotection, and it is endogenously expressed in several human lung cancer cell lines including A549 cells. The interaction of NDs and ND-αBTX complexes was examined in A549 cells or *Xenopus laevis* oocytes (after exogenous expression) with laser scanning confocal microscopy and flow cytometry. The $\sim$300 nm ND-α BTX complex was found to effectively bind onto cell membranes where the α7-nACh receptors were located, compared to unconjugated NDs, which entered the cell cytoplasm. The functionality of the BTX was maintained and led to irreversible, concentration-dependent inhibition of α7-nACh receptor-mediated/choline-evoked inward Ca^{2+} currents in oocytes after incubation for 5 minutes with 12 μg/mL ND-αBTX. The quantification of ND and ND-αBTX with flow cytometry revealed a twofold increase in fluorescent intensity after incubation for 4 hours with 50 μg/mL ND or ND-αBTX compared to control cells.[373]

8.8. Anti-cancer Properties of NDs in Animals and Humans

The positive results for *in vitro* drug delivery or cell targeting via NDs[82,85,96,187] have provided further impetus for studying the medical properties of NDs in animals (mice, dogs) and humans with cancer. In the Af line of mice suffering ascite Erlich carcinoma, the influence of DND upon life expectancy was investigated. These mice were chosen as a model because radiation is traditionally investigated on these laboratory animals and the results may be extrapolated to humans.[338,374,375] Each mouse was injected with 6×10^6 ascite Erlich carcinoma cells, then the influence of DND upon the level of spontaneous mutations in the mice was estimated. The treatment of the experimental mice with the ND suspensions prolonged their life about 38% compared with the control group. Additionally, the mice treated with UNCD were active until the moment of death. Further, the administration of high concentrations (2.5% to 3% aqueous suspensions) of DND produced by the "Diamond Centre" showed no mutagenic properties in the sex cells of the mice.[169] Other investigations in dogs dying of cancer showed that oral suspension of NDs could stop their growling and whining due to pain concomitant with the restoration of intestinal function and strengthening of the immune system.[169]

The research by Dolmatov and colleagues in human patients with stage IV cancer demonstrated the ability of aqueous and oil suspensions of DND to improve health independent of the initial tumor location (i.e., breast, intestine, stomach) after chemical and radio therapies.[169,338,375] In all cases, orally delivered DND showed a pronounced positive effect by increasing life expectancy, enhancing the will to live, reducing pain, restoring intestinal function, allowing mobility, and improving blood indexes. Further, urine color and odor were changed as toxins were actively excreted, polyps were reduced on the internal walls of the urinary bladder, and immune system function was enhanced. Other specific health effects included quick healing of wounds, cuts, and other purulent processes in the mouth and throat, including paradontosis, after rinsing with aqueous suspensions of DND.

8.9. ND Mechanism of Action

One of the proposed mechanisms behind the ability of NDs to induce positive health effects was its ability to act as a polyradical cluster and regulate free radical processes due to its abundance of unpaired electrons.[338,374,376] Additionally, the strong adsorption characteristics (i.e., 1–10 mg-equivalents/m^2 and greatly developed surface of adsorption $\sim$450 m^2/g)[377] and hydrophilic surface groups (–OH, -NH_2, -C(O)NH_2) were hypothesized to be responsible for actively adsorbing pathogenic viruses and other microorganisms.

8.10. Diamonds for Implants and Health Care Products

Several other demonstrated or emerging applications for DNDs including their use in the CVD growth of nanocrystalline

diamond films on medical implants and prospective use of DND in health care products are briefly discussed below.

Different kinds of carbon coatings (among them diamond-like carbon (DLC) and diamond) deposited on the surface of implants increase the implant biocompatibility, hemocompatibility and serve the role of a barrier against corrosion.[378] DLC-coated heart valves and stents are already commercially available from the Cardio Carbon Company offering DLC-coated titanium implants; Sorin Biomedica produces heart valves and stents coated with Carbofilm™; the company PHYTIS sells DLC-coated stents.[378] Nanocrystalline (NC) and ultrananocrystalline diamond (UNCD) coatings on suitable substrates are promising materials for medical orthopaedic implants, for example, hip and knee joint implants[379] and for coating of certain components of artificial heart valves[62,380] due to their extremely high chemical inertness, surface smoothness and good adhesion of the coatings to the substrate. NC and UNCD films can be coated on different materials, such as medical steel AISI316L and titanium and its alloys such as Ti6Al4V.[62,380] Surfaces of NC and UNCD films intended for a new generation of implantable biomedical devices promote cell adhesion, proliferation, and growth. These films are able to coat complex geometrical shapes with good conformal accuracy and with smooth surfaces to produce hermetic bioinert protective coatings, or to provide surfaces for cell grafting through appropriate functionalization.[62] However, as mentioned previously, recent studies show that diamond powders are not bioinactive at the molecular level; they affect cellular gene expression and inhibit stress (oxidative, cellular, genotoxic).[205]

UNCD is a more suitable material than silicon for fabrication of bioMEMS. For example, in the case of a Si microchip implantable in the eye as the main component of an artificial retina to restore sight to people blinded by retina degeneration, Si cannot survive long-term implantation, while UNCD bioinert encapsulation can successfully replace the Si microchip implantation in the eye.[381] In neurodynamic studies using an animal model with an implantable diamond microelectrode, it was possible to integrate neural stimulation and amperometric sensing (e.g., of dopamine, adenosine and serotonin) in the same implantable device.[219]

As a seed material for CVD diamond growth, DND particles play an important role for the development of medical implants.[213,214] Seeding with DND allows obtaining coatings with small grain size and, therefore, smooth surfaces that are important for medical implant applications. Until recently, preparation of the seeding slurry was performed in-house in the laboratories. After advances in DND deagglomeration and fractionation, seeding slurries with consistent properties have become available in the market. Williams et al.[213,214] is developing methods for improving the nucleation density of nanocrystalline diamond film growth using bead-milled DND that is processed to form a stable aqueous colloidal solution of primary particles. This colloid was applied to various substrates to yield a high density of individually spaced diamond nanoparticles (greater than 10^{11}cm^{-2}).[213,214] Seeding slurries of DND with average aggregate size 20 to 30nm in DMSO have been developed at ITC (www.itc-inc.org). Prior to seeding, DMSO-based DND slurry is mixed with methanol or ethanol[382] and the substrate intended for seeding is ultrasonically treated in the slurry, resulting in a monolayer of small DND aggregates. As it was discussed in Section 6, seeding using DND is also important in fabricating biosensor electrodes.

DNDs are considered viable components in bone regeneration, as reported by Pramatarova et al.[383] Hydroxyapatite /DND composites were formed on glass substrate by deposition of DND from supersaturated solution of simulated body fluid (SBF) resembling the composition of human blood plasma. It was revealed that the hydroxyapatite/DND composite is grown both by physical adsorption and chemical bonding of DND with the matrix. The role of OH^- groups in the hydroxyapatite growth on DND surface from SBF is emphasized, providing a negative charge on the surface and attracting Ca^{2+} ions, which in turn attract PO_4^{3-} ions, thus forming apatite nuclei.[383]

Nanodiamonds are also considered for cosmetics and health care applications due to their ability to bond with biological materials, improve durability and robustness of a composition, provide protection from harmful UV light, possibly scavenge free radicals and protect against viruses and bacteria.[161,169,384,385] Sung Chien-Min et al.[384] hypothesize that nanodiamonds dispersed in a biologically acceptable carrier and bonded with biological materials may improve skin cleansing and exfoliation, add mechanical strength, and provide treatment of adverse conditions. The authors consider additions of DND to deodorant, toothpaste, shampoo, antibiotics, dermal strips, DNA test strips, skin cleanser, dental filler, nail polish, eyeliner, lip gloss, and exfoliants. The authors report that nanodiamonds can provide increased resistance to chipping and wear of a nail polish so that it can last from about three to ten times longer than typical nail lacquer formulations. No other specific results, demonstrating improvement in the performance/appearance after addition of ND to healthcare/cosmetic formulations, however, have been demonstrated by Sung Chien-Min et al.[384] Lunkin et al.[385] studied influence of DND formulations on viscoelastic properties of tissue by measuring velocity of surface acoustic waves in skin. Dynamic shear modulus of human skin was increased by 15% after treatment with a skin cream containing 10^{-9}g/g of DND. In experiments with white mice with skin burn wounds, addition 10^{-10}g/g of DND to the treatment gel accelerated the time of healing by twofold.[385] The Environmental Working Group (www.cosmeticdatabase.com)[386] lists eight cosmetic products currently on the market containing diamond powder including nail polishes, nail treatments, anti-aging formulation and facial cleanser. The diamond powder is listed in the formulations as a material with a low hazard score (1 out of 10).

Another potential application of nanodiamond in the healthcare products is protection from ultraviolet radiation (UVR), as

discussed by Shenderova et al.[161] Ultraviolet radiation causes severe damage in humans[387] and natural and synthetic materials. Chemical sunscreens reduce the damaging effects of UVR via absorption, whereas physical sunscreens cause reflection and scattering of UVR.[388] In the case of inorganic sunscreens such as barium sulfate, strontium carbonate, titanium dioxide and zinc oxide nanosuspensions have found applications in sunscreens made for human use.[389] DND has high refractive index (~2.4) and efficiently scatters light. The attenuation of UVR by DND can be enhanced due to absorption by carbon in the sp^2 hybridization state present on the DND surface. Many lattice defects and impurities found in natural and synthetic diamonds absorb UVR,[390] contributing to the radiation attenuation. Photoluminescent defects that can be excited by UV radiation, emit light in the 'safe' visible spectral range. Shenderova et al. demonstrated that detonation nanodiamonds of with sizes ranging from ~50 to 100 nm effectively attenuate UVR without compromising the transparency of a sample in the visible spectral region and, thus, can be used in sunscreens in a variety of applications.[161] The ability of DND to absorb and scatter UVR depends on the concentration and size of nanodiamond particles, their surface composition and can be related to the presence of sp^2 carbon, lattice defects and impurities. Biocompatibility and non-toxicity of nanodiamond in combination with their excellent physical performance make this material a very attractive candidate as a physical sunscreen. Human trials are needed, though, to make a final conclusion of applicability of ND in health care and cosmetic products.

9. FUTURE OUTLOOK FOR ND BIOMEDICAL APPLICATIONS

There are a multitude of nanoparticles currently being examined for biomedical applications (i.e., imaging, diagnostics, drug or gene delivery); however, many have limitations to overcome such as controlling surface properties, increasing dispersion in physiological solutions, expanding on biocompatibility criteria, and effectively targeting intracellular locations. Thus, the interactions of nanoparticles with biological systems will depend highly on the form (i.e., airborne particulate, aqueous suspension, protective coating, solid substrate), presence of impurities (i.e., metal, amorphous carbon), cell type or animal model, and route of administration and exit. Fortunately, nanodiamonds appear to be ideal candidates for biomedical use due to their small primary particle size (~4 to 5 nm), purity, facile functionalization, and retention of high cellular viability. However, the qualities of NDs that must be controlled include their aggregation state, surface chemistry, as well as their localization and accumulation behavior within the body. Therefore, advances in their functionalization and comparisons between *in vitro* and *in vivo* testing for biocompatibility[300] will be required before the full biomedical potential of any nanoparticle, including ND, can be realized. We discuss in greater detail below future ND research and development in bioapplications, biocompatibility studies and specific prospective applications in medicine.

9.1. Designer Nanodiamond for Bioapplications

The most important structural aspects of modern DND have been discussed in Section 3.4. Major structural characteristics that need to be carefully controlled are the size of DND particles (both primary particles and their aggregates), their 'external' composition (surface groups) and 'internal' lattice defects responsible for important physical properties such as photoluminescence (Figure 11). These characteristics are discussed below in the context of cell and animal studies along with their envisioned bioapplication.

9.1.1. Control of Surface Properties

The importance of surface properties and a need for their thorough characterization has been exemplified in studies with particles synthesized through combustion techniques with very low metal content, such as carbon black, which caused inflammation purely due to surface characteristics and not from any impurity soluble species.[279,391] Thus, a suggested set of nanomaterial characteristics considered valuable during the course of cell or animal testing includes size distribution of primary particles, shape, surface area, elemental and phase composition, surface chemistry, homogeneity of surface groups, surface contamination, surface charge, crystal structure, agglomeration state, porosity, method of production, storage conditions, and concentration.[233] Alteration of the diamond core is possible through high-energy beams that enhance PL properties of NDs, however many facile modifications that can be made on a variety of ND surface functional groups formed during their synthesis and processing. It is advantageous that these chemical surface modifications follow standard wet synthetic chemistry techniques. Although the surface of NDs has been utilized for the adsorption of a variety of proteins, microorganisms, and toxins, Perevedentseva et al. demonstrated that NDs do not readily bind *E. coli* until after conjugation with lysozyme.[175] Therefore, the mechanism of surface binding is critical for understanding the specificity of ND toward microbes or other targets, such as enterosorbents.[86] In either case, the rate and efficiency of adsorption and desorption onto the ND surface should be optimized while controlling non-specific binding through steric or chemical means.

9.1.2. Increasing Dispersion

One key aspect related to the use of nanoparticles, including NDs, in biomedical applications is the modification of its surface to produce stable hydrosols that are able to endure necessary medical processing procedures including sterilization (i.e., autoclaving) and freeze-thaw cycles (also see Section 3.3.5). The effect of pH on the stability of fluorescent ND hydrosols in buffer solutions was examined with fluorescence correlation spectroscopy (FCS).[96] The correlation between ND hydrosol stability and pH values greater than 7.5, which promoted

aggregation, was attributed to the pH-dependent dissociation of surface carboxyl groups. Although phosphate buffered saline (PBS) is known to promote the aggregation of NDs, the addition of sodium dodecyl sulfate (SDS) was shown to increase the dispersion of a mixture of NDs and PBS in the pH range of 5.7 to 7.8. Details on the concentration of SDS, actual size of the aggregates, and the effect of size on cell viability would provide valuable information as well as a comparison with other common surfactants. However, the nature of the bonding between detonation-produced NDs is considered to be covalent due to the high-temperature high-pressure synthesis, which forms large agglutinates. Conventional methods such as sonication have not been successful at breaking up the agglutinates, but the isolation of primary particles by wet-milling with zirconia beads continues to be optimized.[392] Therefore, the use of surfactants (i.e., SDS) or other chemical solvents to increase ND dispersion[96] or the attachment of bio-active molecules[80,174] must be taken into consideration for the cellular fate of the NDs throughout the body and in individual cells.

The degree of nanoparticle dispersion or aggregation can impact biocompatibility results, for example by altering the effective dosage. Future studies should strive to take into consideration the constraints of the biological environment (i.e., temperature, media density and viscosity, presence of serum proteins, addition of surfactants) and particle properties (i.e., size, shape, charge, and density), which are related to the diffusion rate and gravitational settling of the nanoparticles.[46,168,246,258,296,345,393,394] For example, the dispersion of NDs in cell culture media containing sugars, salts, and amino acids leads to ND aggregates as large as 2 microns in size.[193] In this respect, it is difficult to predict the effect of size on biocompatibility based upon the primary nanoparticle size as measured with TEM or size in non-physiological solvents. Further, the danger of thrombosis by plasma protein-mediated ND aggregates is of concern if the NDs aggregate *in vivo.* Additional methods of nanoparticle separation according to size, surface charge, and shape with methods such as electrophoresis,[146,395] understanding the properties of various fractions of nanoparticles,[94] and producing pH stable functionalizations (i.e., for the low pH environment of the stomach or lysosomes) will be essential for targeted therapeutics.

9.2. Better Understanding Biocompatibility

A current review of the available data on ND particles overwhelmingly suggests that they are biocompatible with many mammalian cell lines.[75,80,168,246] Regardless of the size of the NDs in cell culture media, after purification, or fluorescent labeling, there was high viability, maintenance of mitochondrial membrane integrity, and no indication of ROS after exposure and internalization at concentrations up to 100 μg/mL over 24 hours. However, the strength of the *in vitro* biocompatibility studies could be improved by providing consistent positive and negative controls and benchmark nanoparticles to assess the validity of the toxicity assays. This includes independent testing of the solvents or surfactants incorporated with the nanoparticles.

Because micron-sized diamond particles were chosen negative control particles for other ceramics, nano-sized diamonds could be proposed as control particles for nano-sized carbon biocompatibility studies. However, the properties would need to be uniform and the binding of the biochemical assay probes (i.e., MTT or ROS) should continue to be scrutinized for directly interfering with the toxicity assay results.[396,397] In this regard, there are currently no standard benchmark nanoparticles. Typically soluble forms of metal/metal oxide nanoparticles (i.e., silver nitrate for Ag nanoparticles or well known toxins such as CdO) and micron-sized counterparts are used as positive and negative controls. However, operating in this fashion assumes that the larger sized or more soluble materials are less toxic, which may not be the case.

It is evident from the above discussion, and abundance of recent publications that have included nanoparticle toxicity as part of their results, that the formation of multidisciplinary teams consisting of chemists, biologists, engineers, and other expert scientists, is critical for developing new protocols and models as well as ensuring the correct interpretation of what might otherwise be attributed to sampling or technical artifacts (i.e., change in microplate reader absorbance due to the adsorbent nature of some carbon nanomaterials). Hoet et al. emphasized the collection of high quality blood samples for clotting studies, differences in thrombogenesis between humans and animals, and highly advised conducting hemostasis and thrombogenesis studies in close collaboration with experts in fields of coagulation and vascular biology.[398] These collaborations could help reveal what caused the damage to blood cells after exposure to NDs, see Table 3.[313] Parameters that can lead to blood hemolysis including physical damage at the time of venipuncture, prolonged or incorrect processing and storage conditions (ie too hot or cold temperature, centrifuging too quickly, or contamination with micro-organisms) should be carefully investigated. Further, an in-depth study of the direct interaction of NDs with the plasma membrane may help elucidate the mechanism of destruction.

The mechanism of positive effects of NDs should be pursued in a more technical fashion. Although the LD50 oral value in rats was $>$7000 mg/kg, the dermal and injection limits are virtually unknown.[169] Before NDs are incorporated into health care products, such as sunscreens and other skin creams, as well as shaving gels and tooth paste, the penetration depth of NDs into the skin or gums would need evaluation for any unforeseen side effects. The preliminary results of the anti-cancer effects of ND need systematic probing of the mechanisms at work, including specific cell signaling pathways and gene expression by high throughput microarrays similar to studies performed with carbon nanotubes.[285,399,400]

9.3. ND Localization

While many studies are ongoing to determine the factors responsible for the biocompatibility of nanomaterials, the

pathways for internalization and degradation at the cellular level are still unknown. Quantum dot-multi-walled carbon nanotube conjugates[401] or multi-photon carbon dots[402] were internalized by temperature/energy-dependent endocytosis after 1 hour at 37°C compared to little or no uptake at 4°C. However, other studies have found non-phagocytic uptake mechanisms based on diffusion or adhesive interactions. For example the uptake of fluorescent polystyrene microspheres into pulmonary macrophages or red blood cells did not result in their containment within membrane bound structures.[403] Other non-specific uptake mechanisms including pinocytosis, patocytosis, or membrane ruffling may unsuspectingly traffic nanomaterials into cells.

The kinetics of both non-fluorescent and fluorescent ND entry and localization inside cells has been examined with microscopic and spectroscopic techniques. Internalized ND aggregates localized within the cytoplasm, but not within the nucleus.[75,76,96,193] Time-and concentration-dependent accumulation in the cytoplasm from 1 to 24 hours showed co-localization to lysosomes between 3 to 6 hours with subsequent release back into the cytoplasm or new ND internalization after 24 hours.[194] However, NDs were not degraded by the cells raising questions about long-term accumulation and damage.

As previously mentioned, the biological fate of nanodiamonds (and many other nanoparticles such as quantum or carbon dots) after internalization into cells is still in an exploratory stage. Not only are there are many different uptake mechanisms (endocytosis, phagocytosis, non-specific) which lead to differential intracellular localization, but the physicochemical properties of the NDs are not yet controllable to consistently allow individual particles to pass through nuclear pores for potential applications such as gene delivery. Further limitations of 'seeing' and recording individual nanoparticles inside the nucleus or other subcellular organelles also continue to be addressed by the scientific community.

Most recently, the authors of this review have worked together to address this issue by using fluorescent NDs to track their localization into cells based on time and concentration. After entering the cytoplasm of the cells, the NDs were routed to lysosomes. However, the NDs were unable to be degraded and appeared to accumulate in the cytoplasm. It is unclear whether the NDs would be released or if the cells would die after long-term repeated accumulated. Because many cells of the body undergo natural cell death, it is anticipated that the body would be capable of clearing small amounts of NDs through natural cellular renewal processes without ROS generation or negative side effects. Cell-specific differences should also be considered in the mechanism of nanoparticle uptake, accumulation, and localization.[246,404]

9.4. Precautionary Measures

As a precaution, people synthesizing or handling nanoparticles should be sufficiently protected from accidental and possibly dangerous contact. The establishment of exposure limits, understanding their undesirable attributes, properly disposing of waste products, and limiting their impact on micro-organisms and plants,[361,405,406] are all required responsibilities during the development of nanoparticles-based products. With this said, the disease potential of supposedly biocompatible nanoparticles in individuals with existing medical conditions can still be high, as well as an increased susceptibility to disease after exposure to nanoparticles.[407] For example, the link between particulate air pollution and increased cardiovascular morbidity and mortality is well documented where increases in respirable particulate matter have been associated with increased plasma viscosity, changes in blood parameters (i.e., fibrinogen, red blood cell counts), arterial vasoconstriction, and increased heart rate variability.[398]

Due to the vast array of compositions and surface properties, the biological effects of nanoparticles have received attention from several U.S. government regulatory agencies, such as the Environmental Protection Agency (EPA), Food and Drug Administration (FDA), National Institute for Occupational Safety and Health (NIOSH), and the Occupational Safety and Health Administration (OSHA). These government agencies, along with public and private organizations, are working closely with scientists to establish safety guidelines and advance the understanding of nanoparticles for the larger global aim of producing sustainable and significant advances for mankind. Although the beneficial effects of nanoparticles are not typically incorporated as part of the risk assessment process, sharing these findings would be beneficial to the scientific community.

9.5. The Bright Future of ND for Biomedical Use

The anticipated major areas for ND biomedical use are in cancer therapeutics (i.e., drug delivery), analytical diagnostics, and imaging. Other clinical uses of NDs for instruments in cell surgery, prosthetic devices for retinal implants, and platforms for nerve stimulation will also undoubtedly impact the field of nanomedicine.[408]

9.5.1. Drug Delivery and Cancer Treatment

ND is unique in its ability as an insoluble solid powder to effectively prevent mutations in normal cells, reduce the reoccurrence of secondary tumors, and counteract the mutagenic effects of cancer medications alone or with the use of chemical and radio therapy.[49,169,375] In addition, the preliminary results of NDs for medical use,[316,334,336,337] have great potential since there are many variations of ND available that may be tailored to a particular drug or delivery application by selecting the most beneficial type of ND (i.e., detonation, HPHT, natural, etc.), dose, surface functionalization, and duration of treatment to maximize their therapeutic value. For example, the time-release and shielding capability of ND agglomerates may be exploited in directed/sustained drug-delivery devices.[372]

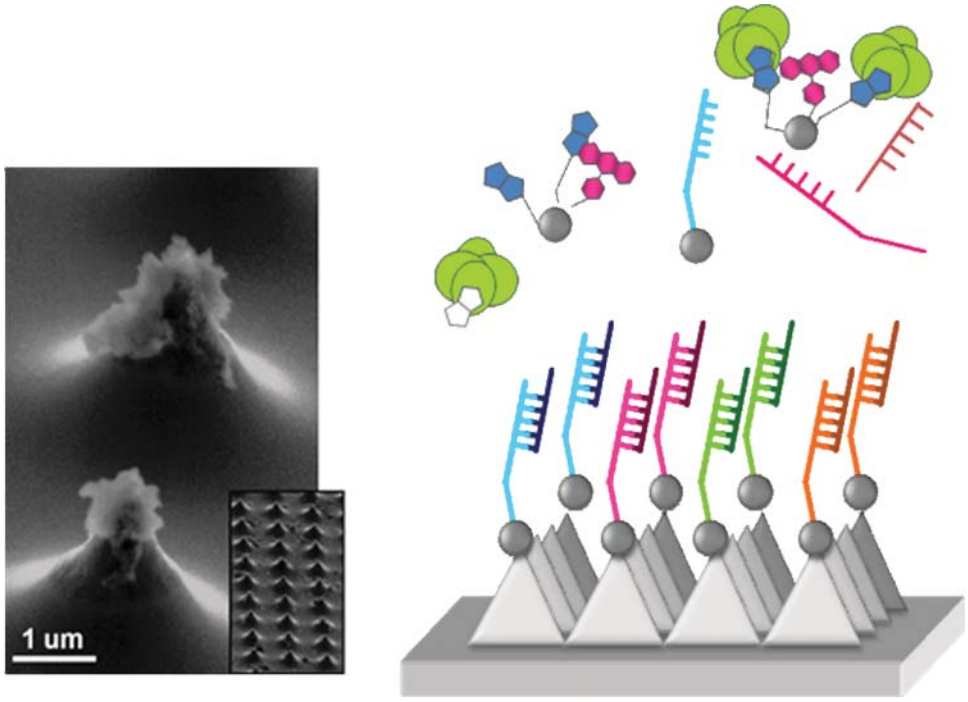

FIG. 29. Schematic of a field tip array (FTA) that can be used to collect solution targets using a ND-probe conjugate by applying a bias on the electrode (*right*). A photograph of nanodiamonds collected on FTAs by applying a modest potential (*left*).

9.5.2. Bioanalytical/Diagnostic

Bioanalytical applications of ND films and particles for adsorption, purification, and collection of analytes are expected to be utilized in the near future. For example, recent work has shown that it is feasible to use ND-probe bioconjugates in diagnostic applications that collect and target proteins,[372] small molecules, nucleic acids, see Figure 29. This work will be expanded to other bio- and organic molecules to determine the breadth of applications, since NDs are biocompatible and may serve as an inert solid support that does not affect chemical/biochemical function of bound molecules.

ND-based biosensors may out-perform traditional silicon and gold-based microelectronic materials by combining rapid detection with high selectivity and sensitivity due to nanodiamond's chemical and physical properties, particularly for high throughput clinical systems.[63] In addition, novel devices may be expansive due to the variations in the type of ND particle or film (i.e., mono-, poly- crystalline) and may exceed current performance criteria with reduced cost.[220] ND particles form ordered assemblies that we call "ND Rainbows" such that the packing distance is dependent upon the spacing of the particles. In addition, size selection of ND particles has produced ordered photonic crystals, which we call 'ND Christmas Lights." Thus, these ordered ND particle assemblies may have applications in biodiagnostics, for example, as a colorimetric indicator platform (see Figure 30).[122]

9.5.3. Imaging

The variety of imaging modalities of ND (PL, optical scattering, Raman mapping, fluorophore tagging) allows dynamic and non-destructive monitoring of its interaction with living systems. In the future, NDs may be used for imaging in biomedicine, which may be targeted to the human body or within single cells. Of course, as means of visualization, optimization may be required to increase the signal output due to endogenous fluorescence of biological tissues and may be accomplished by further functionalizing the surface or developing more sophisticated non-destructive imaging techniques. Never-the-less, current *in vitro* and *in vivo* work shows that ND imaging is facile and does not require such considerations. In the future, nanohybrid fluorescent-magnetic-radioactive nanoparticles could be combined for detection with various forms of near infrared (NIR) fluorescence, tomography (magnetomotive optical coherence, photoacoustic, positron emission, computed scan), ultrasound, or magnetic resonance imaging (MRI).[409–413] Thus, nanodiamonds offer a promising avenue for more sophisticated, and possibly, new imaging modalities in biomedicine.

9.6. Future Applications

Nanodiamonds may be used for biolistic delivery in gene therapy, drug delivery, and vaccines as a solid support matrix that may stabilize and concentrate the bioactive molecules of interest, while maintaining a physically strong matrix that has a large surface area for increased loading of material. Also, NDs

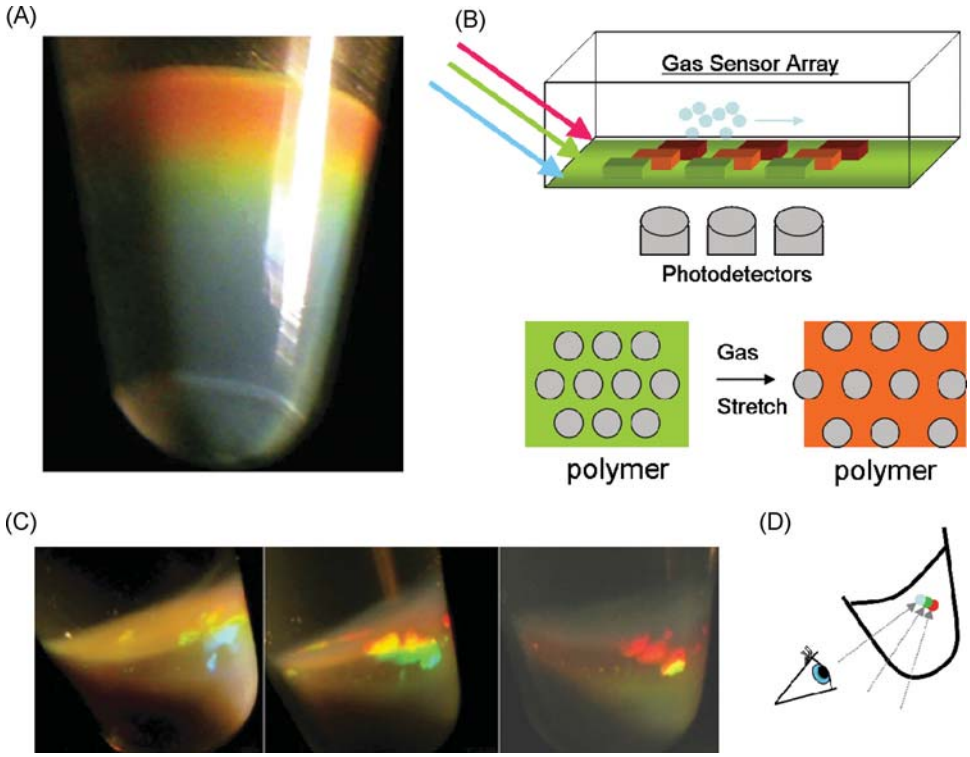

FIG. 30. Nanodiamonds form a rainbow of colors depending upon the spacing between nanodiamond particles (A). Future applications of photonic sensors for analyte detection (B) may employ nanodiamonds that form photonic crystals (C) whereby, the color observed is dependent upon the angle of observation (D). (Adapted from Grichko et al.[85])

may be used as oral adjuvants for drugs and food as a stabilization media, which could be prepared, for example, by hydrogenating NDs to reduce their binding affinity to biomolecules. In biotechnology, genetic screening using gene chips may one day incorporate NDs as the solid support for gene attachments. Similar applications could be transferred to the development of proteomics and metabolomics. Additionally, NDs may be used in immunoassays as either the detection tag or the solid support matrix. Furthermore, NDs may one day be used in humans for labeling biomolecular targets of interest or may be used for immunotherapeutic applications. For example, ND particles may be attached to both an antibody and radiolabel, whereby the high surface area of the ND "protects" the antibody from destruction by the radiolabel. Biosensors in vitro or in vivo may be constructed of ND photonic crystals that change color when targeted molecules bind the sensor surface. NDs may be used in new types of purification procedures that combine high-pressure liquid chromatography with high temperature.

9.7. Conclusions

The highly intense research into ND chemistry and biomedicine in the last several years has lead to a new quality of nanodiamond that is far superior to its predecessors and may be almost unrecognizable. This focused work has lead to ND products that rival other nanoparticles in purity, size selectivity, prevention of aggregation, colloidal stability, surface functionality, and photoluminescence. Thus, the authors of this work expect, that in the near future, NDs will become more widely recognized for their unique surface and diamond core properties and will attract further attention, bring about new applications, and possibly create new scientific fields of research and applications. We believe that forming close working relationships with investigators outside the nanodiamond community is paramount to the successful development of nanodiamond products and is critical in promoting and exploiting their potential in medicine and biotechnology.

ACKNOWLEDGMENTS

The authors would like to acknowledge the help of A. Puzur, V. Bondar, V. Kuznetsov, T.Tyler and B. Palosz for providing illustrations for this review, as well as helpful discussions with G. McGuire.

REFERENCES

1. O.A. Shenderova, V.V. Zhirnov, and D.W. Brenner, Carbon nanostructures, *Crit. Rev. Solid State Mater. Sci.*, **27**, 227 (2002).
2. H. Schwertfeger, A.A. Fokin, and P.R. Schreiner, Diamonds are a chemist's best friend: Diamondoid chemistry beyond adamantane, *Angew. Chem. Int. Ed. Engl.*, **47**, 1022 (2008).

3. T.P. Da. Ros, Medicinal chemistry with fullerenes and fullerene derivatives, *Chem. Commun.* (*Camb.)*, **663** (1999).
4. R.J. Freitas, *Nanomedicine Volume IIA: Biocompatibility*, Landes Bioscience: Georgetown, TX (2003).
5. A. Bianco, Carbon nanotubes for the delivery of therapeutic molecules, *Expert. Opin. Drug. Deliv.*, **1**, 57 (2004).
6. A. Bianco, J. Hoebeke, K. Kostarelos, M. Prato, and C.D. Partidos, Carbon nanotubes: On the road to deliver, *Curr. Drug. Deliv.*, **2**, 253 (2005).
7. A. Bianco, K. Kostarelos, C.D. Partidos, and M. Prato, Biomedical applications of functionalised carbon nanotubes, *Chem. Commun. (Camb.)*, **571** (2005).
8. A. Bianco, K. Kostarelos, and M. Prato, Applications of carbon nanotubes in drug delivery, *Curr. Opin. Chem. Biol.*, **9**, 674 (2005).
9. N.W. Kam and H. Dai, Carbon nanotubes as intracellular protein transporters: Generality and biological functionality, *J. Am. Chem. Soc.*, **127**, 6021 (2005).
10. N.W. Kam, Z. Liu, and H. Dai, Functionalization of carbon nanotubes via cleavable disulfide bonds for efficient intracellular delivery of siRNA and potent gene silencing, *J. Am. Chem. Soc.*, **127**, 12492 (2005).
11. N.W. Kam, M. O'connell, J.A. Wisdom, and H. Dai, Carbon nanotubes as multifunctional biological transporters and near-infrared agents for selective cancer cell destruction, *Proc. Natl. Acad. Sci. USA*, **102**, 11600 (2005).
12. N.W. Kam, Z. Liu, and H. Dai, Carbon nanotubes as intracellular transporters for proteins and DNA: an investigation of the uptake mechanism and pathway, *Angew. Chem. Int. Ed. Engl.*, **45**, 577 (2006).
13. H. Ali-Boucetta, K.T. Al-Jamal, D. Mccarthy, M. Prato, A. Bianco, and K. Kostarelos, Multiwalled carbon nanotube-doxorubicin supramolecular complexes for cancer therapeutics, *Chem. Commun. (Camb.)*, **459** (2008).
14. A. Bianco, K. Kostarelos, and M. Prato, Opportunities and challenges of carbon-based nanomaterials for cancer therapy, *Expert Opin. Drug. Deliv.*, **5**, 331 (2008).
15. M. Prato, K. Kostarelos, and A. Bianco, Functionalized carbon nanotubes in drug design and discovery, *Acc. Chem. Res.*, **41**, 60 (2008).
16. K. Gonsalves, C. Halberstadt, C.T. Laurencin, and Nair L., Eds., *Biomedical Nanostructures*, Wiley-Interscience, Hoboken, NJ (2007).
17. V. Labhasetwar and D.L. Leslie-Pelecky, eds. *Biomedical Applications of Nanotechnology*, Wiley-VCH, Hoboken, NJ (2007).
18. O. Salata, Applications of nanoparticles in biology and medicine, *J. Nanobiotechnology*, **2**, 3 (2004).
19. G.A. Urban, ed. *BioMEMS*, Springer: Dordrecht (2006).
20. M.T. Castaneda, A. Merkoci, M. Pumera, and S. Alegret, Electrochemical genosensors for biomedical applications based on gold nanoparticles, *Biosens. Bioelectron.*, **22**, 1961 (2007).
21. A. Merkoci, Electrochemical biosensing with nanoparticles, *FEBS. J.*, **274**, 310 (2007).
22. O. Shoseyov and I. Levy, Eds., *NanoBioTechnology: Bioinspired devices and materials of the future* Humana Press: Totowa, NJ (2008).
23. B. Dubertret, P. Skourides, D.J. Norris, V. Noireaux, A.H. Brivanlou, and A. Libchaber, In vivo imaging of quantum dots encapsulated in phospholipid micelles, *Science*, **298**, 1759 (2002).
24. Z. Saiyed, S. Telang, and C. Ramchand, Application of magnetic techniques in the field of drug discovery and biomedicine, *Biomagn. Res. Technol.*, **1**, 2 (2003).
25. P. Tartaj, Probing nanomagnets' interactions inside colloidal superparamagnetic composites: aerosol versus surface template methods, *Chemphyschem.*, **4**, 1371 (2003).
26. P. Tartaj and C.J. Serna, Synthesis of monodisperse superparamagnetic Fe/silica nanospherical composites, *J. Am. Chem. Soc.*, **125**, 15754 (2003).
27. M.K. So, A.M. Loening, S.S. Gambhir, and J. Rao, Creating self-illuminating quantum dot conjugates, *Nat. Protoc.*, **1**, 1160 (2006).
28. M.K. So, C. Xu, A.M. Loening, S.S. Gambhir, and J. Rao, Self-illuminating quantum dot conjugates for in vivo imaging, *Nat. Biotechnol.*, **24**, 339 (2006).
29. G. Brumfiel, Nanotechnology: A little knowledge, *Nature*, **424**, 246 (2003).
30. G. Brumfiel, Hydrogen cars fuel debate on basic research, *Nature*, **422**, 104 (2003).
31. V.L. Colvin, The potential environmental impact of engineered nanomaterials, *Nat. Biotechnol.*, **21**, 1166 (2003).
32. P.H. Hoet, A. Nemmar, and B. Nemery, Health impact of nanomaterials?, *Nat. Biotechnol.*, **22**, 19 (2004).
33. P.H. Hoet, Bruske-I. Hohlfeld, and O.V. Salata, Nanoparticles - known and unknown health risks, *J. Nanobiotechnology*, **2**, 12 (2004).
34. F. Proffitt, Nanotechnology. Yellow light for nanotech, *Science*, **305**, 762 (2004).
35. R.F. Service, Nanotoxicology. Nanotechnology grows up, *Science*, **304**, 1732 (2004).
36. A.D. Maynard, R.J. Aitken, T. Butz, V. Colvin, K. Donaldson, G. Oberdorster, M.A. Philbert, J. Ryan, A. Seaton, V. Stone, S.S. Tinkle, L. Tran, N.J. Walker, and D.B. Warheit, Safe handling of nanotechnology, *Nature*, **444**, 267 (2006).
37. A. Nel, T. Xia, L. Madler, and N. Li, Toxic potential of materials at the nanolevel, *Science*, **311**, 622 (2006).
38. R.H. Hurt, M. Monthioux, and A. Kane, Toxicology of carbon nanomaterials: Status, trends, and perspectives on the special issue, *Carbon*, 44 (2006).
39. J.E. Riviere, ed. *Biological concepts and techniques in toxicology: An integrated approach*, Taylor & Francis: New York (2006).
40. O. Shenderova and D. Gruen, eds. *Ultrananocrystalline Diamond*, William-Andrew, Norwich, NY (2006).
41. W.C.W. Chan, Ed. *Bio-applications of nanoparticles*, Landes Bioscience/Springer Science + Business Media, Austin, TX 2007.
42. C. Kumar, ed. *Nanotechnologies for the life sciences Vol. 10: Nanomaterials for medical diagnosis and therapy"* Wiley-VCH Verlag GmbH & Co. KgaA, New York (2007).
43. N.A. Monteiro-Riviere and C.L. Tran, eds. *Nanotoxicology: Characterization, dosing and health effects* Informa Healthcare, New York (2007).
44. M.R. Mozafari, ed. *Nanomaterials and nanosystems for biomedical applications*, Springer Publish Info Dordrecht: The Netherlands 2007.

45. Y. Zhao and H.S. Nalwa, Eds., *Nanotoxicology: Interactions of nanomaterials with biological systems*, American Scientific, Stevenson Ranch, CA (2007).
46. R.C. Murdock, L. Braydich-Stolle, A.M. Schrand, J.J. Schlager, and S.M. Hussain, Characterization of nanomaterial dispersion in solution prior to in vitro exposure using dynamic light scattering technique, *Toxicol. Sci.*, **101**, 239 (2008).
47. A.M. Schrand, J. Johnson, L. Dai, S.M. Hussain, J.J. Schlager, L. Zhu, Y. Hong, and E. Ôsawa, Cytotoxicity and genotoxicity of carbon nanomaterials, in *Safety of nanoparticles: from manufacturing to clinical applications*, Webster, T., Ed., Springer Publishing, Brown University, Providence, RI (2008).
48. D.M. Gruen, Nanocrystalline diamond films, *Annu. Revi. Mater. Sci.*, **29**, 211 (1999).
49. V.Y. Dolmatov, Detonation synthesis ultradispersed diamonds: Properties and applications, *Russ. Chem. Rev.*, **70**, 607 (2001).
50. M. Baidakova and A. Vul, New prospects and frontiers of nanodiamond clusters, *J. Physics D-Appl. Physics*, **40**, 6300 (2007).
51. K.B. Holt, Diamond at the nanoscale: Applications of diamond nanoparticles from cellular biomarkers to quantum computing, *Philos. Transact. A Math Phys. Eng. Sci.*, **365**, 2845 (2007).
52. V.Y. Dolmatov, Detonation nanodiamonds: Synthesis, structure, properties and applications, *USPEKHI KHIMII*, **76**, 375 (2007).
53. A. Krueger, New carbon materials: Biological applications of functionalized nanodiamond materials, *Chem. Eur. J.*, **14**, 1382 (2008).
54. A. Krueger, Diamond nanoparticles: Jewels for chemistry and physics, *Adv. Mater*, **20**, 2445 (2008).
55. A.L. Vereschagin, *Detonation nanodiamonds*, Altai State Technical University, Barnaul, Russian Federation (2001).
56. V.V. Danilenko, *Synthesis and sintering of diamond by detonation*, Energoatomizdat (2003).
57. G. Benedek, P. Milani, and V.G. Ralchenko, *Nanostructured carbon for advanced applications*, ed. Series, N.S., Vol. 24, Kluwer Academic Publishing, Dordrecht (2001).
58. P.I. Belobrov, Nature of nanodiamond state and new applications of diamond nanotechnology, in: *Proceedings of the IX International Conference: High-tech for Russian Industry*, Moscow, Russia (2003).
59. A. Vul, V. Dolmatov, and O. Shenderova, *Detonation nanodiamonds and related materials*. First Edition ed., FIZINTEL, St. Petersburg, Russia (2003).
60. D.M. Gruen, O.A. Shenderova, and A.Y. Vul, *Synthesis, properties, and applications of ultrananocrystallline diamond*, Springer, Dordrecht, The Netherlands (2005).
61. Advanced Diamond Technology, I.W.T.C., Romeoville, IL,
62. P. Bajaj, D. Akin, A. Gupta, D. Sherman, B. Shi, O. Auciello, and R. Bashir, Ultrananocrystalline diamond film as an optimal cell interface for biomedical applications, *Biomed. Microdevices*, **9**, 787 (2007).
63. W.S. Yang, O. Auciello, J.E. Butler, W. Cai, J.A. Carlisle, J. Gerbi, D.M. Gruen, T. Knickerbocker, T.L. Lasseter, J.N. Russell, L.M. Smith, and R.J. Hamers, DNA-modified nanocrystalline diamond thin-films as stable, biologically active substrates, *Nature Mater.*, **1**, 253 (2002).
64. Microdiamant Ag, L., Switzerland, www.microdiamant.com.
65. V.V. Danilenko, On the history of the discovery of nanodiamond synthesis, *Phys. Solid State*, **46**, 595 (2004).
66. A.L. Vereschagin, *Properties of detonation nanodiamonds*, Barnaul State Technical University, Altay Region (2005).
67. *The 3rd International Symposium Detonation Nanodiamonds: Technology, Properties and Applications*, St. Petersburg, Russia (2008).
68. Y. Gogotsi, S. Welz, D.A. Ersoy, and M.J. Mcnallan, Conversion of silicon carbide to crystalline diamond-structured carbon at ambient pressure, *Nature*, **411**, 283 (2001).
69. T.L. Daulton, M.A. Kirk, R.S. Lewis, and L.E. Rehn, Production of nanodiamonds by high-energy ion irradiation of graphite at room temperature, *Nucl. Instr. Meth. Phys. Res. S. B-Beam Inter. Mat. At.*, **175**, 12 (2001).
70. F. Banhart and P.M. Ajayan, Carbon onions as nanoscopic pressure cells for diamond formation, *Nature*, **382**, 433 (1996).
71. M. Frenklach, W. Howard, D. Huang, J. Yuan, K.E. Spear, and R. Koba, Induced nucleation of diamond powder, *Appl. Phys. Lett.*, **59**, 546 (1991).
72. A. Tielens, C.G. Seab, D.J. Hollenbach, and C.F. Mckee, Shock processing of interstellar dust—Diamonds in the sky, *Astrophysical J.*, **319**, L109 (1987).
73. T.L. Daulton, Extraterrestrial nanodiamonds in the cosmos, In: *Ultrananocrystalline diamond*, William-Andrew: Norwich, UK (2006).
74. J.R. Rabeau, A. Stacey, A. Rabeau, S. Prawer, F. Jelezko, I. Mirza, and J. Wrachtrup, Single nitrogen vacancy centers in chemical vapor deposited diamond nanocrystals, *Nano. Lett.*, **7**, 3433 (2007).
75. S.J. Yu, M.W. Kang, H.C. Chang, K.M. Chen, and Y.C. Yu, Bright fluorescent nanodiamonds: no photobleaching and low cytotoxicity, *J. Am. Chem. Soc.*, **127**, 17604 (2005).
76. C.C. Fu, H.Y. Lee, K. Chen, T.S. Lim, H.Y. Wu, P.K. Lin, P.K. Wei, P.H. Tsao, H.C. Chang, and W. Fann, Characterization and application of single fluorescent nanodiamonds as cellular biomarkers, *Proc. Natl. Acad. Sci. USA*, **104**, 727 (2007).
77. Y. Sonnefraud, A. Cuche, O. Faklaris, J.P. Boudou, T. Sauvage, J.F. Roch, F. Treussart, and S. Huant, Diamond nanocrystals hosting single nitrogen-vacancy color centers sorted by photon-correlation near-field microscopy, *Opt. Lett.*, **33**, 611 (2008).
78. P.S. Decarli and J.C. Jamieson, Formation of diamond by explosive shock, *Science*, **133**, 1821 (1961).
79. V.V. Danilenko, Thermal stability of detonation nanodiamond depending on their quality, *Super Hard Mat.* **31**(4), in press (2009).
80. H. Huang, E. Pierstorff, E. Osawa, and D. Ho, Active nanodiamond hydrogels for chemotherapeutic delivery, *Nano. Lett.*, **7**, 3305 (2007).
81. V.S. Bondar, I.O. Pozdnyakova, and A.P. Puzyr, Applications of nanodiamonds for separation and purification of proteins, *Phy. Solid State*, **46**, 758 (2004).
82. L.C. Huang and H.C. Chang, Adsorption and immobilization of Cytochrome c on nanodiamonds, *Langmuir*, **20**, 5879 (2004).
83. X.L. Kong, L.C. Huang, C.M. Hsu, W.H. Chen, C.C. Han, and H.C. Chang, High-affinity capture of proteins by diamond nanoparticles for mass spectrometric analysis, *Anal. Chem.*, **77**, 259 (2005).

84. X. Kong, L.C. Huang, S.C. Liau, C.C. Han, and H.C. Chang, Polylysine-coated diamond nanocrystals for MALDI-TOF mass analysis of DNA oligonucleotides, *Anal. Chem.*, **77**, 4273 (2005).
85. V. Grichko, V. Grishko, and O. Shenderova, Nanodiamond bullets and their biological targets, *Nanobiotechnology*, **2**, 37 (2007).
86. N. Gibson, O. Shenderova, A. Puzyr, K. Purtov, V. Grichko, T.J.M. Luo, Z. Fitgerald, V. Bondar, and D. Brenner, Nanodiamonds for detoxification, In: *Technical Proceedings of the 2007 NSTI NanoTechnology Conference and Trade Show* (2007).
87. A.P. Puzyr, K.V. Purtov, O.A. Shenderova, M. Luo, D.W. Brenner, and V.S. Bondar, The adsorption of aflatoxin B1 by detonation-synthesis nanodiamonds, *Dokl. Biochem. Biophys*, **417**, 299 (2007).
88. J.E. Dahl, S.G. Liu, and R.M.K. Carlson, Isolation and structure of higher diamondoids, nanometer-sized diamond molecules, *Science*, **299**, 96 (2003).
89. R.M.K. Carlson, J.E.P. Dahl, and S.G. Liu, Diamond molecules found in petroleum, In: *Synthesis, properties, and applications of ultrananocrystallline diamond*, Gruen, D.M., Vul, A., and Shenderova, O.A., (Eds.), Springer: Dordrecht, The Netherlands (2005).
90. R.A. Freitas, *Biocompatibility*, Nanomedicine, Vol. IIA, Landes Bioscience, Austin, TX (2003).
91. V. Grichko and O. Shenderova, Nanodiamond designing the bioplatform, In: *Ultrananocrystalline diamond: Synthesis, properties, and applications*, Shenderova, O. and Gruen, D., (Eds.), William-Andrew: Norwich, UK, pp. 529–557 (2006).
92. V. Dolmatov, In *Third International Symposium Detonation Nanodiamonds: Technology, Properties and Applications*, St. Petersburg, Russia (2008).
93. T. Gubarevich, In: *Third International Symposium Detonation Nanodiamonds: Technology, Properties and Applications*, St. Petersburg, Russia (2008).
94. I. Larionova, V. Kuznetsov, A. Frolov, O. Shenderova, S. Moseenkov, and I. Mazov, Properties of individual fractions of detonation nanodiamond, *Diamond Relat. Mater.*, **15**, 1804 (2006).
95. A. Krueger and T. Boedeker, Deagglomeration and functionalization of detonation nanodiamonds, *Diamond Relat. Mater.*, **17**, 1367 (2008).
96. F. Neugart, A. Zappe, F. Jelezko, C. Tietz, J.P. Boudou, A. Krueger, and J. Wrachtrup, Dynamics of diamond nanoparticles in solution and cells, *Nano Lett.*, **7**, 2588 (2007).
97. A. Krueger, J. Stegk, Y. Liang, L. Lu, and G. Jarre, Biotinylated nanodiamond: Simple and efficient functionalization of detonation diamond, *Langmuir*, **24**, 4200 (2008).
98. V.V. Danilenko, Shock-wave sintering of nanodiamonds, *Phys. Solid State*, **46**, 711 (2004).
99. J.A. Viecelli and F.H. Ree, Carbon particle phase transformation kinetics in detonation waves, *J. Appl. Phys.*, **88**, 683 (2000).
100. V.M. Titov, B.P. Tolochko, K.A. Ten, L.A. Lukyanchikov, and E.R. Pruuel, Where and when are nanodiamonds formed under explosion?, *Diamond Relat. Mater.*, **16**, 2009 (2007).
101. V.V. Danilenko, Peculiarities of carbon condensation in a detonation wave and conditions of nanodiamonds optimal synthesis, *Superhard Mater.*, N5, **9** (2006).
102. J.Y. Raty, G. Galli, C. Bostedt, Van T.W. Buuren, and L.J. Terminello, Quantum confinement and fullerenelike surface reconstructions in nanodiamonds, *Phys. Rev. Lett.*, **90**, 037401 (2003).
103. S. Osswald, G. Yushin, V. Mochalin, S.O. Kucheyev, and Y. Gogotsi, Control of sp2/sp3 carbon ratio and surface chemistry of nanodiamond powders by selective oxidation in air, *J. Am. Chem. Soc.*, **128**, 11635 (2006).
104. V. Pichot, M. Comet, E. Fousson, C. Baras, A. Senger, F. Le Normand, and D. Spitzer, An efficient purification method for detonation nanodiamonds, *Diamond Relat. Mater.*, **17**, 13 (2008).
105. I. Petrov and O. Shenderova, History of Russian patents on detonation nanodiamonds, In: *Ultrananocrystalline diamond*, Shenderova, O. and Gruen, D., (Eds.), William-Andrew: Norwich, UK 2006.
106. I. Petrov, O. Shenderova, V. Grishko, V. Grichko, T. Tyler, G. Cunningham, and G. Mcguire, Detonation nanodiamonds simultaneously purified and modified by gas treatment, *Diamond Relat. Mater.*, **16**, 2098 (2007).
107. A.S. Chiganov, Selective inhibition of the oxidation of nanodiamonds for their cleaning, *Phys. Solid State*, **46**, 620 (2004).
108. V.Y. Dolmatov, M.V. Veretennikova, V.A. Marchukov, and V.G. Sushchev, Currently available methods of industrial nanodiamond synthesis, *Phys. Solid State*, **46**, 611 (2004).
109. I.S. Larionova, I.N. Molostov, L.S. Kulagina, and V.F. Komarov, *Method of purification of synthetic ultradispersed diamonds*, RU Patent 2168462 (1999).
110. E.V. Pavlov and J.A. Skrjabin, *Method for removal of impurities of non-diamond carbon and device for its realization*, RU Patent 2019502 (1994).
111. D. Mitev, R. Dimitrova, M. Spassova, C. Minchev, and S. Stavrev, Surface peculiarities of detonation nanodiamonds in dependence of fabrication and purification methods, *Diamond Relat. Mater.*, **16**, 776 (2007).
112. O. Shenderova, I. Petrov, J. Walsh, V. Grichko, V. Grishko, T. Tyler, and G. Cunningham, Modification of detonation nanodiamonds by heat treatment in air, *Diamond Relat. Mater.*, **15**, 1799 (2006).
113. V. Mochalin and Y. Gogotsi, Wet chemistry route to hydrophobic blue fluorescent nanodiamond, *J. Am. Chem. Soc.*, **131**(13), 4594 (2009).
114. V.T. Timofeev and P.Y. Detkov, Diamonds from explosive materials, *Atom*, **4**, 1 (2005).
115. A. Krueger, F. Kataoka, M. Ozawa, T. Fujino, Y. Suzuki, A.E. Aleksenskii, A.Y. Vul, and E. Osawa, Unusually tight aggregation in detonation nanodiamond: Identification and disintegration, *Carbon*, **43**, 1722 (2005).
116. I. Larinova, I. Petrov, and O. Shenderova, Zeta potential of detonation nanodiamonds depending on method of purification, in preparation.
117. S.K. Gordeev and S. Kruglikova, *Method of processing of powders of nanodiamond for obtaining stable suspensions*, RU Patent Application 2004121069 (2004).
118. X.Y. Xu, Z.M. Yu, Y.W. Zhu, and B.C. Wang, Influence of surface modification adopting thermal treatments on dispersion of detonation nanodiamond, *J. Solid State Chem.*, **178**, 688 (2005).
119. B. Spitsyn, J. Davidson, M. Gradoboev, T. Galushko, N. Serebryakova, T. Karpukhina, I. Kulakova, and M. Melnik, Inroad to

modification of detonation nanodiamond, *Diamond Relat. Mater.*, **15**, 296 (2006).
120. S.I. Chukhaeva, P. Detkov, A. Tkachenko, and A. Toropov, Physicochemical properties of fractions isolated from ultradispersed diamonds, *SVERKHTVERD MAT*, **4**, 29 (1998).
121. S.I. Chukhaeva, Synthesis, properties, and applications of fractionated nanodiamonds, *Phys. Solid State*, **46**, 625 (2004).
122. V. Grichko, T. Tyler, V.I. Grishko, and O. Shenderova, Nanodiamond particles forming photonic structures, *Nanotechnology*, **19**, 225201 (2008).
123. K. Iakoubovskii, K. Mitsuishi, and K. Furuya, High-resolution electron microscopy of detonation nanodiamond, *Nanotechnology*, **19**, 155705 (2008).
124. A. Krueger, M. Ozawa, G. Jarre, Y. Liang, J. Stegk, and L. Lu, Deagglomeration and functionalisation of detonation diamond, *Physica Status Solidi a-Appli. Mater. Sci.*, **204**, 2881 (2007).
125. Y.W. Zhu, F. Xu, J.L. Shen, B.C. Wang, X.Y. Xu, and J.B. Shao, Study on the modification of nanodiamond with DN-10, *J. Mater. Sci. Technol.*, **23**, 599 (2007).
126. Y. Morita, T. Takimoto, H. Yamanaka, K. Kumekawa, S. Morino, S. Aonuma, T. Kimura, and N. Komatsu, A Facile and scalable process for size-controllable separation of nanodiamond particles as small as 4 nm, *Small*, **4**, 2154 (2008).
127. M. Ozawa, M. Inaguma, M. Takahashi, F. Kataoka, A. Kruger, and E. Osawa, Preparation and behavior of brownish, clear nanodiamond colloids, *Adv. Mater.*, **19**, 1201 (2007).
128. A. Ozerin, T.S. Kurkin, L.A. Ozerina, and V.Y. Dolmatov, X-ray diffraction study of the structure of detonation nanodiamonds, *Crystallogr. Repo.*, **53**, 60 (2008).
129. E. Osawa, Recent progress and perspectives in single-digit nanodiamond, *Diamond Relat. Mater.*, **16**, 2018 (2007).
130. H.J. Huang, L.M. Dai, D.H. Wang, L.S. Tan, and E. Osawa, Large-scale self-assembly of dispersed nanodiamonds, *J. Mater. Chem.*, **18**, 1347 (2008).
131. K. Xu and Q.J. Xue, Deaggregation of ultradispersed diamond from explosive detonation by a graphitization-oxidation method and by hydroiodic acid treatment, *Diamond Relat. Mater.*, **16**, 277 (2007).
132. N. Gibson, O. Shenderova, T.J.M. Luo, S. Moseenkov, V. Bondar, A. Puzyr, K. Purtov, Z. Fitzgerald, and D. Brenner, Colloidal stability of modified nanodiamond particles, *Diamond Relat. Mater.*, **18**, 620 (2009).
133. S. Hens, S. Wallen, and O. Shenderova, U.S. Patent Application: Nanodiamond fractionation and products thereof (2007).
134. V.S. Bondar and A.P. Puzyr, Nanodiamonds for biological investigations, *Phys. Solid State*, **46**, 716 (2004)
135. A.P. Puzyr and V.S. Bondar, *Method of production of nanodiamonds of explosive synthesis with an increased colloidal stability*, RU Patent 2252192 (2003).
136. T. Tsubota, S. Tanii, S. Ida, M. Nagata, and Y. Matsumoto, Chemical modification of diamond surface with various carboxylic acids by radical reaction in liquid phase, *Diamond Relat. Mater.*, **13**, 1093 (2004).
137. T. Tsubota, T. Ohno, H. Yoshida, and K. Kusakabe, Introduction of molecules containing a NO_2 group on diamond surface by using radical reaction in liquid phase, *Diamond Relat. Mater.*, **15**, 668 (2006).
138. S. Ida, T. Tsubota, S. Tanii, M. Nagata, and Y. Matsumoto, Chemical modification of the diamond surface using benzoyl peroxide and dicarboxylic acids, *Langmuir*, **19**, 9693 (2003).
139. Y. Liu, Z.N. Gu, J.L. Margrave, and V.N. Khabashesku, Functionalization of nanoscale diamond powder: Fluoro-, alkyl-, amino-, and amino acid-nanodiamond derivatives, *Chem. Mater.*, **16**, 3924 (2004).
140. V.F. Loktev, V.I. Makalskii, and I.V. Stoyanova, Surface modification of ultradispersed diamonds, *Carbon*, **29**, 817 (1991).
141. Z. Remes, A. Kromka, M. Vanecek, A. Grinevich, H. Hartmannova, and S. Kmoch, The RF plasma surface chemical modification of nanodiamond films grown on glass and silicon at low temperature, *Diamond Relat. Mater.*, **16**, 671 (2007).
142. M.A. Ray, T. Tyler, B. Hook, A. Martin, G. Cunningham, O. Shenderova, J.L. Davidson, M. Howell, W.P. Kang, and G. Mcguire, Cool plasma functionalization of nano-crystalline diamond films, *Diamond Relat. Mater.*, **16**, 2087 (2007).
143. Lisichkin, G. V. Korolkov, Tarasevich, B. I. Kulakova and Karpukhin, A. Photochemical chlorination of nanodiamond and interaction of its modified surface with C-nucleophiles, *Russ. Chem. Bull.*, **55**, 2212 (2006).
144. Kulakova, Ii, Surface chemistry of nanodiamonds, *Phys. Solid State*, **46**, 636 (2004).
145. A. Krueger, Y.J. Liang, G. Jarre, and J. Stegk, Surface functionalisation of detonation diamond suitable for biological applications, *Journal of Materials Chemistry*, **16**, 2322 (2006).
146. S.C. Hens, G. Cunningham, T. Tyler, S. Moseenkov, V. Kuznetsov, and O. Shenderova, Nanodiamond bioconjugate probes and their collection by electrophoresis, *Diamond Relat. Mater.*, **17**, 1858 (2008).
147. L. Li, Van Der A.E. Ende, J.L. Davidson, and C.M. Lukehart, Nanodiamond/polymer brushes: Synthesis, characterization and application, *Abstr. Papers Am. Chem. Soc.*, 231 (2006).
148. A. Krueger, The structure and reactivity of nanoscale diamond, *J. Mater. Chem.*, **18**, 1485 (2008).
149. S. Ji, T. Jiang, K. Xu, and S. Li, FTIR study of the adsorption of water on ultradispersed diamond powder surface, *Appl. Surface Sci.*, **133**, 231 (1998).
150. T. Jiang and K. Xu, FTIR study of ultradispersed diamond powder synthesized by explosive detonation, *Carbon*, **33**, 1663 (1995).
151. T. Jiang, K. Xu, and S. Ji, FTIR studies on the specrtral changes of the surface functional groups of ultradispersed diamond powder synthesized by explosive detonation after treatment in hydrogen, nitrogen, methane and air at different temperatures, *Faraday Trans.*, **92**, 3401 (1996).
152. T.C. Kuo, R.L. McCreery, and G.M. Swain, Electrochemical modification of boron-doped chemical vapor deposited diamond surfaces with covalently bonded monolayers, *Electrochem. Solid State Lett.*, **2**, 288 (1999).
153. A.E. Aleksenskii, V.Y. Osipov, A.Y. Vul, B.Y. Ber, A.B. Smirnov, V.G. Melekhin, G.J. Adriaenssens, and K. Lakoubovskii, Optical properties of nanodiamond layers, *Phys. Solid State*, **43**, 145 (2001).
154. N. Komatsu, N. Kadota, T. Kimura, and E. Osawa, Solution-phase C-13 NMR spectroscopy of detonation nanodiamond, *Chem. Lett.*, **36**, 398 (2007).
155. G.A. Chiganova, Aggregation of particles in ultradispersed diamond hydrosols, *Colloid J.*, **62**, 238 (2000).

156. X. Xua, Z. Yu, Y. Zhu, and B. Wang, Effect of sodium oleate adsorption on the colloidal stability and zeta potential of detonation synthesized diamond particles in aqueous solutions, *Diamond Relat. Mater.*, **14**, 206 (2005).
157. H.P. Boehm, Surface oxides on carbon and their analysis: a critical assessment, *Carbon*, **40**, 145 (2002).
158. E. Fuente, J.A. Menendez, D. Suarez, and Montes-M.A. Moran, Basic surface oxides on carbon materials: A global view, *Langmuir*, **19**, 3505 (2003).
159. J.B. Donnet, H.P. Boehm, and F. Stoeckli, Third International Conference on Carbon Black Mulhouse (October 2000) - Preface, *Carbon*, **40**, 145 (2002).
160. M.A. Montes-Moran, D. Suarez, J.A. Menendez, and E. Fuente, On the nature of basic sites on carbon surfaces: An overview, *Carbon*, **42**, 1219 (2004).
161. O. Shenderova, V. Grichko, S. Hens, and J. Walsh, Detonation nanodiamonds as UV radiation filter, *Diamond Relat. Mater.*, **16**, 2003 (2007).
162. A.E. Aleksenskii, M.V. Baidakova, A.Y. Vul, and V.I. Siklitskii, The structure of diamond nanoclusters, *Phys. Solid State*, **41**, 668 (1999).
163. S. Sque, R. Jones, and P. Briddon, Structure, electronics, and interaction of hydrogen and oxygen on diamond surfaces, *Phys. Rev. B*, **73**, 85313 (2006).
164. G. Kern and J. Hafner, Ab initio calculations of the atomic and electronic structure of clean and hydrogenated diamond (110) surfaces, *Phys. Rev. B*, **56**, 4203 (1997).
165. V. Borjanovic, W.G. Lawrence, S. Hens, M. Jaksic, I. Zamboni, C. Edson, V. Vlasov, O. Shenderova, and G. Mcguire, Effect of proton irradiation on photoluminescent properties of PDMS nanodiamond composites, *Nanotechnology* **19**, 455701 (2008).
166. A.V. Kvit, V.V. Zhirnov, T. Tyler, and J.J. Hren, Aging effect and nitrogen distribution in diamond nanoparticles, *Composites Part B-Engin.*, **35**, 163 (2004).
167. Y.R. Chang, H.Y. Lee, K. Chen, C.C. Chang, D.S. Tsai, C.C. Fu, T.S. Lim, Y.K. Tzeng, C.Y. Fang, C.C. Han, H.C. Chang, and W. Fann, Mass production and dynamic imaging of fluorescent nanodiamonds, *Nat. Nanotechnol.*, **3**, 284 (2008).
168. A.M. Schrand, H. Huang, C. Carlson, J.J. Schlager, Omacr E. Sawa, S.M. Hussain, and L. Dai, Are diamond nanoparticles cytotoxic?, *J. Phys. Chem. B*, **111**, 2 (2007).
169. V.Y. Dolmatov, Application of detonation nanodiamond, in: *Ultra nanocrystalline diamond: synthesis, properties, and applications*, O. Shenderova and D. Gruen (Eds.), William Andrew Publishing: Norwich, NY, USA, 513 (2006).
170. A.P. Puzyr, A.V. Baron, K.V. Purtov, E.V. Bortnikov, N.N. Skobelev, O.A. Moginaya, and V.S. Bondar, Nanodiamonds with novel properties: A biological study, *Diamond Relat. Mater.*, **16**, 2124 (2007).
171. J.E. Skebo, C.M. Grabinski, A.M. Schrand, J.J. Schlager, and S.M. Hussain, Assessment of metal nanoparticle agglomeration, uptake, and interaction using high-illuminating system, *Int. J. Toxicol.*, **26**, 135 (2007).
172. F. Treussart, V. Jacques, E. Wu, T. Gacoln, P. Grangier, and J.F. Roch, Photoluminescence of single colour defects in 50 nm diamond nanocrystals, *Physica B-Condensed Matter*, **376**, 926 (2006).
173. O. Faklaris, Y. Sonnefraud, A. Cuche, T. Sauvage, V. Joshi, J.P. Boudou, P.A. Curmi, J.F. Roch, S. Huant, and F. Treussart, Diamond nanoparticles as photoluminescent nanoprobes, *Annales De Physique*, **32**, 155 (2007).
174. C.Y. Cheng, E. Perevedentseva, J.S. Tu, P.H. Chung, C.L. Cheng, K.K. Liu, J.I. Chao, P.H. Chen, and C.C. Chang, Direct and in vitro observation of growth hormone receptor molecules in A549 human lung epithelial cells by nanodiamond labeling, *Appl. Phys. Lett.*, **90**, 163903 (2007).
175. E. Perevedentseva, C.Y. Cheng, P.H. Chung, J.S. Tu, Y.H. Hsieh, and C.L. Cheng, The interaction of the protein lysozyme with bacteria E. coli observed using nanodiamond labelling, *Nanotechnology*, **18**, 315102 (2007).
176. Y.T. Lim, S. Kim, A. Nakayama, N.E. Stott, M.G. Bawendi, and J.V. Frangioni, Selection of quantum dot wavelengths for biomedical assays and imaging, *Mol. Imaging*, **2**, 50 (2003).
177. T. Gaebel, I. Popa, A. Gruber, M. Domhan, F. Jelezko, and J. Wrachtrup, Stable single-photon source in the near infrared, *New J. Phys.*, 6 (2004).
178. A.M. Zaitsev, Vibronic spectra of impurity-related optical centers in diamond, *Phys. Rev. B*, **61**, 12909 (2000).
179. F. Jelezko and J. Wrachtrup, Single defect centres in diamond: A review, *Physica Status Solidi a-Appl. Mater. Sci.*, **203**, 3207 (2006).
180. A. Gruber, A. Drabenstedt, C. Tietz, L. Fleury, J. Wrachtrup, and C. Vonborczyskowski, Scanning confocal optical microscopy and magnetic resonance on single defect centers, *Science*, **276**, 2012 (1997).
181. M.E. Kompan, E.I. Terukov, S.K. Gordeev, S.G. Zhukov, and Y.A. Nikolaev, Photoluminescence spectra of ultradisperse diamond, *Phys. Solid State*, **39**, 1928 (1997).
182. A.E. Aleksenskii, V.Y. Osipov, N.A. Kryukov, V.K. Adamchuk, M.I. Abaev, S.P. Vul, and A.Y. Vul, Optical properties of layers of ultradisperse diamond obtained from an aqueous suspension, *Tech. Phys. Lett.*, **23**, 874 (1997).
183. V.S. Gorelik and I.A. Rakhmatullaev, Photoluminescence of diamond films and ultrafine diamond under UV laser excitation, *Inorganic Mater.*, **40**, 686 (2004).
184. F.L. Zhao, Z. Gong, S.D. Liang, N.S. Xu, S.Z. Deng, J. Chen, and H.Z. Wang, Ultrafast optical emission of nanodiamond induced by laser excitation, *Appl. Phys. Lett.*, **85**, 914 (2004).
185. Y. Dumeige, F. Treussart, R. Alleaume, T. Gacoin, J.F. Roch, and P. Grangier, Photo-induced creation of nitrogen-related color centers in diamond nanocrystals under femtosecond illumination, *J. Luminescence*, **109**, 61 (2004).
186. Y.D. Glinka, K.W. Lin, H.C. Chang, and S.H. Lin, Multiphoton-excited luminescence from diamond nanoparticles, *J. Phys. Chem. B*, **103**, 4251 (1999).
187. J.I. Chao, E. Perevedentseva, P.H. Chung, K.K. Liu, C.Y. Cheng, C.C. Chang, and C.L. Cheng, Nanometer-sized diamond particle as a probe for biolabeling, *Biophys. J.*, **93**, 2199 (2007).
188. K.K. Liu, C.L. Cheng, C.C. Chang, and J.I. Chao, Biocompatible and detectable carboxylated nanodiamond on human cell, *Nanotechnology*, 18 (2007).
189. P.H. Chung, E. Perevedentseva, and C.L. Cheng, The particle size-dependent photoluminescence of nanodiamonds, *Surface Sci.*, **601**, 3866 (2007).

190. T.L. Wee, Y.K. Tzeng, C.C. Han, H.C. Chang, W. Fann, J.H. Hsu, K.M. Chen, and Y.C. Yull, Two-photon excited fluorescence of nitrogen-vacancy centers in proton-irradiated type Ib diamond, *J. Phys. Chem. A*, **111**, 9379 (2007).
191. J. Martin, R. Wannemacher, J. Teichert, L. Bischoff, and B. Kohler, Generation and detection of fluorescent color centers in diamond with submicron resolution, *Appl. Phys. Lett.*, **75**, 3096 (1999).
192. C.L. Wang, C. Kurtsiefer, and H. Weinfurter, Single photon emission from SiV centres in diamond produced by ion implantation, *J. Phys. B- Atom. molec. opti. phys.*, **39**, 37 (2006).
193. A.M. Schrand, Characterization and in vitro biocompatibility of engineered nanomaterials, In: *The School of Engineering*, University of Dayton: Dayton, OH. pages 276 (2007).
194. A.M. Schrand, L.K. Braydich-Stolle, J.J. Schlager, S.M. Hussain, and L. Dai, Intracellular destination of fluorophore-conjugated nanodiamonds (in preparation) (2009).
195. S.C. Hens, G. Cunningham, V. Grichko, T. Tyler, S. Moseenkov, V. Kuznetsov, and G.M.O. Shenderova, Biological uses for chemically derivatized detonation nanodiamonds, in *Third International Symposium Detonation Nanodiamonds: Technology, Properties and Applications*, St. Petersburg, Russia (2008).
196. Y. Colpin, A. Swan, A.V. Zvyagin, and T. Plakhotnik, Imaging and sizing of diamond nanoparticles, *Optics Lett.*, **31**, 625 (2006).
197. B.R. Smith, M. Niebert, T. Plakhotnik, and A.V. Zvyagin, Transfection and imaging of diamond nanocrystals as scattering optical labels, *J. Luminescence*, **127**, 260 (2007).
198. E. Perevedentseva, A. Karmenyan, P.H. Chung, Y.T. He, and C.L. Cheng, Surface enhanced Raman spectroscopy of carbon nanostructures, *Surface Sci.*, **600**, 3723 (2006).
199. V.W.K. Wu, Adsorption reaction constants between nanosilica/nanodiamond and lysozyme molecule at pH=11.0, *Chem. Lett.*, **35**, 1380 (2006).
200. W.S. Yeap, Y.Y. Tan, and K.P. Loh, Using detonation nanodiamond for the specific capture of glycoproteins, *Anal. Chem.* (2008).
201. K.V. Purtov, A.P. Puzyr, and V.S. Bondar, Nanodiamond sorbents: new carriers for column chromatography of proteins, *Dokl. Biochem. Biophys.*, **419**, 72 (2008).
202. O.N. Fedyanina and P.N. Nesterenko, Investigation of the properties of sintered nanodiamonds as stationary phase for HPLC, in *Third International Symposium Detonation Nanodiamonds: Technology, Properties and Applications*: St. Petersburg, Russia (2008).
203. T.A. Railkar, W.P. Kang, H. Windischmann, A.P. Malshe, H.A. Naseem, J.L. Davidson, and W.D. Brown, A critical review of chemical vapor-deposited (CVD) diamond for electronic applications, *Crit. Revi. Solid State Mater. Sci.*, **25**, 163 (2000).
204. E. Fortin, Chane-J. Tune, D. Delabouglise, P. Bouvier, T. Livache, P. Mailley, B. Marcus, M. Mermoux, J.P. Petit, S. Szunerits, and E. Vieil, Interfacing boron doped diamond and biology: An insight on its use for bioanalytical applications, *Electroanalysis*, **17**, 517 (2005).
205. K. Bakowicz-Mitura, G. Bartosz, and S. Mitura, Influence of diamond powder particles on human gene expression, *Surface Coatings Technol.*, **201**, 6131 (2007).
206. A.P. Puzyr, I.O. Pozdnyakova, and V.S. Bondar, Design of a luminescent biochip with nanodiamonds and bacterial luciferase, *Phys. Solid State*, **46**, 761 (2004).
207. F.R. Kloss, M. Najam-Ul-Haq, M. Rainer, R. Gassner, G. Lepperdinger, C.W. Huck, G. Bonn, F. Klauser, X. Liu, N. Memmel, E. Bertel, J.A. Garrido, and D. Steinmuller-Nethl, Nanocrystalline diamond—an excellent platform for life science applications, *J. Nanosci. Nanotechnol.*, **7**, 4581 (2007).
208. M. Kalbacova, M. Kalbac, L. Dunsch, A. Kromka, M. Vanecek, B. Rezek, U. Hempel, and S. Kmoch, The effect of SWCNT and nano-diamond films on human osteoblast cells, *Physica Status Solidi B-Basic Solid State Phys.*, **244**, 4356 (2007).
209. M.P. Hughes, AC electrokinetics: Applications for nanotechnology, *Nanotechnology*, **11**, 124 (2000).
210. I. Zhitomirsky, Cathodic electrodeposition of ceramic and organoceramic materials. Fundamental aspects, *Adv. Colloid Interface Sci.*, **97**, 279 (2002).
211. A.N. Alimova, N.N. Chubun, P.I. Belobrov, P.Y. Detkov, and V.V. Zhirnov, Electrophoresis of nanodiamond powder for cold cathode fabrication, *J. Vacuum Sci. Technol. B*, **17**, 715 (1999).
212. I. Zhitomirsky, Cathodic electrophoretic deposition of diamond particles, *Mater. Lett.*, **37**, 72 (1998).
213. M. Daenen, O.A. Williams, J. D'haen, K. Haenen, and M. Nesladek, Seeding, growth and characterization of nanocrystalline diamond films on various substrates, *Physica Status Solidi a-Appli. Mater. Scie.*, **203**, 3005 (2006).
214. O.A. Williams, O. Douheret, M. Daenen, K. Haenen, E. Osawa, and M. Takahashi, Enhanced diamond nucleation on monodispersed nanocrystalline diamond, *Chem. Phys. Lett.*, **445**, 255 (2007).
215. A.M. Affoune, B.L.V. Prasad, H. Sato, and T. Enoki, Electrophoretic deposition of nanosized diamond particles, *Langmuir*, **17**, 547 (2001).
216. L.L. Riveros, D.A. Tryk, and C.R. Cabrera, Chemical purification and characterization of diamond nanoparticles for electrophoretically coated electrodes, *Rev. Adv. Mater. Sci.*, **10**, 256 (2005).
217. A. Kraft, Doped diamond: A compact review on a new, versatile electrode material, *Int. J. Electrochem. Sci.*, **2**, 355 (2007).
218. R.L. McCreery, Advanced carbon electrode materials for molecular electrochemistry, *Chem. Rev.*, **108**, 2646 (2008).
219. J.M. Halpern, S.T. Xie, G.P. Sutton, B.T. Higashikubo, C.A. Chestek, H. Lu, H.J. Chiel, and H.B. Martin, Diamond electrodes for neurodynamic studies in Aplysia californica, *Diamond Relat. Mater.*, **15**, 183 (2006).
220. C.E. Nebel, B. Rezek, D. Shin, H. Uetsuka, and N. Yang, Diamond for bio-sensor applications, *J. Phys. D-Appl. Phys.*, **40**, 6443 (2007).
221. V. Vermeeren, N. Bijnens, S. Wenmackers, M. Daenen, K. Haenen, O.A. Williams, M. Ameloot, A. Vandeven, P. Wagner, and L. Michiels, Towards a real-time, label-free, diamond-based DNA sensor, *Langmuir*, **23**, 13193 (2007).
222. W. Zhao, J.J. Xu, Q.Q. Qiu, and H.Y. Chen, Nanocrystalline diamond modified gold electrode for glucose biosensing, *Biosens. Bioelectr.*, **22**, 649 (2006).
223. K.B. Holt, C. Ziegler, D.J. Caruana, J. Zang, Millan-E.J. Barrios, J. Hu, and J.S. Foord, Redox properties of undoped 5 nm diamond nanoparticles, *Phys. Chem. Chem. Phys.*, **10**, 303 (2008).

224. I.A. Novoselova, E.N. Fedoryshena, E.V. Panov, A.A. Bochechka, and L.A. Romanko, Electrochemical properties of compacts of nano- and microdisperse diamond powders in aqueous electrolytes, *Phys. Solid State*, **46**, 748 (2004).
225. J.B. Zang, Y.H. Wang, S.Z. Zhao, L.Y. Bian, and J. Lu, Electrochemical properties of nanodiamond powder electrodes, *Diamond Relat. Mater.*, **16**, 16 (2007).
226. M.E. Napier and H.H. Thorp, Electrocatalytic oxidation of nucleic acids at electrodes modified with nylon and nitrocellulose membranes, *J. Fluorescence*, **9**, 181 (1999).
227. G. Oberdorster, J.N. Finkelstein, C. Johnston, R. Gelein, C. Cox, R. Baggs, and A.C. Elder, Acute pulmonary effects of ultrafine particles in rats and mice, *Res. Rep. Health Eff. Inst.*, 5 (2000).
228. K. Donaldson, D. Brown, A. Clouter, R. Duffin, W. Macnee, L. Renwick, L. Tran, and V. Stone, The pulmonary toxicology of ultrafine particles, *J. Aerosol. Med.*, **15**, 213 (2002).
229. L. Braydich-Stolle, S. Hussain, J.J. Schlager, and M.C. Hofmann, In vitro cytotoxicity of nanoparticles in mammalian germline stem cells, *Toxicol. Sci.*, **88**, 412 (2005).
230. S.M. Hussain, K.L. Hess, J.M. Gearhart, K.T. Geiss, and J.J. Schlager, In vitro toxicity of nanoparticles in BRL 3A rat liver cells, *Toxicol. In Vitro*, **19**, 975 (2005).
231. K. Donaldson, V. Stone, C.L. Tran, W. Kreyling, and P.J. Borm, Nanotoxicology, *Occup. Environ. Med.*, **61**, 727 (2004).
232. S. Foley, C. Crowley, M. Smaihi, C. Bonfils, B.F. Erlanger, P. Seta, and C. Larroque, Cellular localisation of a water-soluble fullerene derivative, *Biochem. Biophys. Res. Commun.*, **294**, 116 (2002).
233. G. Oberdorster, A. Maynard, K. Donaldson, V. Castranova, J. Fitzpatrick, K. Ausman, J. Carter, et al., Principles for characterizing the potential human health effects from exposure to nanomaterials: elements of a screening strategy, *Part Fibre Toxicol*, **2**, 8 (2005).
234. A.E. Gulyaev, S.E. Gelperina, I.N. Skidan, A.S. Antropov, G.Y. Kivman, and J. Kreuter, Significant transport of doxorubicin into the brain with polysorbate 80-coated nanoparticles, *Pharm. Res.*, **16**, 1564 (1999).
235. P. Calvo, B. Gouritin, I. Brigger, C. Lasmezas, J. Deslys, A. Williams, J.P. Andreux, D. Dormont, and P. Couvreur, PEGylated polycyanoacrylate nanoparticles as vector for drug delivery in prion diseases, *J. Neurosci. Methods*, **111**, 151 (2001).
236. J. Kreuter, Nanoparticulate systems for brain delivery of drugs, *Adv. Drug. Deliv. Rev.*, **47**, 65 (2001).
237. G. Oberdorster, Z. Sharp, A.P. Elder, R. Gelein, W. Kreyling, and C. Cox, Translocation of inhaled ultrafine particles to the brain, *Inhal. Toxicol.*, **16**, 437 (2004).
238. H.F. Wang, Y. Hu, W.Q. Sun, and C.S. Xie, Polylactic acid nanoparticles across the brain-blood barrier observed with analytical electron microscopy, *Sheng Wu Gong Cheng Xue Bao.*, **20**, 790 (2004).
239. A. Elder, R. Gelein, V. Silva, T. Feikert, L. Opanashuk, J. Carter, R. Potter, et al., Translocation of inhaled ultrafine manganese oxide particles to the central nervous system, *Environ. Health Perspect.*, **114**, 1172 (2006).
240. S. Kashiwada, Distribution of nanoparticles in the see-through medaka (Oryzias latipes), *Environ. Health Perspect.*, **114**, 1697 (2006).
241. F.A. Barile, P.J. Dierickx, and U. Kristen, In vitro cytotoxicity testing for prediction of acute human toxicity, *Cell. Biol. Toxicol.*, **10**, 155 (1994).
242. G. Eisenbrand, B. Pool-Zobel, V. Baker, M. Balls, B.J. Blaauboer, A. Boobis, A. Carere, et al., Methods of in vitro toxicology, *Food Chem. Toxicol.*, **40**, 193 (2002).
243. C.W. Lam, J.T. James, R. Mccluskey, and R.L. Hunter, Pulmonary toxicity of single-wall carbon nanotubes in mice 7 and 90 days after intratracheal instillation, *Toxicol. Sci.*, **77**, 126 (2004).
244. D.B. Warheit, B.R. Laurence, K.L. Reed, D.H. Roach, G.A. Reynolds, and T.R. Webb, Comparative pulmonary toxicity assessment of single-wall carbon nanotubes in rats, *Toxicol. Sci.*, **77**, 117 (2004).
245. A.A. Shvedova, E.R. Kisin, R. Mercer, A.R. Murray, V.J. Johnson, A.I. Potapovich, Y.Y. Tyurina, et al., Unusual inflammatory and fibrogenic pulmonary responses to single-walled carbon nanotubes in mice, *Am. J. Physiol. Lung. Cell Mol. Physiol.*, **289**, L698 (2005).
246. A.M. Schrand, L. Dai, J.J. Schlager, S.M. Hussain, and E. Ôsawa, Differential biocompatibility of carbon nanotubes and nanodiamonds, *Diamond Relat. Mater.* **16**, 2118 (2007).
247. A. Swan, B. Dularay, and P. Dieppe, A comparison of the effects of urate, hydroxyapatite and diamond crystals on polymorphonuclear cells: Relationship of mediator release to the surface area and adsorptive capacity of different particles, *J. Rheumatol.*, **17**, 1346 (1990).
248. S.L. Brown, S.M. Brett, M. Gough, J.V. Rodricks, R.G. Tardiff, and D. Turnbull, Review of interspecies risk comparisons, *Regul. Toxicol. Pharmacol.*, **8**, 191 (1988).
249. R.L. Brent, Utilization of juvenile animal studies to determine the human effects and risks of environmental toxicants during postnatal developmental stages, *Birth Defects Res. B Dev. Reprod Toxicol.*, **71**, 303 (2004).
250. R.L. Brent, Utilization of animal studies to determine the effects and human risks of environmental toxicants (drugs, chemicals, and physical agents), *Pediatrics*, **113**, 984 (2004).
251. E.D. Kuempel, Estimating nanoparticle dose in humans: Issues and challenges In: *Nanotoxicology: Characterization, dosing, and health effects* Tran, M.-R.a., Ed., Informa Healthcare, New York, 141 (2007).
252. B. Asgharian and O.T. Price, Deposition of ultrafine (NANO) particles in the human lung, *Inhalation Toxicol.*, **19**, 1045 (2007).
253. L. Dai, Ed., *Carbon nanotechnology: Recent developments in chemistry, physics, materials science and device applications*, Elsevier, Amsterdam (2006).
254. A.A. Shvedova, V. Castranova, E.R. Kisin, Schwegler-D. Berry, A.R. Murray, V.Z. Gandelsman, A. Maynard, and P. Baron, Exposure to carbon nanotube material: assessment of nanotube cytotoxicity using human keratinocyte cells, *J. Toxicol. Environ. Health A*, **66**, 1909 (2003).
255. S. Garibaldi, C. Brunelli, V. Bavastrello, G. Ghigliotti, and C. Nicolini, Carbon nanotube biocompatibility with cardiac muscle cells, *Nanotechnology*, **17**, 391 (2006).
256. V.E. Kagan, Y.Y. Tyurina, V.A. Tyurin, N.V. Konduru, A.I. Potapovich, A.N. Osipov, E.R. Kisin, et al., Direct and indirect effects of single walled carbon nanotubes on RAW 264.7 macrophages: role of iron, *Toxicol. Lett.*, **165**, 88 (2006).

257. K. Pulskamp, S. Diabate, and H.F. Krug, Carbon nanotubes show no sign of acute toxicity but induce intracellular reactive oxygen species in dependence on contaminants, *Toxicol. Lett.*, **168**, 58 (2007).
258. P. Wick, P. Manser, L.K. Limbach, U. Dettlaff-Weglikowska, F. Krumeich, S. Roth, W.J. Stark, and A. Bruinink, The degree and kind of agglomeration affect carbon nanotube cytotoxicity, *Toxicol. Lett.*, **168**, 121 (2007).
259. L.N. Daniel, Y. Mao, T.C. Wang, C.J. Markey, S.P. Markey, X. Shi, and U. Saffiotti, DNA strand breakage, thymine glycol production, and hydroxyl radical generation induced by different samples of crystalline silica in vitro, *Environ. Res.*, **71**, 60 (1995).
260. J.C. Ball, A.M. Straccia, W.C. Young, and A.E. Aust, The formation of reactive oxygen species catalyzed by neutral, aqueous extracts of NIST ambient particulate matter and diesel engine particles, *J. Air. Waste Manag. Assoc.*, **50**, 1897 (2000).
261. J.F. Long, W.J. Waldman, R. Kristovich, M. Williams, D. Knight, and P.K. Dutta, Comparison of ultrastructural cytotoxic effects of carbon and carbon/iron particulates on human monocyte-derived macrophages, *Environ. Health Perspect*, **113**, 170 (2005).
262. J.C. Carrero-Sanchez, A.L. Elias, R. Mancilla, G. Arrellin, H. Terrones, J.P. Laclette, and M. Terrones, Biocompatibility and toxicological studies of carbon nanotubes doped with nitrogen, *Nano. Lett.*, **6**, 1609 (2006).
263. S.K. Manna, S. Sarkar, J. Barr, K. Wise, E.V. Barrera, O. Jejelowo, A.C. Rice-Ficht, and G.T. Ramesh, Single-walled carbon nanotube induces oxidative stress and activates nuclear transcription factor-kappaB in human keratinocytes, *Nano. Lett.*, **5**, 1676 (2005).
264. E. Oberdörster, S. Zhu, T. Blickley, P. Mcclellan-Green, and M. Haasch, Ecotoxicology of carbon-based engineered nanoparticles: effects of fullerene (C60) on aquatic organisms, *Carbon*, **44**, 1112 (2006).
265. Q. Zhang, Y. Kusaka, K. Sato, Y. Mo, M. Fukuda, and Donaldson, K. , Toxicity of ultrafine nickel particles in lungs after intratracheal instillation, *J. Occup. Health*, **40**, 171 (1998).
266. K. Donaldson, P.H. Beswick, and P.S. Gilmour, Free radical activity associated with the surface of particles: a unifying factor in determining biological activity?, *Toxicol. Lett.*, **88**, 293 (1996).
267. Q. Zhang, Y. Kusaka, X. Zhu, K. Sato, Y. Mo, T. Kluz, and K. Donaldson, Comparative toxicity of standard nickel and ultrafine nickel in lung after intratracheal instillation, *J. Occup. Health*, **1**, 23 (2003).
268. Y. Sato, A. Yokoyama, K. Shibata, Y. Akimoto, S. Ogino, Y. Nodasaka, T. Kohgo, et al., Tohji, Influence of length on cytotoxicity of multi-walled carbon nanotubes against human acute monocytic leukemia cell line THP-1 in vitro and subcutaneous tissue of rats in vivo, *Mol. Biosyst.*, **1**, 176 (2005).
269. C.M. Sayes, A.M. Gobin, K.D. Ausman, J. Mendez, J.L. West, and V.L. Colvin, Nano-C60 cytotoxicity is due to lipid peroxidation, *Biomaterials*, **26**, 7587 (2005).
270. M. Bottini, S. Bruckner, K. Nika, N. Bottini, S. Bellucci, A. Magrini, A. Bergamaschi, and T. Mustelin, Multi-walled carbon nanotubes induce T lymphocyte apoptosis, *Toxicol. Lett.*, **160**, 121 (2006).
271. A. Magrez, S. Kasas, V. Salicio, N. Pasquier, J.W. Seo, M. Celio, S. Catsicas, et al., Cellular toxicity of carbon-based nanomaterials, *Nano. Lett.*, **6**, 1121 (2006).
272. G. Jia, H. Wang, L. Yan, X. Wang, R. Pei, T. Yan, Y. Zhao, and X. Guo, Cytotoxicity of carbon nanomaterials: single-wall nanotube, multi-wall nanotube, and fullerene, *Environ. Sci. Technol.*, **39**, 1378 (2005).
273. C. Grabinski, S. Hussain, K. Lafdi, L. Braydich-Stolle and J. Schlager, Effect of particle dimension on biocompatibility of carbon nanomaterials, *Carbon*, **45**, 2828 (2007).
274. M.R. Wilson, J.H. Lightbody, K. Donaldson, and Al., E., Interactions between ultrafine particles and transition metals in vivo and in vitro, *Toxicol. Appl. Pharmacol.* **184**, 172 (2002).
275. P.S. Gilmour, A. Ziesenis, E.R. Morrison, M.A. Vickers, E.M. Drost, I. Ford, et al., Pulmonary and systemic effects of short-term inhalation exposure to ultrafine carbon black particles, *Toxicol. Appl. Pharmacol.*, **195**, 35 (2004).
276. R.L. Price, K.M. Haberstoh, and T.J. Webster, Improved osteoblast viability in the presence of smaller nanometer dimensioned carbon fibres, *Nanotechnology*, **15**, 892 (2004).
277. C. Liu, H. Huang, P. Song, and S. Fan, Machining carbon nanotubes into uniform slices, *J. Nanosci. Nanotechnol.*, **7**, 4473 (2007).
278. T. Ashikaga, M. Wada, H. Kobayashi, M. Mori, Y. Katsumura, H. Fukui, S. Kato, et al., Effect of the photocatalytic activity of TiO(2) on plasmid DNA, *Mutat. Res.*, **466**, 1 (2000).
279. D.M. Brown, V. Stone, P. Findlay, W. Macnee, and K. Donaldson, Increased inflammation and intracellular calcium caused by ultrafine carbon black is independent of transition metals or other soluble components, *Occup. Environ. Med.*, **57**, 685 (2000).
280. D.M. Brown, M.R. Wilson, W. Macnee, V. Stone, and K. Donaldson, Size-dependent proinflammatory effects of ultrafine polystyrene particles: a role for surface area and oxidative stress in the enhanced activity of ultrafines, *Toxicol. Appl. Pharmacol.*, **175**, 191 (2001).
281. D. Hohr, Y. Steinfartz, R.P. Schins, A.M. Knaapen, G. Martra, B. Fubini, and P.J. Borm, The surface area rather than the surface coating determines the acute inflammatory response after instillation of fine and ultrafine TiO2 in the rat, *Int. J. Hyg. Environ. Health*, **205**, 239 (2002).
282. B. Rehn, F. Seiler, S. Rehn, J. Bruch, and M. Maier, Investigations on the inflammatory and genotoxic lung effects of two types of titanium dioxide: Untreated and surface treated, *Toxicol. Appl. Pharmacol.*, **189**, 84 (2003).
283. A. Hoshino, F. Kujioka, T. Oku, M. Suga, Y.F. Sasaki, T. Ohta, M. Yasuhara, K. Suzuki, and K. Yamamoto, Physicochemical properties and cellular toxicity of nanocrystal quantum dots depend on their surface modification, *Nano. Lett.*, **4**, 2163 (2004).
284. M. Muller, S. Mackeben, and C.C. Muller-Goymann, Physicochemical characterisation of liposomes with encapsulated local anaesthetics, *Int. J. Pharm.*, **1-2**, 139 (2004).
285. L. Ding, J. Stilwell, T. Zhang, O. Elboudwarej, H. Jiang, J.P. Selegue, P.A. Cooke, et al., Molecular characterization of the cytotoxic mechanism of multiwall carbon nanotubes and nano-onions on human skin fibroblast, *Nano. Lett.*, **5**, 2448 (2005).
286. C. Kirchner, T. Liedl, S. Kudera, T. Pellegrino, Munoz A. Javier, H.E. Gaub, S. Stolzle, et al., Cytotoxicity of colloidal CdSe and CdSe/ZnS nanoparticles, *Nano. Lett.*, **5**, 331 (2005).
287. K. Soto, A. Carrasco, T. Powell, K. Garza, and L. Murr, Comparative In vitro cytotoxicity assessment of some manufactured

nanoparticulate materials characterized by transmission electron microscopy, *J. Nanopart. Res.*, **7**, 145 (2005).
288. B.D. Chithrani, A.A. Ghazani, and W.C. Chan, Determining the size and shape dependence of gold nanoparticle uptake into mammalian cells, *Nano. Lett.*, **6**, 662 (2006).
289. C.M. Sayes, F. Liang, J.L. Hudson, J. Mendez, W. Guo, J.M. Beach, V.C. Moore, et al., Colvin, Functionalization density dependence of single-walled carbon nanotubes cytotoxicity in vitro, *Toxicol. Lett.*, **161**, 135 (2006).
290. H.W. Chen, S.F. Su, C.T. Chien, W.H. Lin, S.L. Yu, C.C. Chou, J.J. Chen, and P.C. Yang, Titanium dioxide nanoparticles induce emphysema-like lung injury in mice, *FASEB J.*, **20**, 2393 (2006).
291. D.B. Warheit, T.R. Webb, C.M. Sayes, V.L. Colvin, and K.L. Reed, Pulmonary instillation studies with nanoscale TiO2 rods and dots in rats: Toxicity is not dependent upon particle size and surface area, *Toxicol. Sci.*, **91**, 227 (2006).
292. Z.P. Xu, Q.H. Zeng, G.Q.L. Gq, and A.B. Ui, Inorganic nanoparticles as carriers for efficient cellular delivery *Chem. Engineer. Sci.*, **61**, 1027 (2006).
293. S. Pal, Y.K. Tak, and J.M. Song, Does the antibacterial activity of silver nanoparticles depend on the shape of the nanoparticle? A study of the Gram-negative bacterium Escherichia coli, *Appl. Environ. Microbiol.*, **73**, 1712 (2007).
294. A.A. Corona-Morales, A. Castell, and Al., E., Fullerene C60 and ascorbic acid protect cultured chromaffin cells against levodopa toxicity, *J. Neurosci. Res.*, **71**, 121 (2003).
295. G. Bogdanovic, V. Kojic, A. Dordevic, Canadanovic-J. Brunet, M. Vojinovic-Miloradov, and V.V. Baltic, Modulating activity of fullerol C60(OH)22 on doxorubicin-induced cytotoxicity, *Toxicol. In Vitro*, **18**, 629 (2004).
296. N.A. Monteiro-Riviere, A.O. Inman, Y.Y. Wang, and R.J. Nemanich, Surfactant effects on carbon nanotube interactions with human keratinocytes, *Nanomedicine*, **1**, 293 (2005).
297. N.A. Monteiro-Riviere, R.J. Nemanich, A.O. Inman, Y.Y. Wang, and J.E. Riviere, Multi-walled carbon nanotube interactions with human epidermal keratinocytes, *Toxicol. Lett.*, **155**, 377 (2005).
298. F.A. Witzmann and N.A. Monteiro-Riviere, Multi-walled carbon nanotube exposure alters protein expression in human keratinocytes, *Nanomedicine*, **2**, 158 (2006).
299. C.M. Sayes, A.A. Marchione, K.L. Reed, and D.B. Warheit, Comparative pulmonary toxicity assessments of C60 water suspensions in rats: few differences in fullerene toxicity in vivo in contrast to in vitro profiles, *Nano. Lett.*, **7**, 2399 (2007).
300. C.M. Sayes, K.L. Reed, and D.B. Warheit, Assessing toxicity of fine and nanoparticles: Comparing in vitro measurements to in vivo pulmonary toxicity profiles, *Toxicol. Sci.*, **97**, 163 (2007).
301. A.M. Schrand, K. Szcublewski, J.J. Schlager, L. Dai, and S.M. Hussain, Interaction and biocompatibility of multi-walled carbon nanotubes in PC-12 cells, *Int. J. Neuroprotection Neuroregeneration* **3**, 115 (2007).
302. R.L. Tse and P. Phelps, Polymorphonuclear leukocyte motility in vitro. V. Release of chemotactic activity following phagocytosis of calcium pyrophosphate crystals, diamond dust, and urate crystals, *J. Lab. Clin. Med.*, **76**, 403 (1970).
303. F.K. Higson and O.T. Jones, Oxygen radical production by horse and pig neutrophils induced by a range of crystals, *J. Rheumatol.*, **11**, 735 (1984).
304. M. Hedenborg and M. Klockars, Quartz-dust-induced production of reactive oxygen metabolites by human granulocytes, *Lung*, **167**, 23 (1989).
305. J.A. Schmidt, C.N. Oliver, J.L. Lepe-Zuniga, I. Green, and I. Gery, Silica-stimulated monocytes release fibroblast proliferation factors identical to interleukin 1. A potential role for interleukin 1 in the pathogenesis of silicosis, *J. Clin. Invest.*, **73**, 1462 (1984).
306. H.J. Allison Ac, Birbeck M An examination of the cytotoxic effects of silica on macrophages, *J. Exp. Med.* **124**, 141 (1966).
307. L. Nordsletten, A.K. Hogasen, Y.T. Konttinen, S. Santavirta, P. Aspenberg, and A.O. Aasen, Human monocytes stimulation by particles of hydroxyapatite, silicon carbide and diamond: in vitro studies of new prosthesis coatings, *Biomaterials*, **17**, 1521 (1996).
308. H.G. Luhr, Comparative studies on phagocytosis of coal powders of various carbonification grades, also of quartz and diamond powders in tissue cultures, *Arch. Gewerbepathol. Gewerbehyg.*, **16**, 355 (1958).
309. H.S. Cheung, M.T. Story, and D.J. Mccarty, Mitogenic effects of hydroxyapatite and calcium pyrophosphate dihydrate crystals on cultured mammalian cells, *Arthritis Rheum.*, **27**, 668 (1984).
310. I. Dion, L. Bordenave, F. Lefebvre, R. Bareille, C. Baquey, J.R. Monties, and P. Havlik, Physico-chemistry and cytotoxicity of ceramics part II: Cytotoxicity of ceramics *J. Mater. Sci.: Mater. Med.*, **5**, 18 (1994).
311. I. Dion, M. Lahaye, R. Salmon, C. Baquey, J.R. Monties, and P. Havlik, Blood haemolysis by ceramics, *Biomaterials*, **14**, 107 (1993).
312. V. Blanco, Lopez J. Camelo, and N.G. Carri, Growth inhibition, morphological differentiation and stimulation of survival in neuronal cell type (Neuro-2a) treated with trophic molecules, *Cell. Biol. Int.*, **25**, 909 (2001).
313. A.P. Puzyr, D.A. Neshumayev, V.S. Bondar, V.Y. Dolmatov, I.V. Shugalei, N.P. Dubyago, S.V. Tarskikh, and G.V. Makarskaya, The influence of detonation nanodiamond powder on blood cells, in: *Proceedings of NATO Advanced Research Workshop, Innovative superhard materials and sustainable coating*, vol. 200, Springer, Netherlands (2004).
314. A.P. Puzyr, S.V. Tarskikh, G.V. Makarskaya, G.A. Chiganova, I.S. Larionova, P.Y. Detkov, and V.S. Bondar, Damaging effect of detonation diamonds on human white and red blood cells in vitro, *Dokl. Biochem. Biophys.*, **385**, 201 (2002).
315. A.P. Puzyr, D.A. Neshumayev, S.V. Tarskikh, G.V. Makarskaya, V. Dolmatov, and V.S. Bondar, Destruction of human blood vells in interaction with detonation nanodiamonds in experiments in vitro, *Diamond Relat. Mater.*, **13**, 2020 (2004).
316. A.P. Puzyr, D.A. Neshumaev, S.V. Tarskikh, G.V. Makarskaia, V. Dolmatov, and V.S. Bondar, Destruction of human blood cells upon interaction with detonation nanodiamonds in experiments in vitro, *Biofizika*, **50**, 101 (2005).
317. Y. Nosé, What is blood compatibility?, *Aritificial Organs*, **15**, 1 (1991).
318. I. Dion, X. Roques, C. Baquey, E. Baudet, Basse B. Cathalinat, and N. More, Hemocompatibility of diamond-like carbon coating, *Biomed. Mater. Eng.*, **3**, 51 (1993).
319. I. Spilberg, J. Mehta, and L. Simchowitz, Induction of a chemotactic factor from human neutrophils by diverse crystals, *J. Lab. Clin. Med.*, **100**, 399 (1982).

320. J.S. Tu, E. Perevedentseva, P.H. Chung, and C.L. Cheng, Size-dependent surface CO stretching frequency investigations on nanodiamond particles, *J. Chem. Phys.*, **125**, 174713 (2006).
321. J. Muller, F. Huaux, N. Moreau, P. Misson, J.F. Heilier, M. Delos, M. Arras, A. Fonseca, J.B. Nagy, and D. Lison, Respiratory toxicity of multi-wall carbon nanotubes, *Toxicol. Appl. Pharmacol.*, **207**, 221 (2005).
322. K. Donaldson, R. Aitken, L. Tran, V. Stone, R. Duffin, G. Forrest, and A. Alexander, Carbon nanotubes: A review of their properties in relation to pulmonary toxicology and workplace safety, *Toxicol. Sci.*, **92**, 5 (2006).
323. T.K. Leeuw, R.M. Reith, R.A. Simonette, M.E. Harden, P. Cherukuri, D.A. Tsyboulski, K.M. Beckingham, and R.B. Weisman, Single-walled carbon nanotubes in the intact organism: near-IR imaging and biocompatibility studies in Drosophila, *Nano. Lett.*, **7**, 2650 (2007).
324. T. Tsuchiya, I. Oguri, Y.N. Yamakoshi, and N. Miyata, Novel harmful effects of [60]fullerene on mouse embryos in vitro and in vivo, *FEBS Lett.*, **393**, 139 (1996).
325. T.H. Ueng, J.J. Kang, H.W. Wang, Y.W. Cheng, and L.Y. Chiang, Suppression of microsomal cytochrome P450-dependent monooxygenases and mitochondrial oxidative phosphorylation by fullerenol, a polyhydroxylated fullerene C60, *Toxicol. Lett.*, **93**, 29 (1997).
326. C.Y. Usenko, S.L. Harper, and R.L. Tanguay, In vivo evaluation of carbon fullerene toxicity using embryonic zebrafish, *Carbon N Y*, **45**, 1891 (2007).
327. G.L. Baker, A. Gupta, M.L. Clark, B.R. Valenzuela, L.M. Staska, S.J. Harbo, J.T. Pierce, and J.A. Dill, Inhalation toxicity and lung toxicokinetics of C60 fullerene nanoparticles and microparticles, *Toxicol. Sci.*, **101**, 122 (2008).
328. A.A. Tykhomyrov, V.S. Nedzvetsky, V.K. Klochkov, and G.V. Andrievsky, Nanostructures of hydrated C60 fullerene (C60HyFn) protect rat brain against alcohol impact and attenuate behavioral impairments of alcoholized animals, *Toxicology*, **246**, 158 (2008).
329. A. Baun, N.B. Hartmann, K. Grieger, and K.O. Kusk, Ecotoxicity of engineered nanoparticles to aquatic invertebrates: A brief review and recommendations for future toxicity testing, *Ecotoxicology*, **17**, 387 (2008).
330. P. Aspenberg, A. Anttila, Y.T. Konttinen, R. Lappalainen, S.B. Goodman, L. Nordsletten, and S. Santavirta, Benign response to particles of diamond and SiC: Bone chamber studies of new joint replacement coating materials in rabbits, *Biomaterials*, **17**, 807 (1996).
331. M. Doherty, J.T. Whicher, and P.A. Dieppe, Activation of the alternative pathway of complement by monosodium urate monohydrate crystals and other inflammatory particles, *Ann. Rheum. Dis.*, **42**, 285 (1983).
332. A.P. Puzyr, V.S. Bondar, and Al., S.E., Dynamics of the selected physiological responses in laboratory mice under the prolonged oral administration of nanodiamonds suspensions *Siberian Med. Obozrenie (Siberian Med. Rev.) (in Russian)*, **4**, 19 (2004).
333. A.P. Puzyr, V.S. Bondar, Z.Y. Selimhanova, A.G. Tyan, E.V. Bortnikov, and E.V. Injevatkin, Results of studies of possible applications of detonation nanodiamonds as enterosorbents *Siberian Med. Obozrenie (Siberian Med. Rev.) (in Russian)*, 2-3, 25 (2004).
334. V. Bondar, Baron D., et al., Changes in bio-chemical parameters of blood plasma at administration of nanodiamond to laboratory animals, *Bull. Siberian Medi. (in Russian)*, **4**, 182 (2005).
335. A.P. Puzyr, V.S. Bondar, Z.Y. Selimkhanova, A.G. Tyan, E.V. Inzhevatkin, and E.V. Bortnikov, Results of in vitro and in vivo studies using detonation nanodiamonds/complex systems under extreme conditions, *KSC SB RAS, Krasnoyarsk*, **229** (2005).
336. A.P. Puzyr, V.S. Bondar, A.G. Selimkhanova, E.V. Tyan, Inzhevatkin, V.S. Bondar, and D. Baron, Physiological parameters of laboratory animals at oral administration of nanodiamond hydrosols, *Bull. Siberian Medi. (in Russian)*, **4**, 185 (2005).
337. A.P. Puzyr, E.V. Bortnikov, N.N. Skobelev, A.G. Tyan, Z. Yu, G.G. Selimkhanova, G.G. Manashev, and V.S. Bondar, A possibility of using of intravenous administration of sterile colloids of modified nanodiamonds, *Siberian Med. Obozrenie/ Siberian Med. Rev. (in Russian)*, **1**, 20 (2005).
338. V.Y. Dolmatov and L.N. Kostrova, Detonation-synthesized nanodiamonds and the feasibility of developing a new generation of medicinals *Superhard Mater. (in Russian)*, **3**, 82 (2000).
339. H. Maxwell, *The Poisoner's Handbook*, Loompanics Unlimited, Port Townsend, WA (1988).
340. G. Davies, *Diamond*, Adam Hilger Ltd., Bristol (1984).
341. T.S. Huang, Y. Tzeng, Y.K. Liu, Y.K. Chen, K.R. Walker, R. Guntupalli, and C. Liu, Immobilization of antibodies and bacterial binding on nanodiamond and carbon nanotubes for biosensor applications, *Diamond Relat. Mater.*, **13**, 1098 (2004).
342. D.B. Warheit, T.R. Webb, V.L. Colvin, K.L. Reed, and C.M. Sayes, Pulmonary bioassay studies with nanoscale and fine-quartz particles in rats: toxicity is not dependent upon particle size but on surface characteristics, *Toxicol. Sci.*, **95**, 270 (2007).
343. D.E. Gomez, I. Pastoriza-Santos, and P. Mulvaney, Tunable whispering gallery mode emission from quantum-dot-doped microspheres, *Small*, **1**, 238 (2005).
344. J. Lovric, S.J. Cho, F.M. Winnik, and D. Maysinger, Unmodified cadmium telluride quantum dots induce reactive oxygen species formation leading to multiple organelle damage and cell death, *Chem. Biol.*, **12**, 1227 (2005).
345. R. Hardman, A toxicologic review of quantum dots: Toxicity depends on physicochemical and environmental factors, *Environ. Health Perspect.*, **114**, 165 (2006).
346. A.M. Smith, G. Ruan, M.N. Rhyner, and S. Nie, Engineering luminescent quantum dots for in vivo molecular and cellular imaging, *Ann. Biomed. Eng.*, **34**, 3 (2006).
347. A. Hoshino, N. Manabe, K. Fujioka, K. Suzuki, M. Yasuhara, and K. Yamamoto, Use of fluorescent quantum dot bioconjugates for cellular imaging of immune cells, cell organelle labeling, and nanomedicine: Surface modification regulates biological function, including cytotoxicity, *J. Artif. Organs*, **10**, 149 (2007).
348. W. Liu, H.S. Choi, J.P. Zimmer, E. Tanaka, J.V. Frangioni, and M. Bawendi, Compact cysteine-coated CdSe(ZnCdS) quantum dots for in vivo applications, *J. Am. Chem. Soc.*, **129**, 14530 (2007).
349. D. Maysinger and J. Lovric, Quantum dots and other fluorescent nanoparticles: Quo vadis in the cell?, *Adv. Exp. Med. Biol.*, **620**, 156 (2007).
350. D. Maysinger, M. Behrendt, Lalancette-M. Hebert, and J. Kriz, Real-time imaging of astrocyte response to quantum dots: in vivo screening model system for biocompatibility of nanoparticles, *Nano. Lett.*, **7**, 2513 (2007).

351. D. Maysinger, Nanoparticles and cells: Good companions and doomed partnerships, *Org. Biomol. Chem.*, **5**, 2335 (2007).
352. D. Maysinger, J. Lovric, A. Eisenberg, and R. Savic, Fate of micelles and quantum dots in cells, *Eur. J. Pharm. Biopharm.*, **65**, 270 (2007).
353. W.B. Tan, S. Jiang, and Y. Zhang, Quantum-dot based nanoparticles for targeted silencing of HER2/neu gene via RNA interference, *Biomaterials*, **28**, 1565 (2007).
354. A.O. Choi, S.E. Brown, M. Szyf, and D. Maysinger, Quantum dot-induced epigenetic and genotoxic changes in human breast cancer cells, *J. Mol. Med.*, **86**, 291 (2008).
355. W. Liu, M. Howarth, A.B. Greytak, Y. Zheng, D.G. Nocera, A.Y. Ting, and M.G. Bawendi, Compact biocompatible quantum dots functionalized for cellular imaging, *J. Am. Chem. Soc.*, **130**, 1274 (2008).
356. T.C. Liu, H.L. Zhang, J.H. Wang, H.Q. Wang, Z.H. Zhang, X.F. Hua, Y.C. Cao, et al., Study on molecular interactions between proteins on live cell membranes using quantum dot-based fluorescence resonance energy transfer, *Anal. Bioanal. Chem.*, **391**, 2819 (2008).
357. V.N. Anisimov, M.A. Zabezhinski, I.G. Popovich, A.I. Lieberman, and J.L. Shmidt, Prevention of spontaneous and chemically-induced carcinogenesis using activated carbon fiber adsorbent. I. Effect of the activated carbon fiber adsorbent 'Aqualen' on spontaneous carcinogenesis and life-span in mice, *Cancer. Lett.*, **126**, 23 (1998).
358. V.N. Anisimov, M.A. Zabezhinski, I.G. Popovich, L.M. Berstein, I.G. Kovalenko, A.I. Lieberman, and J.L. Shmidt, Prevention of spontaneous and chemically induced carcinogenesis using activated carbon fiber adsorbent. III. Inhibitory effect of the activated carbon fiber adsorbent 'Aqualen' on 1,2-dimethylhydrazine-induced intestinal carcinogenesis in rats, *Cancer Lett.*, **138**, 27 (1999).
359. V.N. Anisimov, M.A. Zabezhinski, I.G. Popovich, A.I. Lieberman, and J.L. Shmidt, Prevention of spontaneous and chemically induced carcinogenesis using activated carbon fiber adsorbent. II. Inhibitory effect of the activated carbon fiber adsorbent 'Aqualen' on N-methyl-N′-nitro-N-nitrosoguanidine-induced gastric carcinogenesis in rats, *Cancer Lett.*, **138**, 23 (1999).
360. T.D. Phillips, Dietary clay in the chemoprevention of aflatoxin-induced disease, *Toxicol. Sci.*, **52**, 118 (1999).
361. V. Grichko, V. Grishko, and O. Shenderova, Nanodiamond bullets and their biological targets, *Nanobiotechnology*, **2**, 37 (2006).
362. K. Ushizawa, Y. Sato, T. Mitsumori, T. Machinami, T. Ueda, and T. Ando, Covalent immobilization of DNA on diamond and its verification by diffuse reflectance infrared spectroscopy, *Chem. Phys. Lett.*, **351**, 105 (2002).
363. H.R. Ibrahim, M. Yamada, K. Matsushita, K. Kobayashi, and A. Kato, Enhanced bactericidal action of lysozyme to Escherichia coli by inserting a hydrophobic pentapeptide into its C terminus, *J. Biol. Chem.*, **269**, 5059 (1994).
364. C.N. Pace, F. Vajdos, L. Fee, G. Grimsley, and T. Gray, How to measure and predict the molar absorption coefficient of a protein, *Protein. Sci.*, **4**, 2411 (1995).
365. T.T.B. Nguyen, H.C. Chang, and V.W.K. Wu, Adsorption and hydrolytic activity of lysozyme on diamond nanocrystallites, *Diamond Relat. Mater.*, **16**, 872 (2007).
366. A.I. Bojkova, O.A. Shilova, E.V. Golikova, N.I. Nikolajchuk, T.V. Khamova, S.V. Hashkovskij, D.Y. Vlasov, O.V. Frank-Kamenetsky, V.Y. Dolmatov, Detonation nanodiamond additives influence on strength and bioproofness of multiphase portland cement clinker materials, in: *Nanotechnology International Forum/Rusanotech '08, Abstracts*, V. 1M, RUSNANO (2008), 488–489.
367. N. Kossovsky, A. Gelman, H.J. Hnatyszyn, S. Rajguru, R.L. Garrell, S. Torbati, S.S. Freitas, and G.M. Chow, Surface-modified diamond nanoparticles as antigen delivery vehicles, *Bioconjug Chem.*, **6**, 507 (1995).
368. A. Bianco, W. Wu, G. Pastorin, C. Klumpp, L. Lacerda, C.D. Partidos, K. Kostarelos, and M. Prato, Carbon nanotube-based vectors for delivering Immunotherapeutics and Drugs, In: *Nanotechnologies for the life sciences* Kumar, C. (Ed.), Wiley-VCH Verlag GmbH & Co. KgaA, New York, 85 (2007).
369. A. Bianco, J. Hoebeke, S. Godefroy, O. Chaloin, D. Pantarotto, J.P. Briand, S. Muller, M. Prato, and C.D. Partidos, Cationic carbon nanotubes bind to CpG oligodeoxynucleotides and enhance their immunostimulatory properties, *J. Am. Chem. Soc.*, **127**, 58 (2005).
370. D. Pantarotto, C.D. Partidos, R. Graff, J. Hoebeke, J.P. Briand, M. Prato, and A. Bianco, Synthesis, structural characterization, and immunological properties of carbon nanotubes functionalized with peptides, *J. Am. Chem. Soc.*, **125**, 6160 (2003).
371. D. Pantarotto, C.D. Partidos, J. Hoebeke, F. Brown, E. Kramer, J.P. Briand, S. Muller, M. Prato, and A. Bianco, Immunization with peptide-functionalized carbon nanotubes enhances virus-specific neutralizing antibody responses, *Chem. Biol.*, **10**, 961 (2003).
372. H.J. Huang, E. Pierstorff, E. Osawa, and D. Ho, Protein-mediated assembly of nanodiamond hydrogels into a biocompatible and biofunctional multilayer nanofilm, *ACS Nano.*, **2**, 203 (2008).
373. K.K. Liu, F. Chen, P.Y. Chen, T.J.F. Lee, C.L. Cheng, C.C. Chang, Y.P. Ho, and J.I. Chao, Alpha-bungarotoxin binding to target cell in a developing visual system by carboxylated nanodiamond, *Nanotechnology*, **19** (2008).
374. V.Y. Dolmatov, *Detonation synthesis ultradispersed diamonds (Russian edition)*, Publ.house of Saint-Petersburg State Polytechnic University Saint-Petersburg (2003).
375. V.Y. Dolmatov, Biologically active detonation synthesis of ultradispersed diamonds, in *Publ. 27.04.*: Russian Federation, A61 K 33/44 2003.
376. T.A. Nachalnaya, Malogolovets V.G., Podzerei G.A., Nikitin Yu.I., Novikov N.V., Polkanov Yu.A., Special features of structure and physico-mechanical properties of natural diamonds of Ukraine, *Superhard materials (in Russian)*, **22**, 33 (2000).
377. T.N. Barushkina, V.G. Aleinikov, B.B. Donster, and G.I. Savvakin, Chemical modification of diamond surface with ozone *(Russian edition)*, In: *Proceedings of Institute of Superhard Materials of Ukrainian Academy of Sciences* (1990).
378. R. Hauert, A review of modified DLC coatings for biological applications, *Diamond Relat. Mater.*, **12**, 583 (2003).
379. M. Amaral and C.S. Abreu, Biotribological performace of NCD coated Si2N4-bioglass composites, *Diamond Relat. Mater.*, **16**, 790 (2007).
380. S. Mitura, A. Mitura, P. Niedzielski, and P. Couvrat, Nanocrystalline diamond coatings, *Chaos Solitons Fractals*, **10**, 2165 (1999).

381. X.C. Xiao, J. Wang, C. Liu, J.A. Carlisle, B. Mech, R. Greenberg, D. Guven, et al., Auciello, In vitro and in vivo evaluation of ultrananocrystalline diamond for coating of implantable retinal microchips, *J. Biomed. Mater. Res. Part B-Appl. Biomater.*, **77B**, 273 (2006).
382. T.I. Feygelson, O. Shenderova, S. Hens, G. Cunningham, K.D. Hobart, and J.E. Butler, Detonation nanodiamond slurries for nucleation of CVD diamond films, in *Third International Symposium Detonation Nanodiamonds: Technology, Properties and Applications*, St. Petersburg, Russia (2008).
383. L. Pramatarova, E. Pecheva, S. Stavrev, T. Spasov, P. Montgomery, A. Toth, M. Dimitrova, and M. Apostolova, Artificial bones through nanodiamonds, *J. Optoelectronics Adv. Mater.*, **9**, 236 (2007).
384. S. Chien-Min, S. Michael, and S. Emily, *Healthcare and cosmetic compositions containing nanodiamond*, US Patent 7, 294, 340.
385. V.V. Lunkin, *Patent: Cosmetic Composition*, RU 2257889.
386. Environmental Working Group, www.cosmeticdatabase.com.
387. F.P. Gasparro, M. Mitchnick, and J.F. Nash, A review of sunscreen safety and efficacy, *Photochemi. Photobiol.*, **68**, 243 (1998).
388. C.S. Cockell and J. Knowland, Ultraviolet radiation screening compounds, *Biol. Rev.*, **74**, 311 (1999).
389. J.F. Nash, Human safety and efficacy of ultraviolet filters and sunscreen products, *Dermatolo. Clin.*, **24**, 35 (2006).
390. A.M. Zaitsev, *Optical Properties of Diamond*, Springer, New York (2001).
391. R. Duffin, P.S. Gilmour, R.P. Schins, A. Clouter, K. Guy, D.M. Brown, W. Macnee, P.J. Borm, K. Donaldson, and V. Stone, Aluminium lactate treatment of DQ12 quartz inhibits its ability to cause inflammation, chemokine expression, and nuclear factor-kappaB activation, *Toxicol. Appl. Pharmacol.*, **176**, 10 (2001).
392. E. Ōsawa, Mono-disperse single-nano diamond particulates, *Pure Appl. Chem.*, **80**, 1365 (2008).
393. J.G. Teeguarden, P.M. Hinderliter, G. Orr, B.D. Thrall, and J.G. Pounds, Particokinetics in vitro: Dosimetry considerations for in vitro nanoparticle toxicity assessments, *Toxicol. Sci.*, **95**, 300 (2007).
394. N. Dutta and D. Green, Nanoparticle stability in semidilute and concentrated polymer solutions, *Langmuir*, **24**, 5260 (2008).
395. M. Hanauer, S. Pierrat, I. Zins, A. Lotz, and C. Sonnichsen, Separation of nanoparticles by gel electrophoresis according to size and shape, *Nano Lett.*, **7**, 2881 (2007).
396. N.A. Monteiro-Riviere, A.O. Inman, B.M. Barlow, and R.E. Baynes, Dermatotoxicity of cutting fluid mixtures: in vitro and in vivo studies, *Cutan. Ocul. Toxicol.*, **25**, 235 (2006).
397. J.M. Worle-Knirsch, K. Pulskamp, and H.F. Krug, Oops they did it again! Carbon nanotubes hoax scientists in viability assays, *Nano. Lett.*, **6**, 1261 (2006).
398. P. Hoet, A. Nemmar, B. Nemery, and M. Hoylaerts, Hemostatic and thrombotic effects of particulate exposure: assessing the mechanisms, In: *Nanotoxicology: characterization, dosing, and health effects* Monteiro-Riviere, N.a.T.C., Editor, Informa Healthcare., 247 (2007).
399. D. Cui, F. Tian, C.S. Ozkan, M. Wang, and H. Gao, Effect of single wall carbon nanotubes on human HEK293 cells, *Toxicol. Lett.*, **155**, 73 (2005).
400. M.J. Cunningham, S.R. Magnuson, and M.T. Falduto, Gene expression profiling of nanoscale materials using a systems biology approach, *Toxicol. Sci.*, **84**, 9 (2005).
401. N. Jia, Q. Lian, H. Shen, C. Wang, X. Li, and Z. Yang, Intracellular delivery of quantum dots tagged antisense oligodeoxynucleotides by functionalized multiwalled carbon nanotubes *Nano. Lett.*, **7**, 2976 (2007).
402. L. Cao, X. Wang, M.J. Meziani, F. Lu, H. Wang, P.G. Luo, Y. Lin, et al., Carbon dots for multiphoton bioimaging, *J. Am. Chem. Soc.*, **129**, 11318 (2007).
403. M. Geiser, B. Rothen-Rutishauser, N. Kapp, S. Schurch, W. Kreyling, H. Schulz, M. Semmler, et al., Ultrafine particles cross cellular membranes by nonphagocytic mechanisms in lungs and in cultured cells, *Environ. Health Perspect.*, **113**, 1555 (2005).
404. M. Ricarda-Lorenz, V. Holzapfel, A. Musyanovych, K. Nothelfer, P. Walther, H. Frank, K. Landfester, et al., Uptake of functionalized, fluorescent-labeled polymeric particles in different cell lines and stem cells *Biomaterials* **27**, 2820 (2006).
405. D. Lin and B. Xing, Phytotoxicity of nanoparticles: Inhibition of seed germination and root growth, *Environ. Pollut.*, **150**, 243 (2007).
406. A.S. Morozan, F. Nastase, A. Dumitru, S. Vulpe, C. Nastase, T. Stamatin, and K. Scott, The biocompatibility microorganisms-carbon nanostructures for applications in microbial fuel cells, *Physica Status Solidi (A)*, **204**, 1797 (2007).
407. K. Inoue, H. Takano, R. Yanagisawa, S. Hirano, M. Sakurai, A. Shimada, and T. Yoshikawa, Effects of airway exposure to nanoparticles on lung inflammation induced by bacterial endotoxin in mice *Environ. Health Perspectives*, **114**, 1325 (2006).
408. S.W. Han, C. Nakamura, I. Obataya, N. Nakamura, and J. Miyake, Gene expression using an ultrathin needle enabling accurate displacement and low invasiveness, *Biochem. Biophys. Res. Commun.*, **332**, 633 (2005).
409. J.H. Choi, F.T. Nguyen, P.W. Barone, D.A. Heller, A.E. Moll, D. Patel, S.A. Boppart, and M.S. Strano, Multimodal biomedical imaging with asymmetric single-walled carbon nanotube/iron oxide nanoparticle complexes, *Nano, Lett.*, **7**, 861 (2007).
410. J. Duryea, M. Magalnick, S. Alli, L. Yao, M. Wilson, and R. Goldbach-Mansky, Semiautomated three-dimensional segmentation software to quantify carpal bone volume changes on wrist CT scans for arthritis assessment, *Med. Phys.*, **35**, 2321 (2008).
411. K. Kim, C.G. Jeong, and S.J. Hollister, Non-invasive monitoring of tissue scaffold degradation using ultrasound elasticity imaging *Acta. Biomaterialia.*, **4**, 783 (2008).
412. J. Yang, E.K. Lim, H.J. Lee, J. Park, S.C. Lee, K. Lee, H.G. Yoon, et al., Fluorescent magnetic nanohybrids as multimodal imaging agents for human epithelial cancer detection, *Biomaterials*, **29**, 2548 (2008).
413. Q. Zhang, Z. Liu, P.R. Carney, Z. Yuan, H. Chen, S.N. Roper, and H. Jiang, Non-invasive imaging of epileptic seizures in vivo using photoacoustic tomography, *Phys. Med. Biol.*, **53**, 1921 (2008).